Development of Paclitaxel-loaded Polymeric Nanoparticles for Treating Liver Cancer

Thesis Submitted

By

DIPIKA MANDAL

Doctor of Philosophy (Pharmacy)

Department of Pharmaceutical Technology
Faculty of Engineering and Technology
Jadavpur University
Kolkata-700 032

2018

JADAVPUR UNIVERSITY

KOLKATA-700032, INDIA

INDEX NO. 147/12/Ph.

1. Title of the thesis:

"Development of Paclitaxel-loaded Polymeric Nanoparticles for Treating Liver Cancer".

2. Name, Designation and Institution of the supervisor/s:

Dr. Amal Kumar Bandyopadhyay,
Ex-Professor,
Department of Pharmaceutical Technology,
Jadavpur University,
Kolkata-700032, India.

3. List of Publications:

i. **Dipika Mandal**, Tapan Kumar Shaw, Goutam Dey, Murari Mohan Pal, Biswajit Mukherjee, Amal Kumar Bandyopadhyay, Mahitosh Mandal. Preferential hepatic uptake of paclitaxel-loaded poly-(D-L-lactide-co-glycolide) nanoparticles — A possibility for hepatic drug targeting: Pharmacokinetics and biodistribution. **Int. J. Bio. Mac**, 2018; 112: 818–830. (I**mpact factor: 3.671**).

ii. Tapan Kumar Shaw, **Dipika Mandal**, Goutam Dey, Murari Mohan Pal, Paramita Paul, Samrat Chakraborty, Kazi Asraf Ali, Biswajit Mukherjee, Amal Kumar Bandyopadhyay, and Mahitosh Mandal. Successful delivery of docetaxel to rat brain using experimentally developed nanoliposome: a treatment strategy for brain tumor. **Drug Deliv**, 2017; 24(1): 346–357. (**Impact factor: 6.402**)

iii. B. Mukherjee, S. Chakraborty, L. Mondal, B.S. Satapathy, S. Sengupta, L. Dutta, A. Choudhury, **D. Mandal**, Multifunctional drug nanocarriers facilitate more specific entry of therapeutic payload into tumors and control multiple drug resistance in cancer, in: A. Grumezescu (Ed.), Nanobiomaterials in Cancer Therapy (Elsevier), 2016, pp. 203–251.

4. List of Patents: NIL

5. List of Presentations in National/International/Conference/Workshops:

International

- Participated DST Sponsored five days International Seminar-cum-Workshop on **"Recent Advances in Clinical Research with a Special Emphasis on BA/BE Study"** organized by Bioequivalence Study Centre, Jadavpur University, India from 11th to 15th September 2014.
- Participated & poster presented in **2nd IAPST International Conference 2014** from 17th to 19th January 2014 in Jadavpur University, Kolkata on **"New Insights into Diseases and Recent Therapeutic Approaches''**.

CERTIFICATE FROM THE SUPERVISOR

*This is to certify that the thesis entitled "**Development of Paclitaxel-loaded Polymeric Nanoparticles for Treating Liver Cancer**" submitted by **Smt. Dipika Mandal**, who got her name registered on 12.09.2012 for the award of Ph.D. (Pharmacy) degree of Jadavpur University is absolutely based upon her own work under the supervision of **Prof. Amal Kumar Bandyopadhyay**, **Ex-Professor**, **Department of Pharmaceutical Technology, Jadavpur University, Kolkata-700032**, **India** and that neither her thesis nor any part of the thesis has been submitted for any degree/diploma or any other academic award anywhere before.*

_____

Signature of the Supervisor
and date with Office Seal


Dedicated to My Family

Acknowledgement

*I take this opportunity to express my heartfelt gratitude and indebtedness to my guide **Prof. Amal Kumar Bandyopadhyay**, Professor (ex), Department of Pharmaceutical Technology, Jadavpur University, Kolkata-32, for giving me the opportunity to do my Ph. D study under his guidance and also for his continuous support, patience, motivation, enthusiasm and faith on me.*

*Besides, I am equally thankful to **Prof. (Dr.) Biswajit Mukherjee,** Ex-Head, Department of Pharmaceutical Technology, Jadavpur University, Kolkata, India for providing me the facility for my Ph. D and research in his laboratory, and also for his continuous support, patience, motivation, enthusiasm and faith on me. His guidance helped me in all the time of research and writing this thesis. His thorough knowledge and suggestions on every new difficulty I faced in my research work, made me possible to complete this work with fruitful results.*

I offer humble gratitude to Dr. K. Kuotsu, Dept. of Pharmaceutical Technology, Jadavpur University, Kolkata for his help and kindness.

I also thanks to Dr. V. Ravichandran Endowment Funds, Centre for Advanced Research in Pharmaceutical Sciences, Jadavpur University, Kolkata and UGC, New Delhi for the financial support to carry out this work.

I also want to take this opportunity to acknowledge the contribution of Indian Association for the Cultivation of Science (IACS), Kolkata for extending cooperation and permission to use premises and facilities during the tenure of my research work.

I would like to thank all my seniors and lab mates in my laboratory of Department of Pharmaceutical Technology, Jadavpur University, Kolkata.

*I would like to express my special thanks to **Soumen Karan** and **Samrat Chakraborty,** Department of Pharmaceutical Technology, Jadavpur University, Kolkata for his their help in my research work.*

Last but not the least, I would like to thanks my family and friends since without their help, love, admiration and encouragement this study would be difficult.

Date:
Place: DIPIKA MANDAL

LIST OF ABBREVIATIONS

µg/ml	Microgram per millilitre
w/v	Weight/volume
µl	Microlitre
AUC	Area under the curve
AUMC	Area under the first moment curve
CC	Calibration control
CL	Clearance
cm	Centimetre
C_{max}	Peak plasma concentration
Da	Daltons
DMSO	Dimethyl sulphoxide
PTX	Paclitaxel
EDTA	Ethylene diamine tetra acetic acid
FBS	Fetal bovine serum
FESEM	Field emission scanning electron microscopy
FITC	Fluorescein isothiocyanate
FTIR	Fourier transform infrared
DSC	Differential scanning calorimetry
PLGA	Poly (D-L-Lactide-co-Glycolide)
g	Gram
h	Hour
HPLC	High performance liquid chromatography
i.v.	Intravenous
IAEC	Institutional Animal Ethical Committee
RH	Relative humidity
IS	Internal standard
L	Litre
LC-MS/MS	Tandem liquid chromatography/ mass spectrometry
mg	Milligram
mg/kg	Milligram per kilogram
min	Minutes
ml	Millilitre
nm	Nanometer
nM	Nano molar
NPs	Nanoparticles
PBCA	Poly butyl cyano acrylate
PBS	Phosphate buffer saline
SLS	Sodium lauryl sulphate
PDI	Polydispersity index
PEG	Polyethylene glycol
PK	Pharmacokinetic
QC	Quality control
QDs	Quantum dots
RES	Reticuloendothelial system
SLNs	Solid lipid nanoparticles
$t_{1/2}$	Half life
TEM	Transmission electron microscopy
US-FDA	United State Food and Drug Administrations
V_{ss}	Steady state volume of distribution
MRT	Mean residence time

Contents

Chapter 1

Introduction

1. INTRODUCTION

1.1. Liver anatomy and function

Liver is the largest organ in the human body. The average weight of the adult human liver is 1.5–2.0 kg. It is situated in the upper right quadrant of the abdomen, below the diaphragm and partially protected by the rib cage **(Abdel-Misih & Bloomston, 2010)**. The liver is covered by a layer of connective tissue called Glisson's capsule. It has two main lobes **(Figure 1.1)**, larger one is the right hepatic lobe and smaller one is the left hepatic lobe which is separated by the course of the middle hepatic vein. Each lobe is composed with numerous lobules which are in general hexagonal in shape **(Figure 1.1)**. The interior of each lobule is occupied by the central vein and the periphery of the lobule is described by a close arrangement of hepatic artery, portal vein, and bile duct; called "portal triads". The liver consists of various types of cells. Oval cells are normally observed near the portal triad. These cells are also called hepatic stem cells. The polygonal hepatic parenchymal cells (hepatocytes) are the main cell-type in the liver. About 80% of hepatocytes are present in the hepatic lobules. They have clear cell membrane; sometimes with two nuclei and contain deposits of glycogen, often with lipid droplets and basophilic materials. They also contain other cellular organelles such as mitochondria, rough endoplasmic reticulum (granular) and smooth endoplasmic reticulum (agranular), golgi apparatus and lysosomes **(Mukherjee et al., 2012)**. Hepatocytes undergo cell division and produce large number of hepatocytes. They metabolize and excrete into sinusoids or bile canaliculi. Besides endothelial cells, liver sinusoids also contain phagocytic cells that obtained from monocytes, known as Kupffer cells. Kupffer cells are tissue resident macrophages and they phagocytose and destroy pathogens and other foreign bodies and materials in the blood. These macrophages are also engaged in the recycling of erythrocytes and the digestion of apoptotic cells. Other hepatic cell-type is known as the ito cell which is also called adipose or perisinusoidal cells or hepatic stellate cells. These are involved with the secretion and maintenance of extracellular matrix. They maintain a large reservoir of vitamin A in the liver and respond to damaged hepatocytes and immune cells by differentiating into tissue-regenerating myofibroblasts **(Yin et al., 2013)**.

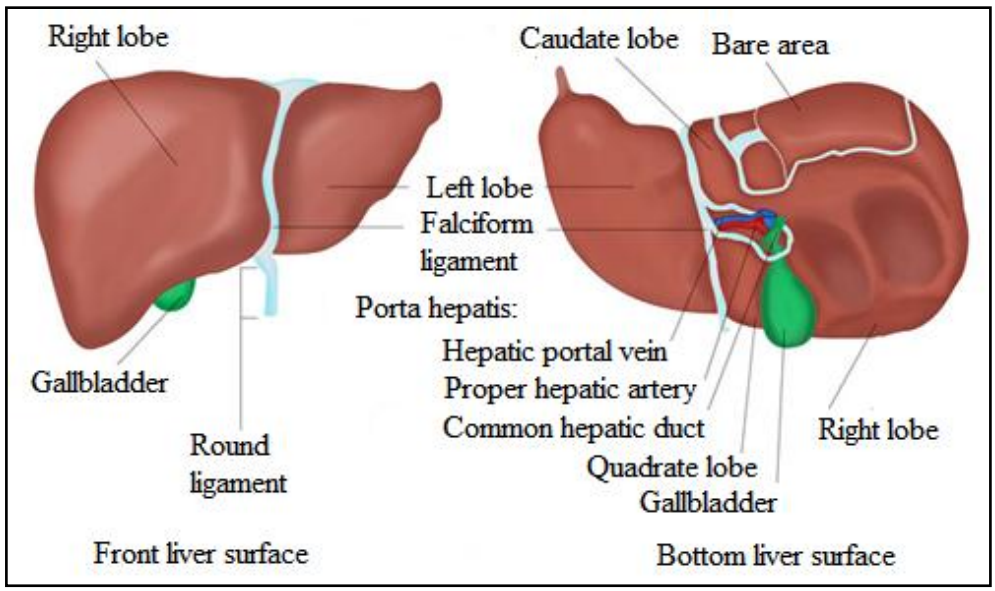

Figure 1.1. Liver anatomy diagram: anterior and inferior surface.

The two major sources of blood supply in liver are the hepatic artery and portal vein **(Abdel-Misih & Bloomston, 2010; Mishra et al., 2013)**. The left and right hepatic arteries supply oxygen-rich blood to the liver from the heart. The portal vein carries nutrient-rich blood (but relatively less oxygenated) from the spleen, pancreas and intestines to the liver and comprises the remaining 65-70% of blood volume. The majority of the blood is then drained from the liver through the left, middle and right hepatic veins **(Reddy & Couvreur, 2011)**.

The main functions of the liver are;

- Production and secretion of bile, which contains bile salts (sodium glycocholate, sodium taurocholate). The bile salts emulsify fats and oils and thus help in the digestion of them.
- Storage of iron, vitamins, trace elements and glycogen.
- Metabolism of carbohydrates, fat and hemoglobin and synthesis of lipid.
- Volume reservoir and filter for blood.
- Hormonal balance and detoxification and removal of many toxic chemicals, including drugs, carcinogens and various toxins through bile from the body.
- Production of immune factors to fight infection against pathogens and
- Conversion of waste products for excretion by the kidneys and intestines **(Hoekstra et al., 2013; Ghibellini et al., 2006; Pond & Tozer, 1984; Wang et al., 2015)**.

1.2. Liver cancer and its types

Cancer, one of the most devastating diseases having a tremendous morbidity and mortality impact in the developing world, caused nearly 8.8 million deaths in 2015 (**http://www.who.int/mediacentre/factsheets/fs297/en/**). In 2018, 1,735,350 new cancer cases and 609,640 cancer deaths are expected to occur in the United States **(Siegel et al., 2018)**. Globally, 1 in 6 deaths is due to cancer. It is characterized by an abnormal growth of cells. When healthy cells become cancerous, they begin to grow and divide rapidly and forming a tumor. Healthy cells are unable to compete with the cancerous cells which rapidly consume the nutrient supplied from the blood stream **(Hu & Zhang, 2009)**. The healthy cells will ultimately be overcrowded by the tumor cells. Although, the excess demand of nutrition cannot be supported continuously by the vasculature, because of this reason, some of the cancer cells die, but most of them will survive and still divide continuously in an environment that lacks nutrition. Among all the cancers, liver cancer is common and second-leading cause of cancer deaths after lung cancer (**http://www.who.int/mediacentre/factsheets/fs297/en/**). Liver cancer more commonly occurs in sub-Saharan Africa and Southeast Asia than in the US. Men are more susceptible than woman in case of liver cancer **(Jemal et al., 2011)**. Uncontrolled proliferation of the cells causes solid mass formation in the liver, resulting hepatic tumor. The main causes of liver cancer are chronic infection with hepatitis B virus (HBV), hepatitis C virus (HCV), alcoholic cirrhosis and cirrhosis associated with genetic liver diseases **(Bosch et al., 2004)**.

1.2.1. Primary liver cancer

Primary liver cancer is the most common type of liver cancer. It starts primarily in the liver not from the cancerous cells present surrounding the liver. It is much more common in men than in women and older people are more likely to affect with this cancer. The causes of primary liver cancer are chronic viral infections such as hepatitis B or C, some toxins, chemical induced hepatic damage, radiation-induced hepatic damage and chronic liver diseases such as cirrhosis. Different types of primary liver cancer are as follows.

Hepatocellular carcinoma (HCC)

HCC is the most common type of primary liver cancer which starts from the main liver cells, called hepatocytes. HCC is also known as hepatoma. It is more common in adult people. The main causes of HCC are the result of infection with hepatitis B or C, or cirrhosis of the liver caused by alcoholism. A rare type of HCC called fibrolamellar HCC generally affects younger women and is not related to previous liver disease and it is more responsive to treatment than other types of liver cancer.

Cholangiocarcinoma

It occurs in the small, tube-like bile ducts within the liver and accounting about 10-20 percent of all liver cancers.

Angiosarcoma

It is also called hemangiocarcinoma and accounts for about 1 percent of all liver cancers. Angiosarcomas start in the blood vessels of the liver and develop rapidly. They are typically diagnosed at an advanced stage.

1.2.2. Secondary liver cancer

Secondary liver cancer develops when primary cancer from any part of the body invades hepatic tissues. This is also known as liver metastasis. The spreading of malignant cells from other part of the body to liver occurs through the blood flow or through the lymphatic system, the anchorage of the cells in liver, angiogenesis (formation of new blood vessels for supply of food and oxygen for new cells) and cellular proliferation leading to solid growth of mass are the possible sequences of secondary liver cancer. More than half of people diagnosed with colorectal cancer build up secondary liver cancer.

1.3. Current treatments strategy of liver cancer

1.3.1. Surgical resection

Surgical resection is the treatment of choice for noncirrhotic patients, when the lesion is superficial and of small dimensions. In earlier days, survival was rare but recently, the 5-

years survival rate after resection has increased up to 41%-74% **(Allemann et al., 2013)**. The resectability of the tumor is dependent on the tumor size, location, underlying liver function and the remaining liver volume. In the United States and Europe, selection of perfect candidates for resection is generally based on the assessment of portal hypertension, which is assessed by cannulation of the hepatic vein and calculation of the hepatic portal venous gradient. In patients with normal synthetic function, standardized levels of bilirubin and the pressure gradient of <10 mmHg in the hepatic vein (Grade II recommendation) are the potential candidates for liver surgery **(Bruix & Sherman, 2011; Bruix et al., 1996)**. Operative mortality depends on the presence (10%) or absence (5%) of cirrhosis **(Colleoni et al., 1998)**. Instead of curative resection, recurrence is common **(Hwang et al., 2015)**. After 5 years of surgery recurrence rates may be as high as 70%. Recurrence occurs either from the microscopic residual disease that remains after resection or from *de novo* cancer that comes about in hepatitis or cirrhosis **(Cha et al., 2003)**. The majority of liver cancer recurrences develop within a short period (1-2 years) which is believed to be due to the dissemination or micrometastasis from the primary tumor and not from inadequate surgical resection **(Crissien & Frenette, 2014)**. Contraindications to the resection are the occurrence of extrahepatic metastasis or invasion of the main portal trunk by the tumor.

1.3.2. Liver transplantation (LT)

Liver transplantation is a potential curative treatment for patients with decompensated cirrhosis, and only solid tumor. LT provides a better oncological outcome than surgical resection because it not only removes all precancerous and cancerous lesions within the liver but also cures the co-existing liver disease. But, selection of the candidates is a difficult matter, due to worldwide organ shortage, controlling the amount of tumor present during the time till transplant, exploring live donors and different immunosuppressive or supplementary therapy **(Clavien et al., 2012)**. In early days back to the 1980s the 5-year survival rates after liver transplantation was less than 40%. Recently, LT is proposed for the patients whose tumor is within the Milan criteria for liver cancer (one lesion not larger than 5 cm, or up to 3 lesions with each 3 cm or smaller). LT according to this selection procedure results in a 5-year overall survival rate more than 70% and a tumor recurrence rate of less than 15%

(Mazzaferro, 1996, 2007 & 2011). The shortage of liver donor remains the main problem for liver cancer patients and increases the waiting time for transplantation.

1.3.3. Local ablative therapy

Local ablative therapy is two types such as, chemical ablation and thermal ablation. Ethanol and acetic acid are used as chemical ablation and thermal ablation uses radiofrequency, microwaves, cryoablation, lasers and ultrasound. Local ablation is an alternative treatment for cirrhotic patients with early-stage HCC and contraindications for surgical treatment. The complication rate of this treatment is low, and is suitable in patients with good liver function. The 5-year survival rate of up to 50% may be achieved **(Llovet et al., 2012)**. Radiofrequency ablations (RFA) are effective to all other local ablative therapies. For unresectable liver cancer, local ablative therapy has also been shown better efficacy when combined with transarterial chemoembolization (TACE). In a randomized trial comparing TACE followed by RFA versus RFA in patients with HCC < 7 cm in size, the combination therapy resulted in 1-, 3-, and 4-year overall survival rates of 93, 67, and 62%, respectively, compared to 85, 59, and 45% respectively in the RFA-alone **(Xie et al., 2014)**. The corresponding recurrence-free survivals were 79, 61, and 55% as well as 67, 44, and 39%, respectively.

1.3.4. Transarterial chemoembolization (TACE)

For intermediate-stage of liver tumors TACE is the treatment of choice **(Llovet et al., 2012; Bruix & Sherman, 2011)**. TACE is based on the simultaneous application of a chemotherapeutic agent and embolization with occluding particles. The successful TACE depends on the presence of a hypervascularized tumor. Selective administration of the mixture of chemotherapeutic agent and occluding particles results in a high local concentration of the chemotherapeutic agent in the tumor with low systemic distribution. The chemotherapeutic agents remain in the tumor region due to occlusion of the tumor vessels and the resulting hypoxia improves the effect of the chemotherapeutic agent. Procedures for TACE are not standardized. Commonly used chemotherapeutic agents are doxorubicin, mitomycin C and cisplatin. Lipiodol as an oily suspension has an affinity to HCC and acts as a carrier for the chemotherapeutic agent. TACE is either performed as ‘on demand’ (repeated in case of persistent vascularization) or as ‘continuous’ (repeated every 4-6 weeks until

devascularization) schedule. TACE and oral tyrosine kinase inhibitor sorafenib are the active treatments for HCC. Liu et al. **(Liu et al., 2014)** studied a meta-analysis on this subject and concluded that the combination seems to be more active than each single approach.

1.3.5. Systemic therapy

Most of the liver cancer patients were diagnosed in advanced stage. Up to 2008, there was no systemic therapy available which could improve the survival rate. Recently, there are many chemotherapeutic agents which are identified as anticancer drugs. Among these drugs, some are available in the market as formulated drugs and some of them are in the clinical trials. Sorafenib, an oral multiple kinase inhibitor, is approved by United State Food and Drug Administration (US-FDA) for advanced liver cancer treatment. Another oral multi-kinase inhibitor, regorafenib has also been shown to improve overall survival of advanced liver cancer patients after a phase 3 trial **(Bruix et al., 2017)**. In 2017, regorafenib has been approved by FDA due to the efficacy and safety. Other liver cancer targeted drugs that have been evaluated in clinical trials include sunitinib and linifanib (multi-targeted tyrosine kinase inhibitor), erlotinib and gefitinib (inhibitors for epidermal growth factor receptor), brivanib (selective inhibitor of fibroblastic growth factor receptor and vascular endothelial growth factor), tivantinib (oral Met receptor tyrosine kinase inhibitor), everolimus (inhibitor of mammalian target of rapamycin) and bevacizumab (humanized monoclonal antibody against vascular endothelial growth factor) **(Fu & Wang, 2018)**.

1.4. Nanoparticle targeting

Targeting can be attained by designing nanocarriers, conjugated with ligands that have high affinity to the specific receptors present on the cancer cells. Hence, higher drug concentration can be achieved to the target sites, depending on the extent of receptor-ligand interaction, concentration of ligand on the surface of NPs, and the extent to which these receptors are expressed by cells. The targeting ligands are used to modify the surface of different types of nanoparticles, like polymeric, lipid-based, metallic nanoparticles etc. **(Elsabahy et al., 2015; Zhang et al., 2012; Ma et al., 2016; Meng et al., 2015; Tomuleasa et al., 2012)**.

There are several advantages of nanoparticle targeting in liver cancer.

- Increase drug concentration in the tumor through:
  (i) Passive targeting
  (ii) Active targeting
- Decrease drug concentration in normal tissue.
- Improve pharmacokinetic and pharmacodynamic profiles.
- Improve the solubility of drug to allow intravenous administration.
- Release maximum drug during transit.
- Release maximum drug at the targeted site.
- Increase drug stability and reducing drug degradation.
- Improve internalization and intracellular delivery.
- Biocompatible and biodegradable.

1.4.1. Passive targeting

This targeting approach exploits the pathophysiological conditions, such as leaky vasculature, pH, temperature, and surface charge surrounding the tumor for specific delivery of NPs.

- ***Enhanced permeation and retention (EPR) effect***

Passive targeting of nanoparticulate systems in the liver tumor can occur by enhanced permeability and retention (EPR) effect that was first described by Matsumura and Maeda in 1986 **(Matsumura & Maeda, 1986)**. When the tumor volume reaches more than 2 mm^3, diffusion limitation takes place, which ultimately impairs nutrition intake, waste excretion and oxygen delivery **(Byrne et al., 2008)**. Such rapidly growing cancer cells generate new blood vessels, a phenomenon called angiogenesis (or neovascularization). As a result unusual tortuosity, abnormalities in the basement membrane and the lack of pericytes lining endothelial cells are produced which imperts leaky vessels with gap sizes of 100 nm to 2 μm, depending upon the tumor type **(Maeda, 2001)**. Poor lymphatic drainage occurs due to the high interstitial pressure at the core of the tumor than at the periphery. This combination of leaky vasculature and poor lymphatic flow results in enhanced permeation and retention (EPR) effect. Thus, NPs can favorably localize in the cancerous tissues owing to their smaller

size than the blood vessel fenestration and be entrapped in to the tumor due to higher retention ability than the normal tissues **(Figure 1.2) (Carmeliet & Jain, 2000)**.

- ***Tumor microenvironment***

Passive targeting also depends on microenvironment surrounding the tumor cells, and it differs from that of the normal cells. Generally cancer cells show high metabolic rate. Glycolysis can occur to of nutrients and oxygen to the tumor cells, which results in acidic environments in cancer cells **(Pelicano et al., 2006)**. The pH sensitive nanoparticles are designed to remain stable at physiological pH (pH 7.4), but they release the active material at the pH lower than physiological pH such as acidic environment of tumor cells **(Yatvin et al., 1980)**. Hyperthermia is produced in many types of cancers such as ovarian carcinoma. Thermo-sensitive polymeric nanoparticles contain polymer that reveals a low critical solution temperature (LCST) and that have a tendency to release drug at the temperature above LCST in the tumor cells. Localized hyperthermia in tumors can be induced by physical methods such as ultrasound or photothermal means **(Brewer et al., 2011, Cheng et al., 2010)**.

- ***Surface charge***

Tumor cells bear relatively high negative surface charge than the normal cells and they favor binding of cationic nanoparticulate systems **(James et al., 1956)**. Targeting of cationic nanoparticles is achieved by electrostatic binding to negatively charged phospholipid head groups presented on tumor endothelial cells **(Ran et al., 2002; Krasnici et al., 2003)**. The cytotoxicity potential of polymeric nanoparticles largely depends on cellular internalization and subcellular localization of the NPs, which is governed by the nature of polymeric surface charge (anionic, cationic, or neutral) **(Asati et al., 2010)**.

1.4.2. Active targeting

In active targeting, nanoparticles containing the chemotherapeutic agents are designed in such a way that the surface of nanoparticle is modified to target the cancerous cells. Non-uniform drug distribution may cause incomplete cancer treatment and drug targeting may be one of the most suitable options to tackle the problem. By targeted drug delivery system drug accumulates in the targeted organ or tissue in a selective way independent of site and method of administration. Thus, drug at the disease site becomes more while its concentration at the

non-targeted tissues will be minimum **(Danhier et al., 2010)**. Active targeting utilizes either by ligand-receptor interaction or antibody-antigen recognition **(Figure 1.2) (Guo & Szoka, 2003; Nie et al., 2007; Cho et al., 2008)**. Nanoparticles with targeted ligand such as antibody, antibody fragments, aptamers, polysaccharide, peptide and small biomolecules like folic acid etc. **(Zhong et al., 2014)** are being used to target cells through ligand-receptor interactions. Various ligands used against the receptors of hepatic stellate cells include mannose-6 phosphate, human serum albumin, galactocyte and galactosamine and those of hepatocytes are glycyrrahizin, linoleic acid and apolipoprotein A1 **(Mukherjee et al., 2016)**. Active targeting by nanoparticulate system has three main components namely, (i) an apoptosis-inducing agent (anticancer drug), (ii) a targeting moiety-penetration enhancer and (iii) a carrier. Several materials are used to construct a nanoparticle and they include ceramic, polymers, lipids and metals **(Yezhelyev et al., 2006)**. Nanoparticles containing chemotherapeutic agents are engulfed by phagocytes and quickly cleared by the reticuloendothelial system (RES). Various methods have been developed to sustain the nanoparticles in blood stream like alteration of the polymeric composition of the carrier and coating of nanoparticles with hydrophilic polymers to avoid wash out that can sufficiently target the cancerous cells. Hydrophilic polymer coating on the nanoparticle surface repels plasma proteins and escapes from being opsonized and cleared. This is described as a "cloud" effect **(Brigger et al., 2002; Jeon et al., 1991; Tallury et al., 2009; Francis et al., 2004)**. Commonly used hydrophilic polymers are polyethylene glycol (PEG), poloxamines, poloxamers, polysaccharides etc **(Storm et al., 1995; Torchilin & Trubetskoy, 1995)**. Specific receptors are present on the cell surface of the cancer cells but, they are absent on normal cells. Some receptors of cancer cells may be altered due to over expression or mutation. Active targeting develops after functionalization of nanoparticles with specific ligand that has a high affinity towards tumor cell differentiating target receptor. Various targeting cells of human liver are non-parenchymal sinusoidal endothelial cells (SECs), kuffer cells (KCs), hepatic stellate cells (HSCs) and the predominant parenchymal hepatocytes.

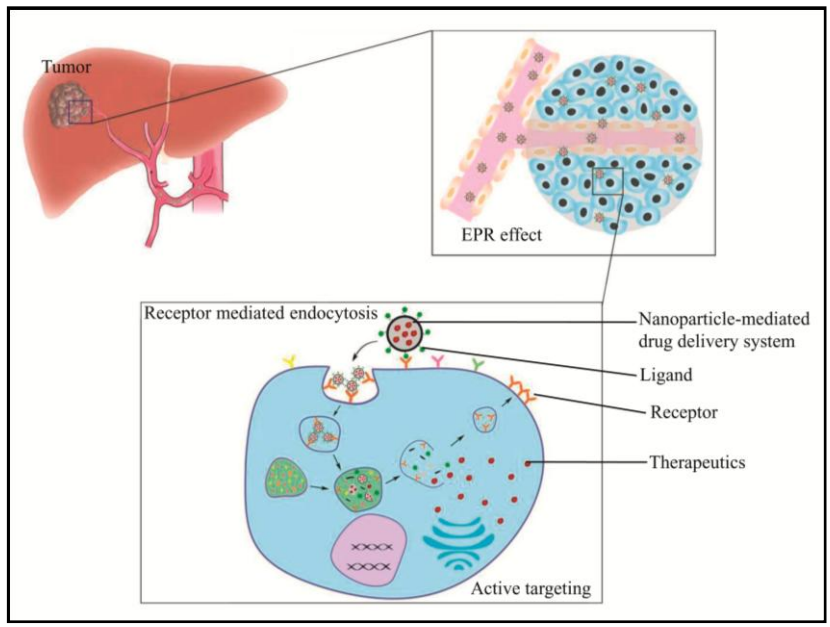

Figure 1.2. The schematic diagram of ligand-based targeted therapy through EPR effect and active targeting. **(Li et al., 2016).**

1.5. Liver cell specific targeting

There are five different cell types present in liver for active targeting of drug. They are hepatocytes, Kupffer and sinusoidal endothelial cells, hepatic stellate cells (HSC), bile duct epithelial cells.

1.5.1. Hepatocytes

Hepatocytes may be affected with many liver diseases like viral hepatitis (hepatitis A, B or C), alcohol-induced steatohepatitis (ASH), nonalcohol induced steatohepatitis (NASH) and some genetic diseases like Wilson‘s disease, hemochromatosis, α-1 antitrypsin deficiency and several other metabolic disorders. Many methods have been developed for hepatocytes selective drug targeting for reduction of side effects and enhancement of the therapeutic effect of drugs. The most prevalent and attractive method is asialoglycoprotein receptors (ASGP-R) targeting strategy. Asialoglycoprotein receptors (ASGP-R) are situated at the basolateral membrane of hepatocytes and, therefore, are in direct contact with the bloodstream. They show high affinity for binding to a broad range of molecules mainly galactose and N-acetyl-galactosamine residues such as asialoorosomucoid, asialofetuin (AF),

sterylglucoside, lactose and poly-(N-ρ-vinylbenzyl-O-β-D-galactopyranosyl-[1-4]-D-gluconamide (PVLA). Clerc et al. **(Clerc et al., 1995)** showed that the number of binding sites for glycyrrhetinic acid (GA) is much more than that for glycyrrhizin (GL) in hepatocytes. Tian et al. **(Tian et al., 2010)** prepared glycyrrhetinic acid-modified chitosan/poly(ethylene glycol) nanoparticles for liver-targeted delivery and found that the cellular uptake of nanoparticles modified with glycyrrhetinic acid by rat hepatocytes was 19-fold higher than that of unmodified ones. The delivery of novel drug delivery system like liposomes, niosomes, nanoparticles, and proteins to the hepatocytes using ASGP-R as a target receptor is one of the first options for the cell specific delivery to the liver cells.

1.5.2. Kupffer and sinusoidal endothelial cells

Kupffer cells are located within the space of disse (perisinusoidal space) in the surrounding area of the hepatocytes **(Gratton et al., 2008)**. Kupffer cells may be involved in the pathogenesis of various liver diseases like hepatitis, steatohepatitis, alcoholic liver disease, intrahepatic cholestasis, and activation or rejection of the liver during liver transplantation and liver fibrosis **(Sharma et al., 2010)**. Kupffer and sinusoidal endothelial cells can enhance the uptake of drug delivery systems and showed high phagocytic capacity. Accumulation of targeted carrier systems in Kupffer and endothelial cells occurs either by nonspecific or specific uptake mechanism via designated receptors. Drug delivery systems like liposomes, micelles and viral particles are taken up by nonspecific uptake mechanism due to their largest phagocytic activity **(Arnida et al., 2011)**. Targeting to Kupffer cells is directed through mannose receptor using sugar moieties (like mannose and fucose) which are coupled to delivery system while targeting to sinusoidal endothelial cells is possible using hyaluron receptor as the target receptor **(Banquy et al., 2009; You & Auguste, 2009)**. Yamashita et al. **(Yamashita et al., 1991)** observed that when liposome surface was modified by cetylmannoside then it could be useful for targeting to Kupffer cells. Melgert et al. investigated that when dexamethasone was combined to mannosylated albumin, it was selectively delivered to the Kupffer cells **(Melgert et al., 2001)**.

1.5.3. Hepatic Stellate Cells (HSC)

Hepatic stellate cells (HSC) play an important role for the development of liver fibrosis due to production and regulation of vascular tone in extracellular matrix, and production of inflammatory mediators such as transforming growth factor-beta (TGF-β) and platelet-derived growth factor (PDGF). These processes are dearranged during fibrosis and at a certain time point, the HSC continue the fibrogenesis by generating several autocrine loops. Thus, this process is maintaining without contribution of the other cell types. These cells are major target for antifibrotic drugs **(Merkel et al., 2011; Hillaireau & Couvreur, 2009; Schuppan et al., 2001; Benyon & Arthur, 2001; Rockey, 2001)**. The first target receptor chosen was the mannose-6-phosphate (M6P)/insulin-like growth factor II (M6P/IGFII) receptor, because it was reported to be highly unregulated on the cell membranes of activated HSC. Mannose-6-phosphate hepatic stellate cell (M6P-HSA) binds to the activated HSC and rapid internalization of the protein occurs via a receptor mediated endocytotic route. Greupink et al. **(Greupink et al., 2005)** showed that targeted delivery of coupled mycophenolic acid to the HSC-selective drug carrier mannose-6-phosphate modified human serum albumin results in a decrease in HSC activation, which is the first drug that is successfully delivered to this cell type.

1.6. Nanoparticle therapeutics for liver cancer

Over the last few decades, nanocarriers in the form of nanoparticles (NPs) have been developed for drug delivery in liver cancer treatment for increased efficiency and reduced drug side effects **(Marinina et al., 2000; Sachdeva, 1998)**. Therapeutic agents that have been incorporated with the drug carriers include chemotherapeutic agents such as paclitaxel, docetaxel and doxorubicin; the antibiotic, thiostrepton; gene therapy (TNF); the flavanoid-like antioxidant, wogonin; toad toxins (bufadienolides) and a licorice root extract, glycyrrhizin **(Souza et al., 2015)**. There are many types of nanocarriers that have been used for the treatment of liver cancer. But, other than NPs, a number of small molecule drugs and monoclonal antibodies are in clinical trials now. All the NP systems currently used for the therapy of liver cancer are characterized by their unique properties **(Surendran et al., 2017)**.

1.6.1. Polymeric nanoparticles

Recently, polymeric nanoparticles, a novel drug delivery system, may be a promising approach for beginning of new era as chemotherapeutic agent to treat liver cancer **(Figure 1.3)**. The main advantages of polymeric nanoparticles include increase in water solubility, reduction of side-effects and toxicity, improvement of pharmacokinetic properties and tissue distribution through the leaky neovasculature and premature lymphatic system of tumor cells, improvement of anti-tumor efficacy of anticancer agents **(Ryu et al., 2012; Greish, 2007; Lu et al., 2012)**. Most polymeric nanoparticles are biodegradable and biocompatible. They demonstrate good potential for surface modification and functionalization with different ligands and provide potent pharmacokinetic control and are suitable for encapsulating and delivering anti-cancer drugs for liver cancer. The most commonly used polymers are poly(lactic-co-glycolic acid), polybutyl cyanoacrylate, poly(caprolactone) etc. Biodegradable materials used for the formulation of nanoparticles provide sustained drug release within the target site over a prolong period of time. In order to prolong the blood circulation and increase tumor accumulation of nanoparticles, few researchers have been proposed for modification of polymer with hydrophilic poly(ethylene glycol) (PEG) **(Liu et al., 2012)**. Various polymeric-based NPs have also been developed to deliver drugs and other therapeutic moieties for the treatment of liver cancer. For example, sorafenib is a tyrosine kinase inhibitor that has recently been proven to be a potential antifibrotic agent. Poly(ethylene glycol)-β-poly(lactic-co-glycolic acid) (PEG-PLGA) copolymers with PLGA were developed recently for the systemic delivery of sorafenib into the fibrotic livers of CCl_4-induced fibrosis mouse models. The results showed decreased alpha-smooth muscle actin (α-SMA) content and collagen production in the liver with significantly shrunken abnormal blood vessels and decreased microvascular density, leading to vessel normalization in fibrotic livers **(Lin et al., 2016)**.

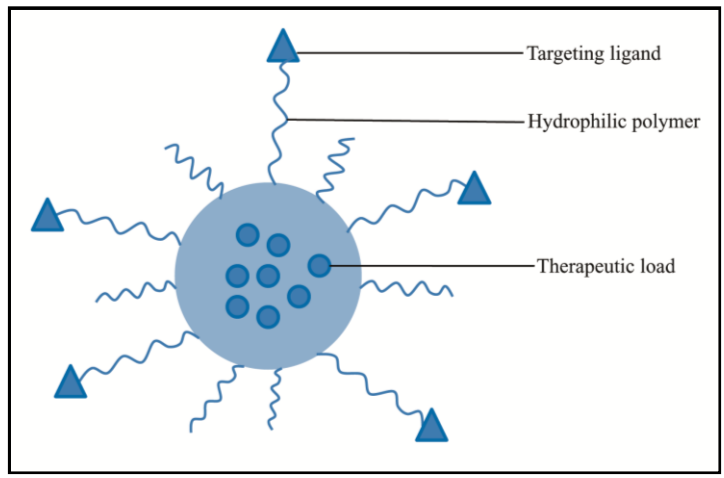

Figure 1.3. Polymeric nanoparticles **(Cerqueira et al., 2015).**

1.6.2. Inorganic nanoparticles

Inorganic nanoparticles have achieved significant attention in the recent years for the treatment of liver cancer due to their distinctive properties such as material- and size-dependent physicochemical properties. These NPs consist of a metal oxide or metal core, which is covered with an organic layer **(Figure 1.4)**. These metal cores give them unique optical, electrical and magnetic properties according to their size and shape. Up to now, the inorganic NPs are in the preclinical stage of studies due to their lack of biocompatible characteristics **(Mudshinge et al., 2011; Anselmo & Mitragotri, 2015; Paul & Sharma, 2010; Giner et al., 2016; Sipai et al., 2012)**. The widely used inorganic NPs for the liver cancer therapy are cerium oxide NPs (CeO_2 NPs), gold NPs and silver NPs **(Hendi, 2011)**. Most of the inorganic NPs are inert in nature **(Tomuleasa et al., 2012)**. Conjugated gold NPs containing thiolterminated PEG-paclitaxel revealed superior properties, including enhanced water solubility, drug loading and targeted drug release inside tumor cells, resulting in an enhanced tumor cell killing ability *in vitro* and tumor therapeutic efficacy in mice bearing liver tumors **(Ding et al., 2013)**. Silica NPs have been also used as drug carriers to improve the treatment of liver tumors. PEGylated silica nanorattle (SN-PEG) loaded with docetaxel (Dtxl; SN-PEG-Dtxl) exhibited high therapeutic efficacy in a murine hepatocarcinoma 22 (H22) subcutaneous model. The average inhibition rate calculated from tumor weight by the SN-PEGDtxl group was 72%, in comparison to the untreated group. Further, SN-PEG-Dtxl showed low toxicity *in vivo* **(Li et al., 2010)**.

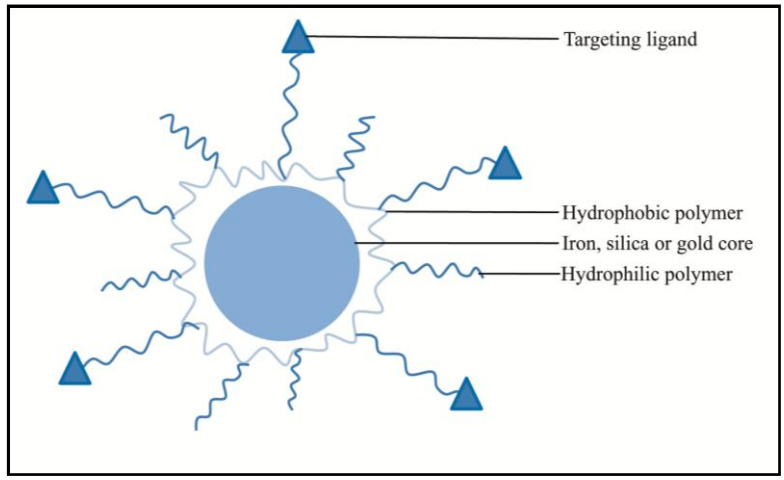

Figure 1.4. Inorganic nanoparticle **(Cerqueira et al., 2015).**

1.6.3. Lipid-based nanoparticles

Lipid-based nanocarriers are the alternative colloidal carrier systems to emulsions, liposomes and polymeric nanoparticles for controlled drug delivery. Lipid nanoparticles have many advantages than other particulate carriers, like good tolerability, biodegradability and high bioavailability. Mainly, two types of lipid nanocarriers such as lipid nanocapsules and solid lipid nanoparticles are used for liver cancer therapy. Lipid nanocapsules are biomimetic carriers that mimic physiological lipoproteins **(Huynh et al., 2009)**. They have size ranges from 20 to 100 nm and are characterized by a hybrid structure between polymer nanocapsules and liposomes. Lipid nanocapsules have an oily core, corresponding to medium-chain triglycerides surrounded by a membrane made from a mixture of lecithin and pegylated surfactant **(Heurtault et al., 2002)**. In the other way, solid lipid nanoparticles are particles made from solid lipid and stabilized by surfactant. Several studies have been carried on lipid nanocapsules and solid lipid nanoparticles which show controlled drug delivery, enhancement of bioavailability of entrapped drugs, improvement of tissue distribution and targeting of drugs. Jimenez et al. **(Jimenez et al., 2015)** examined lipid NPs loaded with siRNA and the results have shown that remarkably down regulated procollagen α I(I) gene expression and, therefore, reduced the total hepatic collagen content, which in turn reduced hepatic fibrosis in carbon tetrachloride $(CCl_4)^-$ induced liver fibrosis in Balb/c mice.

1.6.4. Albumin-based nanoparticles

Albumin is also a natural carrier of endogenous hydrophobic molecules (such as vitamins, hormones and other water-soluble plasma substances), which are bound in a relatively non-specific manner and enhance penetration by albumin receptor-mediated endothelial transcytosis. It is used as the wall material for nanoencapsulation due to biocompatibility and biodegradability. After coating to the anticancer drugs, albumin assists in the transport of the nanoparticles to the interior of the tumor cell that preferentially takes in albumin as a nutrient through the gp60 pathway. Albumin that binds to the therapeutic peptide or protein enhances the stability and efficacy of the anticancer drugs. It also provides controlled delivery and targeting of drugs for liver cancer therapy.

1.6.5. Liposomes

In the recent years, liposome is one of the most promising areas of research interest in both preclinical and clinical stages **(Figure 1.5)**. Liposome can entrap both hydrophilic and hydrophobic drugs and release them in the appropriate target sites. The main advantages of liposomal delivery systems are biocompatibility, biodegradability and low toxicity. However, the low solubility, high cost of production and chance of leakage of drugs are challenging for researchers as well as clinicians **(Akbarzadeh et al., 2013; Toh & Chiu, 2013)**. Various researchers studied the therapeutic potential of dexamethasone-loaded liposomes and it was confirmed that the treatment reduced both liver inflammation and liver fibrosis. The reduction of liver inflammation and fibrosis were due to reduction of T-cells in the liver through an immune reaction **(Bartneck et al., 2015)**. Most of the NP systems for liver fibrosis therapy are in the preclinical stage of study; however, the only type of NPs in the clinical stage of study is liposomal nucleic acid carrier. The gene delivery system of vitamin A-conjugated siRNA lipid NPs is now under clinical Phase I trials for the treatment of hepatic fibrosis. siRNA delivery through PLK-1 targeting lipid particles, as well as double-stranded RNA-encapsulated liposomes, is also now being studied in Phase II and Phase I trials, respectively, for the treatment of HCC. In that study, the successful delivery of siRNA to HSC against gp46 using vitamin A-coupled liposomes resulted in the suppression of

collagen secretion and therefore reduced liver fibrosis in a CCl_4 and bile duct-ligated fibrosis mouse model **(Bansal et al., 2016)**.

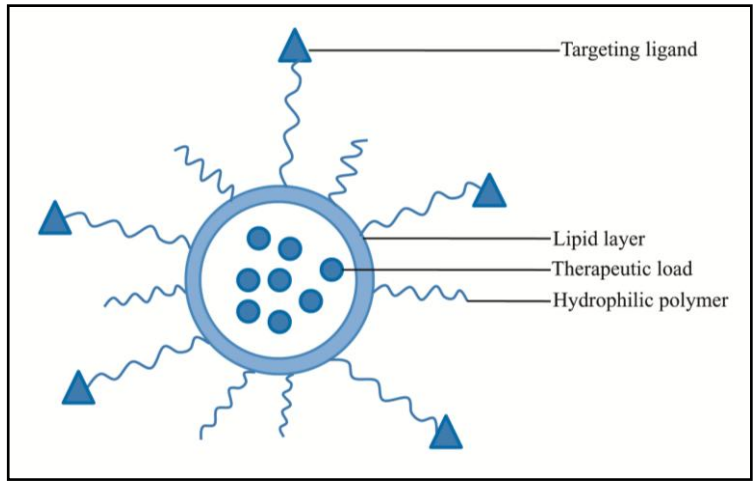

Figure 1.5. Liposome **(Cerqueira et al., 2015).**

1.6.6. Nanomicelles

Nanomicelles with a core-shell architecture composed of a semisolid hydrophobic core which entraps water-insoluble drugs **(Figure 1.6)**. These NPs can be used in wide variety of cancer because most of the anticancer drugs are water insoluble. The stability of entrapped drug will increase and provides effective drug targeting. The size of these NPs is very small. One of the main advantages of polymeric micelles is that stimuli-responsive drug release is possible. Apart from many advantages, these NPs have a number of challenges. The small size of the polymeric micelles limits the drug loading of the particles and there is a long-term stability problem of these NPs **(Movassaghian et al., 2015)**.

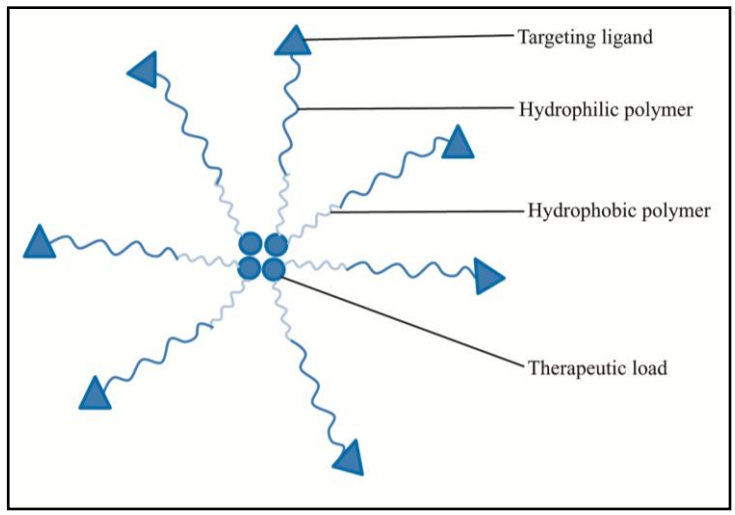

Figure 1.6. Polymeric micelles **(Cerqueira et al., 2015).**

1.7. Methods for preparation of polymeric nanoparticles

1.7.1. Emulsification-solvent evaporation method

The most commonly used method of preparation of polymeric nanoparticles (NPs) preparation is single (oil-in-water (o/w)) or double emulsion solvent evaporation technique (water-in-oil-in-water (w/o/w)). Single emulsion method is conducted for the formulation of hydrophobic drugs (oil soluble); while double emulsion is adopted for the encapsulation of hydrophilic drugs (peptide and protein drugs) **(Ansary et al., 2014)**.

The w/o/w double emulsion solvent evaporation method has been commonly used for NPs preparation due to simple process, convenience in controlling process parameters and ability to produce with inexpensive instrument **(Ruan et al., 2002)**. At first, polymer is dissolved in an organic solvent like dichloromethane (DCM). Other solvents like chloroform, ethyl acetate or methylethyl ketone have also been used. An aqueous solution of hydrophilic drug is added drop-wise in to the polymer solution and the mixture is homogenized by a high speed homogenizer to form w/o emulsion **(Figure 1.7)**. Then, the primary emulsion (w/o) is added gently in to aqueous poly(vinyl alcohol) (PVA) solution with continuous homogenization to form w/o/w double emulsion **(Maji et al., 2014)**. PVA is used as surfactant or stabilizers. The organic solvent is removed by either solvent extraction or solvent evaporation to harden the NPs and the nanoparticles are collected by filtration or centrifugation.

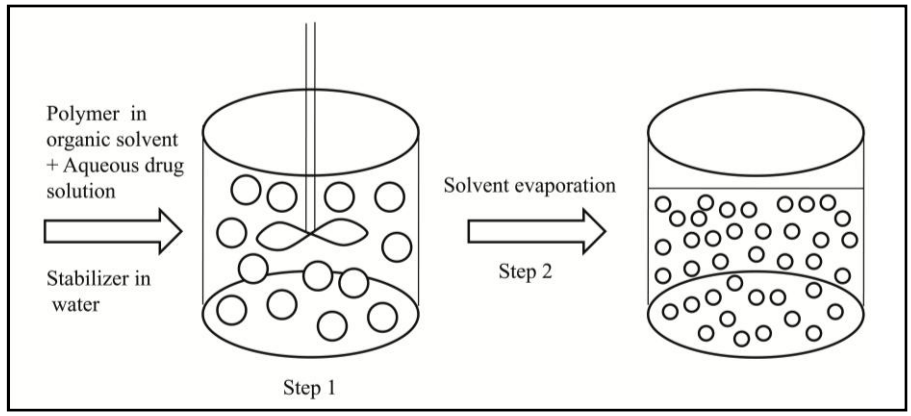

Figure 1.7. Schematic representation of the emulsification-evaporation technique.

1.7.2. Emulsification solvent diffusion (ESD) method

In this method, the polymer(s) and drug are dissolved in an organic solvent and the mixture is emulsified in an aqueous PVA solution by using a high speed homogenizer to form o/w emulsion. Water is then added under constant stirring to the above formed emulsion which cause phase transformation and outward diffusion of the solvent from the internal phase, leading to the nanoprecipitation of the polymer and the formation of colloidal nanoparticles **(Figure 1.8)**. Finally, the solvent can be removed by vacuum steam distillation or evaporation.

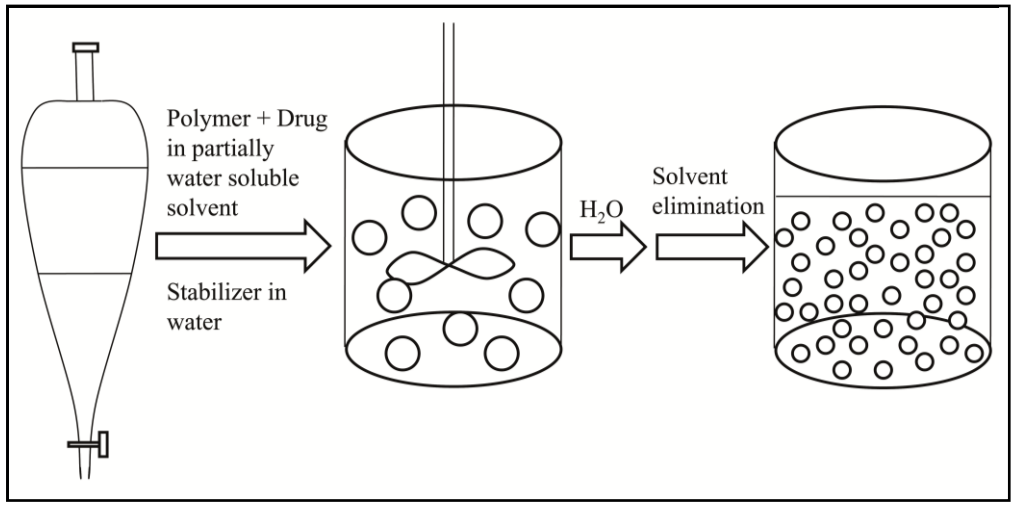

Figure 1.8. Schematic illustration of the ESD technique

1.7.3. Emulsification reverse salting-out method

In this method, initially the polymer is dissolved in a water miscible organic solvent such as tetrahydrofuran (THF) or acetone. Then, the oil phase is emulsified in an aqueous phase containing surfactant and salt of high concentration under strong shearing force by an overhead mechanical stirrer. The most commonly used salts are magnesium chloride hexahydrate or magnesium acetate tetrahydrate with a ratio of 1:3 (polymer to salt) **(Eley et al., 2004)**. The water miscible organic solvents migrate from the oil phase to the aqueous phase resulting in the formation of nanoparticles **(Figure 1.9)**. Finally, the salting out agent is removed by centrifugation.

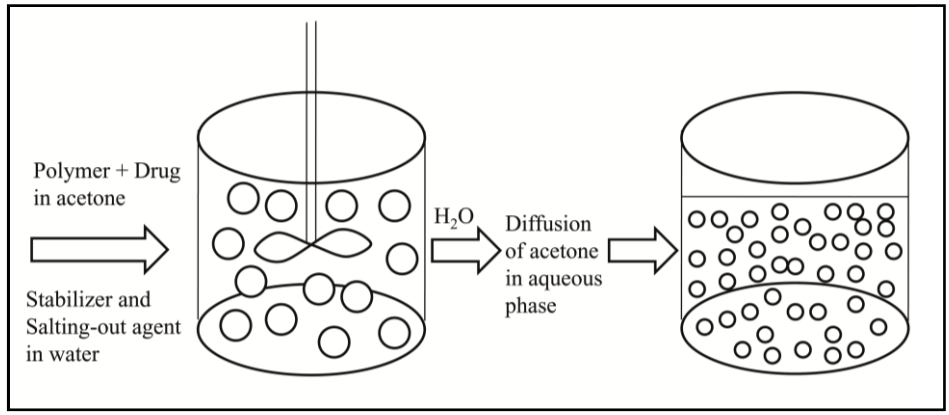

Figure 1.9. Schematic of the salting-out technique

1.7.4. Nanoprecipitation method

Nanoprecipitation or solvent displacement method is a popular technique to prepare nanoparticles due to narrow size distribution, absence of shear stress and absence of surfactants for amphiphilic polymers **(Fessi et al., 1989)**. The polymer and drug are dissolved in a water miscible organic solvent like acetone or methanol. The solution is then added into an aqueous solution of surfactant under continuous magnetic stirring. Particles are formed spontaneously by precipitation and subsequent solidification of the polymer upon rapid solvent diffusion. Finally, the solvents are removed under reduced pressure. The mechanism of formation of NPs by this technique has been explained by the interfacial turbulence generated at the interface of the solvent and non-solvent. Thus, the process is also called solvent displacement or interfacial deposition.

Chapter 2

Aim & Objectives

2. AIM & OBJECTIVES

2.1. Aim of the work

Except surgery, chemotherapy is the main treatment for liver cancer. Its clinical application is restricted due to some limitations such as side-effects like non-specific dose-limiting organ toxicities, short circulating half-life, poor solubility, stability and pharmacokinetic properties and development of drug resistance **(Nag et al., 2016)**. Thus, there is an urgent need to develop some alternative approach to treat liver cancer which can nullify the existing drawbacks. Polymeric nanoparticles, a novel drug delivery system, may be a promising approach for beginning of new era as chemotherapeutic agent to treat liver cancer.

In this work, we have selected paclitaxel as a model drug. PTX is one of the most useful and effective antineoplastic agents for treatment of liver cancer **(Bernabeu et al., 2014)**. It is advantageous to use PTX for the treatment of liver cancer over other drugs owing to its broad spectrum antitumor activity, effectiveness on both solid and disseminated tumors and a unique mechanism of action as it stabilizes the microtubule and selectively disrupts the microtubule dynamics, thus inducing mitotic arrest that leads to cell death. PTX binds with β-tubulin and promotes the assembly of microtubules which prevents microtubular depolymerization and causes cell death **(Priyadarshini & Keerthi, 2012)**. It shows activity against several cancers such as advanced ovarian cancer, breast cancer, lung cancer and liver cancer **(Cho et al., 2015; Danhier et al., 2015)**. There are several reasons for formulation of PTX. Intravenous infusion of paclitaxel is painful and often causes hypersensitive reactions **(Wang et al., 2013)**. Its systemic bioavailability is less than 8% due to low aqueous solubility (0.3 ± 0.02 g/ml). The low solubility is due to its highly lipophilic nature (log P, 3.96) and bulky polycyclic structure (molecular weight 853 Da). The poor oral bioavailability is also attributed to its significant –first-pass" metabolism by cytochrome P450 in liver and p-glycoprotein mediated effluxing by intestinal cells **(Scripture et al., 2006)**. So, it is important to formulate the paclitaxel to avoid such drawbacks. In the recent years, the use of biodegradable nanomaterials has gained impressive attention to bypass those properties for efficacious treatment **(Raza & Sood, 2014)**.

Clinical formulation of PTX (Taxol®) is used with 1:1 mixture of Cremophore EL (polyethoxylated castor oil) and ethanol due to its low aqueous solubility. The solvent is harmful and shows severe toxic effects such as hypersensitivity reactions, nephrotoxicity and neurotoxicity **(Battogtokh et al., 2015; Danhier et al., 2009; Lv et al., 2011)**. Thus, Cremophore EL free formulation of PTX can eliminate the solvent related toxicity, improve stability, bioavailability and present sustained drug release **(Aygul et al., 2013)**.

PTX is very little soluble in water and phosphate buffer. PLGA (85:15) is also very non-polar polymer. Hence drug release from the formulation is very slow. PTX will be formulated to improve the efficacy of the drug and reduce the adverse effects associated with Cremophore EL. The prepared PLGA formulation may have better pharmacokinetic properties. Thus, the aim of the present study is to develop paclitaxel-loaded poly-(D-L-lactide-co-glycolide) nanoparticles for intravenous administration of PTX for prolonged drug release and sustained drug action to successfully treat hepatocellular tumor.

2.2. Objectives of the work

The objectives of the present study are given more precisely below:

- Investigation of drug excipients interaction.
- Preparation of PTX-loaded nanoparticles by emulsification solvent evaporation method.
- Measurement of particle size, shape, morphology by Field Emission Scanning Electron Microscopy (FESEM) and drug distribution and internal morphology of nanoparticles by Transmission electron microscope (TEM).
- Determination of drug loading and drug loading efficiency.
- Study on comparative *in vitro* drug release pattern of different formulations.
- Determination of kinetics of drug release from the prepared nanoparticles.
- Comparison of hydrolytic degradation of nanoparticles at different pH conditions.
- Determination of *in vitro* antitumor efficacy of experimental nanoparticles in comparison to free-drug and Pacliall® by MTT assay method.
- Study on cellular uptake of PTX-loaded nanoparticles by fluorescent microscopy in HepG2 cells lines.
- Determination of lipid peroxidation of formulation in HepG2 cells and normal liver cells.
- Determination of different pharmacokinetic parameters after the administration of PTX-loaded nanoparticles in rats and
- Investigation of deposition of the formulation in rat liver.

Chapter 3

Literature review

3. LITERATURE REVIEW

Worldwide, liver cancer is one of the most common cancers, with a rising incidence. It is increased with age. Surgical resection is one of the most common treatments for liver cancer. Unfortunately, only 10% to 20% of patients undergo surgery due to the advanced stage of the disease at diagnosis **(Sitzmann, 1995 & 1987)**. Liver transplantation is another treatment of liver cancer which can completely resect the tumors and also improve the liver function of the patients. It is the only radical surgical treatment for patients who cannot undergo liver resection. But, metastatic and recurrent tumors significantly reduce the effectiveness of transplantation. **Calne et al. (Calne et al., 1993)** reported that 37.5% of patients died between 2 months to 5 years after surgery due to recurrence of the tumor. The 5 years survival rate is 18.6%. Chemotherapy is the alternative treatment for patients who cannot tolerate surgical resection or bear high risk of recurrence and metastasis after surgery and transplantation. Systemic drugs used in the treatment for cancer are tyrosine kinase inhibitor like sorafenib, anti-angiogenic drugs, MET inhibitors, and immunotherapeutics which are currently under advanced clinical investigation **(Trojan et al., 2016).** However, chemotherapy can control the growth of tumor but, poor targeting, low sensitivity, short circulation half-life, high toxicity restrict its clinical application **(Tang, 2006; Thomas & Zhu, 2005; Wu, 2009)**. Therefore, it is essential to develop newly active and well-tolerated formulations to improve the survival rate of liver cancer patients.

Colloidal drug carriers have attracted great interest in the recent years for administration of anticancer drugs to overcome existing clinical problems.

Zhang et al. (**Zhang et al., 1996)** prepared mitoxantrone loaded polybutyl cyanoacrylate nanoparticles (PBCA-NPs) by the emulsion polymerization method for antineoplastic targeting drug delivery system. They studied surface charge, drug loading, stability, morphology, size, *in vitro* release characteristics and the distribution of drugs in animals for their prepared formulations. After giving i.v. injection of 3H-mitoxantrone PBCA-NPs, they observed that the radioactivity was mainly concentrated in the liver and it was higher in liver tumors than in liver tissue. Finally, the authors suggested that the method of preparation

might be helpful towards increasing the anti-tumor efficacy and decreasing the toxicity of mitoxantrone.

Lacoeuille et al. (Lacoeuille et al., 2007) developed paclitaxel-loaded lipid nanocapsules (PX-LNC) and the biodistribution studies were performed using ^{14}C-trimyristin (^{14}C-TM) or ^{14}C-phosphatidylcholine (^{14}C-PC) whereas antitumoral activity of PX-LNC formulations was based on the animal survival in a chemically induced hepatocellular carcinoma (HCC) model with Wistar rats. They observed that (i) blood concentration-time profiles for both labeled ^{14}C-TM-LNC and ^{14}C-PC-LNC were similar (ii) the $t_{1/2}$ and MRT (mean residence time) values indicated the long circulating properties of the LNC carrier with a slow distribution and elimination phase (iii) survival curves of paclitaxel treated groups showed a statistically significant difference when compared to the control survival curve (iv) animals treated with 4×70 mg/m^2 of PX-LNC showed the most significant increase in mean survival times compared to the controls (IST_{mean} 72%) and cases of long-term survivors were preferentially observed in the PX-LNC treated group (37.5%; 3/8). Finally, they concluded that therapeutic equivalency of the paclitaxel loaded nanocapsules was comparable with classical paclitaxel formulation and PX-LNC exhibited the great advantage in avoiding the use of Cremophor® EL for the solubilization and formulation of paclitaxel.

Qi et al. (Qi et al., 2007) attempted to develop chitosan nanoparticles (CNP) and evaluated the antitumor effects on various cell lines both *in vitro* and *in vivo*. They analyzed cell viability, ultrastructural changes, surface charge, mitochondrial membrane potential, reactive oxygen species (ROS) generation, lipid peroxidation, DNA fragmentation and fatty acid composition by MTT assay, electron microscopy, zetasizer analysis, flow cytometry, spectrophotometric thiobarbituric (TBA) assays, DNA agarose gel electrophoresis and GC/MS respectively. They have also studied the size, body weight and morphologic changes of tumor and liver tissues of mice after oral administration of chitosan, saline, and CNP with different mean particle sizes. CNP showed high antitumor activities with an IC_{50} value of 15.01 μg/ml, 6.19 μg/ml and 0.94 μg/ml after treatment for 24 h, 48 h and 72 h respectively. The tumor growth inhibitory rates on BEL7402 cells in nude mice treated with chitosan and CNP with different mean particle size (40, 70 and 100 nm) were 24.07%, 61.69%, 58.98% and 34.91% with no liver abnormalities. Their results showed a strong antitumor effect of

CNP on human hepatoma cell line BEL7402 both *in vitro* and *in vivo*. Finally, the authors concluded that CNP could be a kind of promising agent for further evaluations in the treatment of HCC.

Again, **Morille et al. (Morille et al., 2009)** developed galactosylated DNA lipid nanocapsules (LNCs), with a size suitable for systemic injection (109±6 nm) for efficient hepatocyte targeting. The LNCs were stabilized by long chains of poly(ethylene glycol) (PEG), which was obtained either from a PEG lipid derivative (DSPE-mPEG 2000) or from an amphiphilic block copolymer (F108). A specific ligand (galactose) was added at the distal end of the PEG chains in order to provide active targeting of the asialoglycoprotein-receptor present on hepatocytes. Their study showed that DNA LNCs were as efficient as positively charged DOTAP (1,2-dioleoyl-3-trimethylammonium-propane)/DOPE (1,2-dioleyl-sn-glycero-3-phosphoethanolamine) lipoplexes for transfection. It was also reported that in primary hepatocytes, non-galactosylate nanocapsules significantly decreased the transfection, probably by creating a barrier around the DNA LNCs. Finally, the authors claimed that galactosylated F108 coated DNA LNCs led to an 18-fold increase in luciferase expression compared to non-galactosylated ones.

Further, **Xu et al. (Xu et al., 2009)** designed and prepared docetaxel-loaded hepatoma-targeted solid lipid nanoparticles (tSLNs) with galactosylated dioleoylphosphatidyl ethanolamine. They studied the cellular cytotoxicity, cellular uptake, subcellular localization, *in vivo* toxicity, therapeutic effect, biodistribution and histology of tSLNs. The cytotoxicity of tSLNs was compared with conventional formulation (Taxotere®) and non-targeted SLNs (nSLNs) against HCC and it was reported that tSLNs was superior to the conventional formulation and non-targeted SLNs. The tSLNs also showed better tolerant and antitumoral efficacy in murine model bearing hepatoma than Taxotere® or nSLNs. The authors claimed that better antitumor efficacy of tSLNs was due to both increased accumulation of drug in tumor and more cellular uptake by hepatoma cells. Targeted nanocarrier of docetaxel can enhance its antitumor effect *in vivo* with low systemic toxicity for the treatment of locally advanced and metastatic HCC.

Tian et al. (Tian et al., 2010) reported a liver-targeted drug delivery nanoparticle (CTS/PEG-GA) composed of poly(ethylene glycol)-glycyrrhetinic acid (PEG-GA) and chitosan (CTS), prepared by ionic gelation process and characterized the nanoparticles both *in vitro* and *in vivo*. Cellular uptake was studied by single-photon emission computed tomography and human hepatic carcinoma cells (QGY-7703 cells). Biodistribution and anti-neoplastic effect of the DOX-loaded nanoparticles were also studied. They also observed that CTS/PEG-GA nanoparticles accumulated extensively in the rat liver cells within a few minutes and maintained a high level (around 50%) even higher than that of the nanoparticles without GA. They found that the DOX-loaded nanoparticles were cytotoxic to human hepatic carcinoma cells (QGY-7703), and the IC_{50} (50% inhibitory concentration) for the free doxorubicin-HCl (DOX-HCl) and the DOX-loaded CTS/PEG-GA nanoparticles were 47 and 79 ng/ml respectively. They claimed that introduction of GA to the nanoparticles could increase the affinity towards human hepatic carcinoma cells significantly and DOX-loaded CTS/PEG-GA nanoparticles showed remarkable cytotoxicity towards QGY-7703 cells. Finally, the authors concluded that DOX-loaded CTS/PEG-GA nanoparticles might be an effective formulation for liver-targeted drug delivery system.

Maeng et al. (Maeng et al., 2010) developed multifunctional doxorubicin loaded superparamagnetic iron oxide nanoparticles (YCC-DOX) which was composed of poly (ethylene oxide)-trimellitic anhydride chloride-folate (PEO-TMA-FA), doxorubicin (DOX), superparamagnetic iron oxide (Fe_3O_4) and folate for chemotherapy and magnetic resonance imaging in liver cancer. They performed the efficacy of the nanoparticles in rats and rabbits with hepatocarcinoma. The authors compared the results with free-DOX (FD) and a commercial liposome drug, DOXIL® and reported that YCC-DOX have anticancer efficacy, thereby increasing the bioavailability and efficacy of DOX. They found that the relative tumor volume was decreased two to four fold. From immunohistochemical analysis, the authors found that YCC-DOX group showed lower expression of CD34 and Ki-67 which are markers for angiogenesis and cell proliferation respectively while apoptotic cells were significantly rich in the YCC-DOX group in terminal deoxynucleotidyl transferase dUTP nick end labeling (TUNEL) assay. Finally, they proposed that YCC-DOX had potential

value for drug delivery therapy and diagnostic imaging in the future nanomedicine to treat human liver cancer and other diseases.

Kang et al. (Kang et al., 2010) developed a novel hepatoma-targeted gene delivery system which was prepared by combining a human liver cell-specific bionanocapsule (BNC) and a tumor cell-specific gene regulation polymer responding to hyperactivated protein kinase Cα in hepatoma cells. They observed that the developed system showed increased transfection efficiency which resulted in cell-specific gene expression in hepatoma cells and tissues (HuH-7) but no gene expression was observed in normal human hepatocytes or human epidermoid tumor cells (A431). The author and co-workers claimed that their system could be a useful method with applications in hepatoma-specific gene therapy and molecular imaging.

Zhou et al. (Zhou et al., 2011) developed albumin-bound paclitaxel nanoparticles for the treatment of hepatocellular carcinoma. They have utilized gene expression profiling on 43 paired HCC tumors and adjacent non-tumoral liver for this study. The authors examined the potential use of microtubule targeting taxane drugs including paclitaxel and docetaxel and compared it with the results obtained from doxorubicin, a common chemotherapeutic agent used in HCC. Their studies showed that drug delivery by nanoparticles have enhanced efficacy with reduced side effects and IC_{50} dose was lowered by 15-fold than paclitaxel alone or the derivative analogue of docetaxel (showed ~450-fold less IC_{50} compared to doxorubicin). They also performed flow cytometric analysis to confirm the cell cycle blockade at G2/M phase and increased apoptosis following nab-paclitaxel treatment. From *in vivo* animal studies, they showed that nab-paclitaxel readily inhibited xenograft growth with less toxicity for host cells compared to other anti-microtubule drugs and doxorubicin. Gene silencing of the microtubule regulatory gene STMN1 by RNAi showed synergistic effect during the combined treatment with nab-paclitaxel. Finally, they concluded that the microtubule assembly might be a promising therapeutic target development for HCC.

Again, **Sha et al. (Sha et al., 2011)** investigated the cytotoxicity of titanium dioxide nanoparticles (TiO_2 NPs) *in vitro* using four liver cell lines such as, human hepatocellular carcinoma cell line (SMMC-7721), human liver cell line (HL-7702), rat hepatocarcinoma

cell line (CBRH-7919) and rat liver cell line (BRL-3A). They checked cell viability, cell morphology and levels of reactive oxygen species (ROS) and glutathione (GSH) after TiO_2 exposure with different concentrations (0.1-100 μg/ml) and for different rate of exposure (12-48 h). They found that four cell lines exposed to TiO_2 NPs showed cytotoxicity in a dose-dependent and time-dependent manner after comparing with NP-free control. They also found that carcinomatous liver cells and human liver cells exhibited more tolerance towards TiO_2 NPs exposure for 24 h as compared to normal liver cells and rat liver cells. Their results suggested that *in vitro* cytotoxicity induced by NPs should be assessed with great caution before the use of nanocomposites and that there was a need to standardize the cytotoxicity testing procedure of nanoscale components in composites when using different cell lines.

In another study, **Albarran et al. (Albarran et al., 2011)** developed controlled release IFC-305 (derivative of 6-aminoribofuranosil purine) encapsulated in silica nanoparticles for liver cancer synthesized by sol-gel. They characterized the IFC-silica nanoparticles by Fourier transform infrared spectroscopy (FTIR), X-ray diffraction (XRD), thermal analysis (DTA-TGA), transmission electron microscopy (TEM), and N_2 adsorption-desorption isotherms (BET). They claimed that the slow release rate was obtained due to strong carboxylic acid-amine interactions. They proposed that the rate of drug release was a combination of dissolution and diffusion processes and the release rates could be controlled by the internal structure of the particles for a desired diffusion profile. Finally, they concluded that IFC-silica nanoparticles could be used for liver targeted drug delivery reservoirs.

Cao et al. (Cao et al., 2011) synthesized and characterized two di-block copolymers (PEI-PCL) of poly(ε-caprolactone) (PCL) and linear poly(ethylene imine) (PEI) and assembled them to biodegradable nanocarriers for co-delivery of BCL-2 siRNA and doxorubicin (DOX) to observe synergistic effect. They used folic acid as a tumor-targeting ligand which was conjugated to the polyanion, poly(ethylene glycol)-block-poly(glutamic acid) (FA-PEG-PGA). FA-PEG-PGA was coated onto the surface of the prepared nanoparticles which potentiate a ligand-directed delivery to human hepatic cancer cells Bel-7402. They observed that at certain N/P to C/N ratios (N/P: PEI-PCL nitrogen to siRNA phosphate; C/N: FA-PEG-PGA carboxyl to PEI-PCL amine), the nanoparticles showed high transfection efficiency and controlled drug release. They also found that folate-targeted delivery of BCL-2 siRNA

showed better gene suppression at BCL-2 mRNA and protein expression levels, inducing cancer cell apoptosis and improving the therapeutic efficacy of the co-administered DOX compared to non-specific delivery. Finally, they claimed that their results showed potential hierarchical nano-assembly as a facile nano-platform for siRNA and hydrophobic drug co-delivery in biomedical applications.

Again, **Qin et al. (Qin et al., 2012)** prepared carboxylated polyethylene glycol-polylactide block copolymer based brucine immuno-nanoparticles (BINPs) for HCC. They performed *in vitro* studies for evaluation of size, shape, zeta potential, drug loading, encapsulation efficiency and release of immune-nanoparticles and also studied targeting, growth, invasion and metastasis inhibitory effects of these nanoparticles on liver cancer cells (SMMC-7721). After comparing with conventional brucine formulation and brucine nanoparticles, the authors reported that BINPs had higher tumor specific cell targeting effect, more local drug concentration and effectively inhibited cancer cell growth, matrix adhesion, invasion and metastasis. Finally, the authors suggested that BINPs might be potentially promising anticancer targeting drug for inhibiting the growth, recurrence and metastasis of HCC.

Further, in another study, **Liu et al. (Liu et al., 2012)** developed docetaxel (DOC)-loaded polyethylene glycol-poly(caprolactone) (mPEG-PCL) nanoparticles and characterized the formulations by both *in vitro* and *in vivo*. They claimed that in case of *in vitro* cytotoxicity test, DOC-NPs inhibited the murine hepatic carcinoma cell line H22 in a dose-dependent manner which was similar to commercial formulation of docetaxel (Taxotere®). The *in vivo* biodistribution studies showed that the nanoparticles achieved higher concentration and longer retention in tumors than in non-targeted organs. The *in vivo* antitumor evaluation studies also showed that DOC-NPs significantly inhibited tumor growth. The researchers concluded that high effectiveness and biocompatibility of their simultaneous delivery system might provide a promising approach for future targeted therapy against hepatic carcinoma.

Wang et al. (Wang et al., 2012) prepared and evaluated paclitaxel-loaded poly(lactic-co-glycolic acid) (PLGA) nanoparticle incorporated with galactose-carrying polymer poly(vinyl benzyl lactonamide) (PVLA). They used polyvinyl alcohol (PVA) as co-emulsifier to facilitate the hepatocyte cell targeted delivery of paclitaxel via ligand-receptor mediated

endocytosis. They investigated the presence of PVLA on the particle surface through the change of zeta potential and surface hydrophobicity. They used HepG2 cells for evaluating cellular uptake and cytotoxic activity. The authors observed that presence of PVLA in the nanoparticles led to increased zeta potential, reduced particle surface hydrophobicity, slight promotion of paclitaxel encapsulation efficiency and more homogeneous particle size, whereas excessive PVLA accelerates the burst release. The PVLA incorporated nanoparticles with enhanced attachment and cellular uptake efficiency, exhibited significant cytotoxicity to HepG2 cells. They have also been found that the nanoparticles with higher PVLA-to-PLGA ratio showed much higher cytotoxicity due to the larger drug capacity and faster release rate. Lastly, they concluded that PVLA incorporated paclitaxel-loaded nanoparticles could enhance the anti-tumor efficiency of paclitaxel by facilitating the drug targeting to the hepatocyte cells and alleviating the elimination in the course of transport.

Guan et al. (Guan et al., 2012), synthesized N-trimethyl chitosan (TMC) and prepared lactosyl-norcantharidin TMC nanoparticles (Lac-NCTD-TMC-NPs) using an ionic cross-linkage process. They observed that average particle size of Lac-NCTD-TMC-NPs was 120.6 ± 1.7 nm with an entrapment efficiency of 69.29% ± 0.76%, drug-loading amount of 9.1% ± 0.07%, sustained *in vitro* drug release and the half-maximum inhibiting concentration (IC_{50}) of 24.2%. After comparing with chitosan free Lac-NCTD, they found that Lac-NCTD-CS-NPs showed strong antitumor activity on the murine hepatocarcinoma 22 subcutaneous model.

Wang et al. (Wang et al., 2012) designed a monoclonal antibody-conjugated gene nanocomplex for targeted therapy of HCC to enhance tumor targeting abilities and therapeutic efficiency. The authors used biodegradable cationic polyethylenimine-grafted-α,β-poly(N-3-hydroxypropyl)-DL-aspartamide (PHPA-PEI) for complexing pDNA to form the PHPA-PEI/pDNA nanoparticle and 9B9 mAb, an anti-epidermal growth factor receptor (anti-EGFR) monoclonal antibody for conjugation to produce the PHPA-PEI/pDNA/9B9 mAb (PP9mN) complex. The authors performed *in vitro* studies which showed that the PP9mN complex was highly efficient in gene delivery to the HCC whereas in case of *in vivo* studies, PP9mN could target the tumor tissue effectively. Finally, they proposed that

monoclonal antibody-conjugated gene complex might be a safe and effective delivery agent for liver cancer gene therapy.

Yu et al. (Yu et al., 2012) designed and synthesized lipid nanoparticles (LNPs) for siRNA delivery, based on cationic lipids, with multiple tertiary amines and hydrophobic linoleyl chains. LNPs named TRENL3 which contains tris-(2-aminoethyl) amine (TREN) and 3-linoleyl chains showed high siRNA transfection efficacy that was markedly superior to lipofectamine. They reported that incorporating of linoleic acid and linolenic acid in the formulation further enhanced the siRNA delivery efficiency. They concluded that the new LNPs have shown preferential uptake by the liver and hepatocellular carcinoma in mice, thereby leading to high siRNA gene-silencing activity might serve as valuable nanocarriers for *in vivo* targeting and siRNA therapeutic for use in liver diseases.

Bao et al. (Bao et al., 2014) developed a combinative drug delivery system of two drug delivery strategies in one system that composed of organic and inorganic materials. In their work, gold nanoparticles (GNPs) and liposomes had taken to observe the performance of Paclitaxel (PTX) in tumor therapy. They observed that the hybrid liposomes resolved the solubility and stability problems of gold conjugates and produced high drug loading capacity and sustained drug release behavior. The authors also observed that, the stability and liver targeting performance of hybrid liposomes was higher than Taxol$^{(R)}$ and gold conjugates before the protection by liposomes. At last, the authors concluded that the improved circulation longevity and liver targetability not only afforded the hybrid liposomes better antitumor treatment efficacy in the tumor bearing mice, but also provided a great possibility to develop a super long-acting drug delivery system of antineoplastics.

In a study, **Gao et al. (Gao et al., 2015),** formulated sorafenib in C-X-C receptor type 4 (CXCR4)-targeted lipid-coated poly(lactic-coglycolic acid) (PLGA) nanoparticles for hepatocellular carcinoma treatment. The authors reported that AMD3100 attached to the sorafenib-loaded CXCR4-targeted NPs could block CXCR4/Stromal-derived factor 1α (SDF1α) and produced reduction of tumor-associated macrophages, enhancement of anti-angiogenic effect, delayed in tumor progression and increased overall survival in the orthotopic HCC model compared with other control groups. The authors claimed that their

results highlighted the clinical potential of CXCR4-targeted NPs for delivering sorafenib and overcoming acquired drug resistance in liver cancer.

Qi et al. (Qi et al., 2015) prepared doxorubicin (DOX) loaded glycyrrhetinic acid-modified recombinant human serum albumin nanoparticles (DOX/GA-rHSA NPs) for liver cancer targeting therapy. The formulated NPs showed spherical particle of 170 nm size and high stability in plasma with negative zeta potential. The encapsulation efficiency of the NPs was 75.8%. The authors also reported that the targeted NPs produced higher cytotoxic activity and cellular uptake in liver tumor cells than the non-targeted NPs. Biodistribution study showed that DOX/GA-rHSA NPs exhibited a much higher level of tumor accumulation than non-targeted NPs after certain time point. The authors finally suggested that the DOX/GA-rHSA NPs could be considered as an efficient nanoplatform for targeting drug delivery system for liver cancer.

Di-Wen et al. (Di-Wen et al., 2016) also studied epirubicin-loaded CXCR4-targeted nanoparticles composed of PLGA/TPGS (D-α-Tocopheryl polyethylene glycol succinate) and the surface of nanoparticle was conjugated with LFC131 peptide. They reported that the nanoparticle had size less than 150 nm, sustained drug release kinetics, higher affinity to HepG2 cells and 3-fold improvement in cellular uptake than non-targeted one. *In vivo* study showed that the nanoparticles distributed mostly in the xenograft tumor and remained in the blood for at least 24 h. Their results suggested that CX-EPNP could effectively inhibit the growth of liver tumors *in situ* and could potentially reduce the systemic side effects.

Loutfy et al. (Loutfy et al., 2016) synthesized water-soluble chitosan nanoparticles (CS-NPs) and evaluated their properties using transmission electron microscopy (TEM), Fourier transform infrared spectroscopy (FT-IR) and zeta analysis. The cytotoxic effects of the CS-NPs on HepG2 cells were conducted by sulforhodamine B colorimetric assays for cytotoxicity screening and flow cytometric analysis. The authors also conducted molecular investigations including DNA fragmentation and the expression of some apoptotic genes on the transcriptional RNA level. They reported that after 24 h of HepG2 cell exposure with different concentrations of 150 nm diameter CS-NPs did not show any alteration of cell morphology but, after 48 h of cell exposure with 100 μg/ml of CS-NPs showed 12% of cell

death with IC_{50} value of 239 μg/ml. They found that flow cytometry analysis produced mild accumulation of NPs in the G2/M phase followed by cellular DNA fragmentation after 48 h of cell exposure. Extensive evaluation of the cytotoxic effect of the CS-NPs showed messenger RNA (mRNA) apoptotic gene expression (p53, Bak, Caspase3) after 24 h of cell exposure with no expression of the mRNA of the caspase 3 gene after 48 h of cell exposure. Finally, the authors suggested that CS-NPs were effective against liver cancer cells at a concentration of 100 μg/ml.

Again, **Marakby et al. (Marakby et al., 2017)** developed valeric acid modified chitosan nanoparticles for the delivery and liver-targeting of a natural chemotherapeutic agent like Ferulic acid. They characterized the modified nanoparticles for particle size, PDI and zeta potential and subjected to *ex-vivo* stability study in serum and cytotoxicity studies in HepG2 cell lines. The nanoparticles were also surface-decorated with glycyrrhizin for active liver targeting. The authors observed that *in vivo* biodistribution study showed highest accumulation (13.34% ID/g) of the glycyrrhizin containing nanoparticles in liver than the drug solution and glycyrrhizin free nanoparticles after 6 h. Their results suggested that the proposed selected system could be efficiently utilized as a successful platform for targeting a natural chemotherapeutic agent viz. ferulic acid to the liver.

Further, **Zhang et al. (Zhang et al., 2017)** prepared Bufalin-loaded bovine serum albumin nanoparticle by desolvation method and evaluated *in vitro* and *in vivo*. The authors observed that, (i) the average particle size of NPs was 125.1 nm with sustained drug release behavior, (ii) the uptake of liver for Bufalin NPs was 352.045 ± 35.665 ng/g while for Bufalin was 164.465 ± 48.080 ng/g ($P < 0.01$) at 5 min, (iii) the uptake of tumor for Bufalin NPs was significantly higher than that of Bufalin both at 5 min (50.169 ± 11.708 ng/g, 93.415±13.828 ng/g, $P < 0.01$) and 15 min (43.683 ± 11.499 ng/g, 64.219 ± 17.684 ng/g, $P > 0.05$), (iv) both had similar antitumor activity *in vitro* and finally, (v) pharmacokinetics study showed that the half-life, blood plasma area under the curve and apparent volume of distribution of Bufalin NPs group were higher than that of Bufalin treated group, whereas the clearance rate was lower than Bufalin group. Lastly, the authors concluded that, Bufalin-loaded bovine serum albumin nanoparticle was a promising liver-targeted drug delivery system with higher liver uptake and stronger antitumor activity against hepatocellular carcinoma.

Several researchers studied the gene therapy to overcome the poor responses and toxicity associated with standard treatments. **Zamboni et al. (Zamboni et al., 2017)** developed and evaluated non-viral strategy for effective and cancer-specific DNA delivery to human HCC using biodegradable poly(beta-amino ester) (PBAE) nanoparticles (NPs). They reported that the polymeric NPs, composed of 2-((3-aminopropyl) amino) ethanol end-modified poly(1,5-pentanediol diacrylate-co-3-amino-1-propanol) (_536‘) at a 25 polymer-to-DNA weight-to-weight ratio led to high transfection efficacy to all of the liver cancer lines, but not to hepatocytes. It has also been reported that each individual HCC line had a significantly higher percentage of exogenous gene expression than the healthy liver cells. The authors suggested that the biodegradable end-modified PBAE gene delivery vector was not cytotoxic and maintained the viability of hepatocytes above 80%. The *in vivo* study confirmed an effective DNA transfection. Finally, the researchers concluded that PBAE-based NPs might be a promising technology to deliver therapeutic genes to liver cancer.

In a study, **Wang et al. (Wang et al., 2018)** developed and evaluated paclitaxel-loaded poly(ethylene oxide)-b-poly(butylene oxide) (PEO-PBO) nanoparticles for tumour targeting. Their results showed that the size of the nanoparticles was about 92.71 nm and the zeta potential was −5.06 mV. The authors also reported that the PEO-PBO nanoparticles showed superior pharmacokinetic, biodistribution and tumor inhibitory properties than commonly used block copolymer poly(ethylene glycol)-b-poly-D,L-(lactic acid) (PEG-PDLLA). They found that the PEO-PBONPs had excellent biocompatibility and antitumor efficacy. The researchers concluded that PEO-PBO was promising novel polymeric materials with potential application in liver cancer.

Further, **Wang et al. (Wang et al., 2018)** established doxorubicin (DOX) loaded hyaluronic acid-glycyrrhetinic acid succinate (HSG) conjugates based nanoparticles (HSG/DOX nanoparticles) for liver-targeted therapy. The researchers reported that the nanoparticles were sub-spherical in shape with particle size in the range of 180–280 nm, the drug loading was dependent on drug-to-carrier ratio and GA graft ratio and *in vitro* drug release was in sustained manner. Pharmacokinetics study demonstrated the HSG/DOX nanoparticles could prolong blood circulation time of DOX and had a higher AUC value than that of DOX solution. The authors also reported that biodistribution of HSG/DOX nanoparticles increased

the accumulation and decreased the cardiotoxicity and nephrotoxicity of DOX. The accumulation of HSG-20/DOX, HSG-12/DOX and HSG-6/DOX nanoparticles in the liver was 4.0-, 3.1-, and 2.6-fold higher than that of DOX solution. Their results suggested that HSG conjugates prepared via modifying the hydroxyl groups of HA had promising potential as a liver targeting nanocarrier for the delivery of hydrophobic anti-tumor drugs.

Chapter 4

Experimental

4. EXPERIMENTAL

4.1. Materials

The drug and various other excipients and reagents used in this work are enlisted in the following **Table 4.1**.

Table 4.1.
Drug, excipients and reagents used in this work

Serial No.	Chemical name	Source
1.	Paclitaxel	Fresenius Kabi Oncology Ltd. Kolkata, India.
2.	Poly-D-L-lactide-co-glycolide (ratio 85:15)	Sigma-Aldrich Co, Mumbai, India.
3.	Polyvinyl alcohol	S.D. Fine Chem. Pvt. Ltd, Mumbai, India.
4.	Dichloromethane	Merck, Mumbai, India.
5.	Potassium dihydrogen phosphate	Merck, Mumbai, India.
6.	Disodium hydrogen phosphate	Merck, Mumbai, India.
7.	Sodium chloride	Merck, Mumbai, India.
8.	Sodium carbonate	Merck, Mumbai, India.
9.	Sodium hydrogen carbonate	Merck, Mumbai, India.
10.	Fluorescein isothiocyanate 98%	HiMedia Laboratories, Mumbai, India.
11.	4', 6-Diamidino-2-phenylindole) (DAPI)	HiMedia Laboratories, Mumbai, India.
12.	3-(4,5-Dimers dimethylthiazol-2-yl)-2,5-diphenyltetrazolium bromide (MTT)	HiMedia Laboratories, Mumbai, India.
13.	Dulbecco‘s Modified Eagle‘s Medium (DMEM) containing fetal bovine serum (FBS) and Minimum Essential Medium (MEM)	HiMedia Laboratories, Mumbai, India.
14.	Antibiotics (1% penicillin streptomycin	HiMedia Laboratories, Mumbai, India.
15.	Pacliall® injection (100 mg vial)	Panacea Biotec Limited, Mumbai, India.

4.2. Profile of drug

4.2.1. Paclitaxel (PTX)

CAS Number: 33069-62-4

Chemical name: 5β,20-Epoxy-1,2α,4,7β,10β,13α-hexahydroxytax-11-en-9-one 4,10-diacetate 2-benzoate 13-ester with (2R,3S)-N-benzoyl-3-phenylisoserine.

Structural formula:

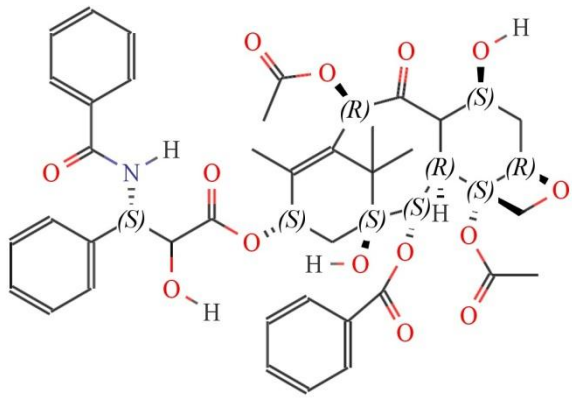

Chemical formula: $C_{47}H_{51}NO_{14}$

Molecular weight: 853.9 Da.

Bioavailability: <8%.

Description: Paclitaxel is obtained by a semi-synthetic process from *Taxus baccata*. It is a white to off-white crystalline powder.

Solubility: Soluble in DMSO at 200 mg/ml; soluble in ethanol at 40 mg/ml; very poorly soluble in water; maximum solubility in plain water is estimated to be about 10-20 µM.

Melting point: 216-217° C

Mechanism of action: PTX binds with β-tubulin and promotes the assembly of microtubules which prevent microtubular depolymerization. Chromosomes are thus unable to achieve a metaphase spindle configuration. This blocks the progression of mitosis and prolonged

activation of the mitotic check-point triggers apoptosis or reversion to the G-phase of the cell cycle without cell division.

Uses: Paclitaxel (PTX) is a powerful anticancer chemotherapeutic agent. It is used to treat different types of cancer such as, ovarian cancer, breast cancer, lung cancer, Kaposi sarcoma, cervical cancer, pancreatic cancer and liver cancer. It is advantageous to use PTX for the treatment of liver cancer over other drugs owing to its broad spectrum antitumor activity, effectiveness on both solid and disseminated tumors and a unique mechanism of action as it stabilizes the microtubule and selectively disrupts the microtubule dynamics, thus inducing mitotic arrest that leads to cell death.

Storage: The drug should be stored the product at 2-8°C and protected from the light.

4.3. Profile of excipients

4.3.1. Poly(D,L-lactide-co-glycolide) (PLGA) 85:15

Synthesis: PLGA is a linear copolymer that can be prepared at various ratios between its constituent monomers, lactic (LA) and glycolic acid (GA).

Chemical structure of poly(lactic-co-glycolic acid) and its monomer:

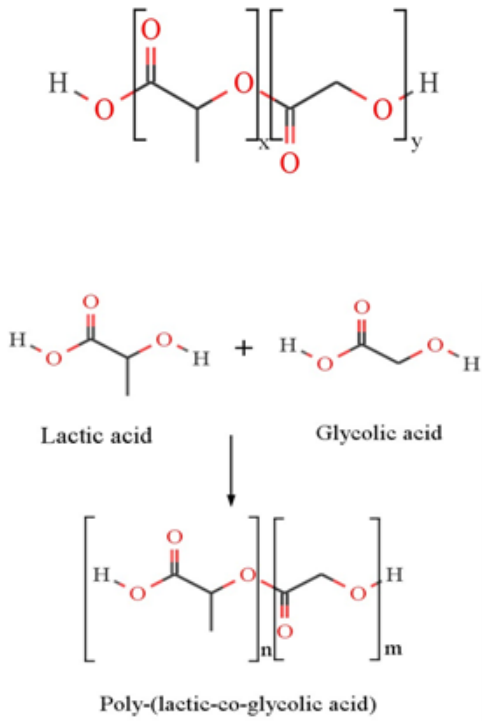

Where n=number of units of lactic acid, m=number of units of glycolic acid.

Molecular weight: 17,000 g/mol.

Crystallinity: Amorphous

Solubility: The polymer is soluble in chlorinated solvents, tetrahydrofuran, acetone or ethyl acetate.

Degradation: There are four steps of PLGA degradation; (i) hydration: water penetrates into the amorphous region and disrupts the van der Waals forces and hydrogen bonds, causing a decrease in the glass

transition temperature (T_g), (ii) initial degradation: cleavage of covalent bonds, with a decrease in the molecular weight, (iii) constant degradation: carboxylic end groups autocatalyze the degradation process and mass loss starts by massive cleavage of the backbone covalent bonds, resulting in loss of integrity and (iv) solubilization: the fragments are further cleaved to molecules that are soluble in the aqueous environment.

Use: PLGA is used as biodegradable polymers for the development of nanocarrier because it undergoes hydrolysis in the body to produce the biodegradable metabolite monomers, lactic acid and glycolic acid. These monomers are metabolized in the body via Krebs cycle and removed as carbon dioxide and water which result minimal systemic toxicity.

Storage: The polymer should be stored in a cool and dry place.

4.3.2. Polyvinyl alcohol (PVA)

CAS Number:	9002-89-5
Chemical formula:	$(C_2H_4O)_x$
Description:	Polyvinyl alcohol is a synthetic resin prepared by the polymerization of vinyl acetate, followed by partial hydrolysis of the ester in the presence of an alkaline catalyst. It is odourless, translucent, white or cream-coloured granular powder.
Molecular weight:	44.053 g/mol.
Melting point:	200°C
Solubility:	The polymer is soluble in water and sparingly soluble in ethanol.
Uses:	PVA is a well-known hydrophilic polymer usually acts as stabilizer. Although PVA has hydrophilic –OH group, it has also a nonpolar vinyl part. Thus, it reduces the surface tension between the aqueous part and the nonpolar non-aqueous part, where vinyl group remains towards non-polar part and OH-group faces towards aqueous part. Thus, it stabilizes primary emulsion. Other uses of polyvinyl alcohol include: (i) paper adhesive with boric acid in spiral tube winding and solid board production, (ii) thickener, modifier, in polyvinyl acetate glues, (iii) as a surfactant for the formation of polymer encapsulated nanobeads etc.
Storage:	The polymer should be stored in a cool and dry place.

4.4. Instruments and equipments

Various instruments/equipments used in this work are enlisted in the following Table 4.2.

Table 4.2.
List of instruments/equipments used.

Serial No.	Name and Make/model	Availed at
1.	High speed homogenizer, IKA Laboratory Equipment, Model T10B Ultra-Turrax, Staufen, Germany.	Department of Pharmaceutical Technology, Jadavpur University, Kolkata.
2.	Cold centrifuge, 3K30 Sigma Lab Centrifuge, Merrington Hall Farm, Shrewsbury, UK.	Department of Pharmaceutical Technology, Jadavpur University, Kolkata.
3.	Freeze dryer, Laboratory Freeze Dryer, Instrumentation India Ltd., Kolkata, India.	Department of Pharmaceutical Technology, Jadavpur University, Kolkata.
4.	Fourier transform infrared spectroscopy, Perkin-Elmer RX-1, USA.	Department of Inorganic Chemistry, Jadavpur University, Kolkata.
5.	UV-visible spectrophotometer, Advanced Microprocessor UV-Visible single beam, Intech 295, AP, India.	Department of Pharmaceutical Technology, Jadavpur University, Kolkata.
6.	Liquid chromatography-Mass Spectrophotometer, LC: Shimadzu Model 20AC, MS: AB-SCIEX, Model: API4000, Software: Analyst 1.6.	Department of Pharmaceutical Technology, Jadavpur University, Kolkata.
7.	Particle size analyzer, Zetasizer Nano ZS 90, Malvern Instruments, Malvern, UK.	Department of Pharmaceutical Technology, Jadavpur University, Kolkata.
8.	Bath sonicator, Trans-o-sonic, Mumbai, India.	Department of Pharmaceutical Technology, Jadavpur University, Kolkata.
9.	Fluorescent microscope, Carl Zeiss, Oberkochen, Germany.	School of Medical Science and Technology, Indian Institute of Technology, Kharagpur.

10.	Digital balance, Sartorius, Goettingen, Germany.	Department of Pharmaceutical Technology, Jadavpur University, Kolkata.
11.	Deep freeze (-80°C), New Brunswick Scientific, U410, Swedesboro, USA.	Department of Pharmaceutical Technology, Jadavpur University, Kolkata.
12.	Magnetic stirrer, Remi Equipments, Mumbai, India.	Department of Pharmaceutical Technology, Jadavpur University, Kolkata.
13.	Field emission scanning electron microscope, JEOL JSM 6700 F, JEOL, Tokyo, Japan.	Indian Association for Cultivation of Science, Kolkata.
14.	Transmission electron microscope, FEI type FP5018/40 Tecnai G2 Spirit Bio TWIN.	Indian Association for Cultivation of Science, Kolkata.
15.	pH meter, Toshniwal Inst. Mfg. Pvt. Ltd., Ajmer, India.	Department of Pharmaceutical Technology, Jadavpur University, Kolkata.

4.5. Methodology

4.5.1. Preparation of calibration curve of paclitaxel in phosphate buffered saline (PBS) containing 0.5% (w/v) sodium lauryl sulphate (SLS)

Preparation of PBS, pH 7.4

Phosphate buffer saline, pH 7.4 was prepared as per the formula mentioned in Indian Pharmacopoeia (volume 1). According to above formula, NaCl 0.8 g, Na_2HPO_4 0.238 g and KH_2PO_4 0.019 g were taken in a 100 ml volumetric flask and dissolved with double distilled water. The solution was sonicated for some time using a bath sonicator and pH was adjusted to 7.4. Finally, volume was made up to the mark. After that 0.5 g of SLS was added into the above prepared PBS and ultrasonicated for 5 min using a bath sonicator to dissolve properly.

Determination of absorption maxima (λ_{max}) of PTX in PBS containing 0.5% (w/v) SLS

A solution of PTX (10 µg/ml) in PBS containing 0.5% (w/v) SLS was scanned from wavelength 200 nm to 400 nm in UV/VIS spectrophotometer by using PBS, pH 7.4 containing 0.5% (w/v) SLS with reference to PBS, pH 7.4 containing 0.5% (w/v) SLS as blank solution.

Preparation of standard curve for drug loading study

A stock PTX solution of 100 µg/ml was prepared by adding 10 mg PTX in 100 ml water-acetonitrile mixture (HPLC grade) in ratio of 40:60 in a borosilicate glass volumetric flask followed by ultrasonication for about 2 min for complete dissolution of PTX in the solvent. From this stock solution, different volumes, 0.2 ml, 0.5 ml, 1.0 ml, 1.5 ml, 2.0 ml and 2.5 ml were withdrawn and diluted with water-acetonitrile mixture to 10.0 ml to obtain five different solutions having different concentrations of PTX, namely 2 µg/ml, 5 µg/ml, 10 µg/ml, 15 µg/ml, 20 µg/ml and 25 µg/ml. Absorbance of each solution was measured using UV-visible spectrophotometer against water-acetonitrile mixture as blank, at 218 nm.

Preparation of standard curve for drug release study

To make a stock solution of PTX (100 µg/ml), 10 mg of drug was taken in a 100 ml volumetric flask. Then 100 ml of PBS, pH 7.4 containing 0.5% (w/v) SLS was added and ultrasonicated for about 10 min for complete dissolution of PTX in PBS. From this stock

solution, various volumes 0.2 ml, 0.5 ml, 1.0 ml, 1.5 ml, 2.0 ml and 2.5 ml were placed in five different 10 ml volumetric flasks and diluted with PBS, pH 7.4 containing 0.5% (w/v) SLS to obtain concentrations of PTX namely, 2 μg/ml, 5 μg/ml, 10 μg/ml, 15 μg/ml, 20 μg/ml and 25 μg/ml. Absorbance of individual solution was measured using UV-visible spectrophotometer against PBS, pH 7.4 containing 0.5% (w/v) SLS as blank, at 218 nm.

4.5.2. Preparation of buffers for hydrolytic stability study

Preparation of citrate buffer pH 3.0 and pH 5.0

A solution of 1.134 g of citric acid and 1.204 g of sodium citrate dihydrate was prepared with 80 ml of double distilled water in 100 ml volumetric flask. Adjust the desired pH (pH 3.0 or 5.0) using hydrochloric acid or sodium hydroxide. Finally, the volume was made up to 100 ml with double distilled water.

Preparation of bicarbonate buffer pH 9.2

A solution of 0.105 g of sodium bicarbonate and 0.927 g of sodium carbonate (anhydrous) was prepared with 80 ml of double distilled water in 100 ml volumetric flask. Finally, the volume was made up to 100 ml with double distilled water.

4.5.3. Fourier transform infrared spectroscopy (FTIR)

FTIR (Perkin-Elmer RX-1, USA) was carried out to observe infrared spectra of pure drug (paclitaxel), PLGA, PVA, their physical mixture, blank formulation and prepared nanoparticles. During analysis, sample was mixed with potassium bromide in the ratio of 1:100 and compressed into pellets using a hydraulic press at 5.5 metric ton pressure. The pellets were scanned with FTIR spectroscope in a range of 4000–400 cm^{-1}. The spectra were recorded as % transmittance (ordinate) against wave number (abscissa).

4.5.4. Differential scanning calorimetry (DSC) study

The physical state of PTX and PTX in PTX-loaded PLGA nanoparticles were investigated by differential scanning calorimetry (Jade DSC, Perkin Elmer, Japan). The samples were weighed from 1.18 to 2.784 mg and heated at a scanning rate of 10°C min^{-1} under dry

nitrogen flow at 20 ml/min over a temperature range of 32°C to 310°C **(Mandal et al., 2010)**.

4.5.5. Preparation of nanoparticles

Paclitaxel-loaded PLGA nanoparticles were prepared using multiple-emulsion solvent evaporation method **(Mosafer et al., 2017; Maji et al., 2014)**. In the first step, 2.5% (w/v) and 1.5% (w/v) aqueous solutions of PVA were prepared separately. After that, an organic solution of drug and PLGA was prepared in dichloromethane (2 ml). The amounts of drug and polymer used for various formulations were shown later in **Table 5.3**. Previously prepared 0.5 ml of 2.5% PVA solution was added drop-wise into the drug-polymer mixture and homogenized at 20,000 rpm with a high speed homogenizer (IKA Laboratory Equipment, Model T10B Ultra-Turrax, Staufen, Germany) for 5 min at room temperature and primary emulsion was formed (water-in-oil). This primary emulsion was then added drop-wise into 75 ml of 1.5% PVA solution with constant homogenization at 20,000 rpm for 8 min. PVA is a well-known hydrophilic polymer usually acts as stabilizer **(Ibraheem et al., 2014)**. Although PVA has hydrophilic –OH group, it has also a nonpolar vinyl part. Thus, it reduces the surface tension between the aqueous part and the nonpolar non-aqueous part, where vinyl group remains towards non-polar part and OH-group faces towards aqueous part. Thus, it stabilizes primary emulsion. The resulting mixture was stirred overnight using a magnetic stirrer for removal of organic solvent. The nanoparticles were then separated by centrifugation using a cold centrifuge (3K30 Sigma Lab Centrifuge, Merrington Hall Farm, Shrewsbury, UK) at 15,000 rpm for 45 min and washed three times with double distilled water at the same speed for removal of free drug and PVA. The separated nanoparticles were poured in a petridish and kept it at −40°C overnight. Then the frozen nanoparticles were lyophilized using freeze dryer (Laboratory Freeze Dryer, Instrumentation India Ltd., Kolkata, India) for 8 h. This method has been well-standardized with PVA as stabilizer. In this method, no other cryoprotectant (such as sucrose) was required. Cryoprotectants (such as sucrose, lactose, manitol) mostly function because of the presence of number of poly hydroxyl group. In PVA, there is also the presence of number of hydroxyl group, owing to which it could have acted as cryoprotectant by itself. Finally, the product was collected and kept in an air tight container at 4°C. We have prepared nanoparticle formulation without drug

using the same procedure as discussed above. Fluorescent nanoparticles of PTX were also prepared to visualize the distribution of nanoparticles in the cancer cells. FITC-stock solution was prepared by dissolving FITC in ethanol:chloroform (1:3 ratio). During emulsification, 100 µl of this solution was added into the organic phase of drug-polymer mixture and all other steps were same as mentioned above.

4.5.6. Physicochemical characterization of nanoparticles

Drug loading and loading efficiency

Drug loading was carried out to identify the amount of drug entrapped in the experimental formulations. The required amount of nanoparticles (2 mg) was suspended with 2 ml of water-acetonitrile mixture (40:60 v/v). The mixture was vortexed for 5 min followed by shaking in an incubator shaker for 3–4 h at 37°C. Finally, it was centrifuged at 10,000 rpm for 5 min and the supernatant was collected. After appropriate dilution, the absorbance was measured spectrophotometrically at 218 nm. The same procedure was also followed for blank formulation and absorbance was measured. The actual amount of drug present in nanoparticles was calculated from the difference between the absorbance of nanoparticle formulation and blank formulation. The percentage of actual drug loading and loading efficiency were calculated using the following equations:

$$\text{Percentage of actual drug loading} = \frac{\text{Amount of drug present in nanoparticles}}{\text{Weight of nanoparticle sample analyzed}} \times 100$$

$$\text{Percentage of loading efficiency} = \frac{\text{Actual drug loading}}{\text{Theoretical drug loading}} \times 100$$

Yield percentage

The amount of nanoparticles obtained was determined with respect to the total amount of raw materials used for the formulation. The lyophilized nanoparticles were weighed and the percentage yield of the formulations was calculated by using the following formula:

$$\text{Percentage yield} = \frac{\text{Amount of nanoparticles obtained}}{\text{Total amount of drug and polymer used}} \times 100$$

Particle size, size distribution and zeta potential

The particle size distribution of nanoparticles is important to understand size range of the particles. Zeta potential is the measurement of surface charges of nanoparticles which implies the stability of colloidal dispersion. Average particle size, size distribution and zeta potential of paclitaxel-loaded PLGA nanoparticles were studied by dynamic light scattering technique (Zetasizer Nano ZS90, Malvern Instrument, Malvern, UK). The analysis was performed at 25°C with scattering angle of 90°. Samples were dispersed with Milli-Q water before observation **(Maji et al., 2014)**.

Surface morphology by field emission scanning electron microscopy (FESEM)

Surface morphology of the nanoparticles was analyzed using field emission scanning electron microscope (Model-JSM-6700F; JEOL, Tokyo, Japan). The samples were coated with platinum under vacuum for 6 min before observation **(Ghosh et al., 2017)**.

Transmission electron microscopy (TEM)

Drug distribution and internal morphology of nanoparticles were determined by transmission electron microscope (FEI type FP5018/40 Tecnai G2 Spirit Bio twin, Praha, Czech Republic). Small amount of nanoparticles were uniformly distributed in Milli-Q water and a drop was placed on a carbon coated grid. The grid was then air-dried overnight and examined using TEM.

4.5.7. In vitro drug release and release kinetics

In vitro drug release study was carried out in phosphate-buffered saline (PBS), pH 7.4 containing 0.5% sodium lauryl sulfate **(Acharya & Reddy, 2016)** to check the release of the drug from the formulations. To see the drug release, we have taken 5 mg of the prepared nanoparticles in a microcentrifuge tube containing 2 ml of release medium. The tube was placed in an incubator shaker at 37°C. At different time intervals (0.5, 2, 4, 6, 8, 24, 48, 72, 168, 360, 528 and 720 h), the tube was removed from incubator shaker followed by centrifuged at 15,000 rpm for 10 min. The supernatant portion of the sample was collected from the tube. The tube was again filled up with 2 ml of fresh medium and the nanoparticles were resuspended and incubated under the same condition as mentioned above. The absorbance of the supernatant of the collected sample was measured using a UV

spectrophotometer at 218 nm. The concentration of the drug was calculated from the calibration curve. The same procedure was repeated in three times to check the reproducibility.

We have used different mathematical models such as zero order, first order, Higuchi, Korsmeyer-Peppas, and Hixon Crowell model to evaluate *in vitro* drug release kinetic patterns using drug release data. The best kinetic model was selected based on the highest correlation coefficient (R^2) values, calculated by using Microsoft Excel software **(Costa & Lobo, 2001; Dash et al., 2010)**.

4.5.8. Hydrolytic stability study

Required amount (10 mg) of NP3 and pure PTX were taken separately in 2 ml buffer of different pH (3.0, 5.0, 7.4 and 9.2) to measure the hydrolytic degradation of nanoparticles as compared with pure drug. Buffers used were citrate buffer pH 3 and 5, phosphate buffered saline pH 7.4 and bicarbonate buffer pH 9.2. The solutions were kept in an incubator at 37±2°C with mild shaking. After the scheduled time intervals that is, 7^{th} day, 14^{th} day, 21^{st} day and 28^{th} day, the samples were removed from incubator, centrifuged and washed two times with double distilled water and dried in speed vac for 30 min and then mass of nanoparticles was measured. The incubation medium was completely replaced with fresh medium. For determination of mass loss, the weight of each sample was carefully measured before the hydrolytic degradation measurement. After drying, the weight of the samples was taken to evaluate the change of weight. The weight change was calculated according to the following formula **(Jain et al., 2010; Chen et al., 2013)**:

$$\text{Weight change } \% = \frac{W_0 - W_t}{W_0} \times 100$$

Where, W_0 and W_t represent the initial weight and the weight at time t respectively.

4.5.9. Cancer cell culture and culture condition

Human liver hepatocellular carcinoma HepG2/Huh-7 cells were cultured in Dulbecco's Modified Eagle's Medium (DMEM) containing fetal bovine serum (FBS) and antibiotics (1% penicillin streptomycin). Normal Chang liver cells were cultured similarly in Minimum Essential Medium (MEM) medium. Cancer cells were maintained at 37°C in CO_2 incubator.

The atmosphere inside the incubator was kept humidified. Cells were grown in T-25 culture flask and taken for further experiments.

(4, 5-Dimethylthiazol-2-yl)-2, 5-diphenyltetrazolium bromide assay (MTT assay)

MTT assay was performed in cancer cells **(Bharti et al., 2016)** to evaluate anti-proliferative potential of free drug, marketed formulation of paclitaxel (Pacliall®) and NP3 (selected as the best experimental formulation upon physicochemical evaluation). We have now performed MTT assay using multiple cell lines, HepG2 cells and Huh-7 cells and further, in normal cell type (Chang liver cells). Human liver cancer (HepG2, Huh-7) cells and normal cell type (Chang liver cells) were cultured, collected and resuspended in complete DMEM medium (for HepG2, Huh-7) and MEM (Chang liver cells) medium. 2.0×103 cells were seeded in each well of 96 well plates. After overnight incubation, complete medium was removed and incomplete medium containing free paclitaxel/Pacliall®/NP3 (Dose dependent treatment) was added in each well. After 48 h of incubation, drug containing medium was discarded and MTT solution (1 mg/ml) was added. After 4 h of incubation, MTT solution was discarded and 100 µl DMSO was added. After 20 min, optical density was measured at 560 nm by plate reader (Biorad, Hercules, CA, USA).

Cellular uptake assay

Cellular uptake study was performed according to earlier reported method **(Panja et al., 2016)** to evaluate the entry of NP3 inside HepG2 cancer cells. Briefly, cells were cultured on sterile lysine-coated cover slips. After attaining the 50-60% confluence, cells were starved with incomplete medium. Cells were then treated with low doses of FITC conjugated NP3 for 1 h and 4 h. Then, cells were incubated in 4% formalin solution followed by washing with sterile PBS and staining with DAPI. Florescent images were captured by using Zeiss Observer microscope (Carl Zeiss, Oberkochen, Germany) at 20× magnification. For quantitative uptake, HepG2 cells were grown in 13 mm petridish at a concentration 10^6 cells/well for a period of 24 h. After that, FITC conjugated paclitaxel-loaded nanoparticle was added and the cells were incubated with the formulation for different time period such as 1 h and 4 h. Then the cells were collected by trypsinization and suspended in PBS for analysis by flow cytometry (FACS Canto II cell sorter, BD Biosciences, San Jose, CA) using

FACS Diva Software (BD Biosciences) to measure cellular uptake of nanoparticles. Cells without treatment were considered as control.

4.5.10. Lipid peroxidation

Lipid peroxidation in HepG2 cells and normal liver cells (Chang liver cells) was estimated by the method available **(Maia et al., 2010)**. Malondialdehyde (MDA), a product of lipid peroxidation was determined spectrophotometrically by using Thiobarbituric Acid-Reactive Substances (TBARS). Lysate supernatant (0.2 ml) was mixed with 0.8 ml of phosphate buffered saline (pH 7.4) followed by 0.025 ml of butylated hydroxyl toluene solution (8.8 gl^{-1}) and 0.5 ml of 30% trichloroacetic acid. The mixture was incubated at 37°C for 1 h. From the above solution 1 ml was mixed with 0.25 ml of 1% thiobarbituric acid in 0.05 N NaOH and 0.075 ml of 0.1 M EDTA. The solution was vortexed and heated on a water-bath at 95°C for 20 min and then cooled under tap water. The absorbance of the mixture was read at 532 nm and the calculated lipid peroxidation value was expressed in nM MDA/h/mg protein using a molar extinction coefficient of 1.56×105/M/cm **(Chowdhury et al., 2013)**.

4.5.11. In vivo study

Plasma and liver pharmacokinetic study

Pharmacokinetic studies were performed using Sprague-Dawley rats (male) with an average body weight 150±20 g to investigate various pharmacokinetic parameters of drug in plasma and to determine hepatic drug concentration upon i.v. administration from NP3, marketed formulation (Pacliall®) and free drug suspension. The study protocol was approved by Institutional Animal Ethical Committee (IAEC), Jadavpur University, Kolkata and the study was conducted following the IAEC guideline. The animals were housed and maintained under standard laboratory conditions as mentioned below. The temperature and relative humidity (RH) were maintained at 25±2°C and 55±5%, respectively. The animals were maintained in 12 h light and dark cycle **(Choudhury et al., 2014)**. The animals were fasted for 12 h with free access of water before sacrifice. The animals were divided into four groups. First group of animals was treated with nanoparticle formulation (NP3), the second group of animals received commercial paclitaxel formulation and animals of the third group received free drug suspension. Doses were calculated as equivalent dose of 5 mg/kg body

weight of rat **(Wang et al., 2013)**. The fourth group of animals received no treatment and was considered as control group. The animals of group A-C were treated with the experimental formulations (NP3), Pacliall® and free drug containing equivalent amount of drug by intravenous injection in tail vein. After the scheduled time intervals (15 min, 30 min, 1 h, 2 h, 4 h, 8 h, 10 h, 12 h, 24 h and 48 h), the animals were anaesthetized and sacrificed. Around 0.5 ml of blood was collected by terminal heart puncture of the animals and placed in microcentrifuge tube containing small amount of EDTA solution. Plasma was separated immediately using centrifugation at 5000 rpm for 6min at 4°C. We have also collected the liver of corresponding animals at the same time intervals. The plasma and liver organs were preserved in −80°C until analysis. The concentrations of PTX upon treatment of NP3, marketed formulation (Pacliall®) and free drug suspension were estimated by tandem liquid chromatography-mass spectroscopy (LC-MS/MS) **(Zeng et al., 2012)**.

Sample analysis by LC-MS/MS

PTX stock solution was prepared by serial dilution with HPLC grade methanol. Calibration control (CC) and quality control (QC) samples were prepared by spiking the working stock solutions in blank plasma. Here, protein precipitation technique was used to extract the CC, QC and PTX from the study samples. Protein of plasma sample (100 µl) was precipitated with 300 µl ice cold 50:50 acetonitrile-methanol mixture containing 200 ng/ml docetaxel as internal standard (IS). The mixture was vortex-mixed for 10 min, centrifuged at 10,000 rpm at 4°C for 5 min. Supernatant (100 µl) was mixed with 100 µl of water and loaded into LC-MS/MS (LC: Shimadzu Model 20AC, MS: AB-SCIEX, Model: API4000, Software: Analyst 1.6). Analytes were eluted using YMC Triat C18 column (30×2.1 mm, 5 µ) and gradient elution technique of two mobile phases (mobile phase A: 0.1% formic acid in water and mobile phase B: 0.1% formic acid in methanol-acetonitrile-water mixture (45:45:10)) was conducted with injection volume 20 µl, flow rate 0.8 ml/min and total run time 3.0 min. Liver samples were weighed and diluted with four times water, homogenized and processed following the above mentioned protein precipitation technique using liver homogenate. Plasma data were plotted against time and various pharmacokinetic parameters such as maximum plasma concentration (C_{max}), area under curve to the last measurable concentration (AUC_{0-t}), half-life ($t_{1/2}$), clearance, steady state volume of distribution (V_{ss}) and mean

residence time (MRT) were determined by WinNonlin software (Certara, Princeton, NJ). Further, hepatic drug concentration was also determined.

Statistical analysis

All the experimental works were carried out at least three times for checking reproducibility. Data was expressed as the mean±standard deviation (SD). Statistical significance was evaluated using one-way ANOVA followed by Tukey post hoc test using Origin Pro 8 software (Origin Lab, Northampton, MA). Differences were considered statistically significant when $p<0.05$ at 95% confidence level.

Chapter 5

Results

5. RESULTS

5.1. Determination of absorption maxima of PTX in PBS (pH 7.4) containing 0.5% (w/v) SLS and water-acetotonitrile mixture:

Drug absorption maxima was determined in different working solution such as PBS containing 0.5% (w/v) SLS and in water:acetonitrile=40:60 by using a UV/VIS spectrophotometer. The results were shown in **Figure 5.1 & 5.2**.

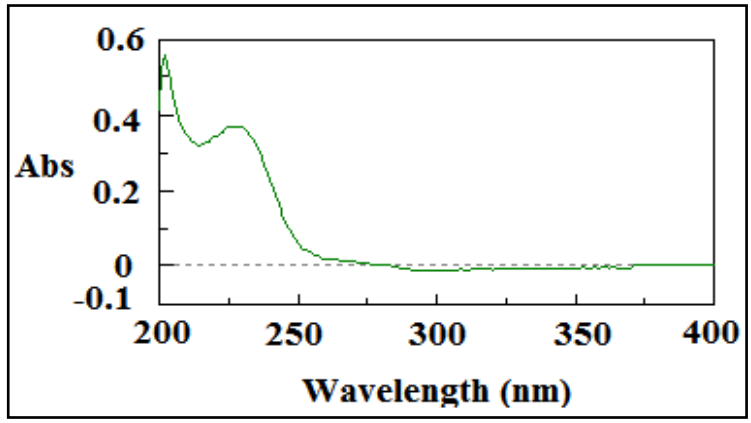

Figure 5.1. The absorption maxima of PTX in phosphate buffer (pH 7.4) containing 0.5% (w/v) SLS was detected at 218 nm.

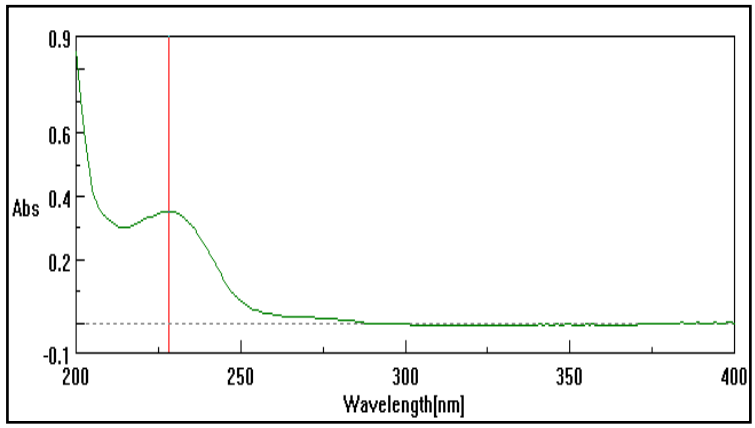

Figure 5.2. The absorption maxima of PTX in water: acetonitrile=40:60 was detected at 218 nm.

5.2. Preparation of calibration curve of PTX

Respective absorbance against concentrations was determined in PBS of pH 7.4 **(Table 5.1)** and water-acetonitrile mixture **(Table 5.2)**. The data were plotted to develop the respective calibration curves shown in **Figure 5.3 & 5.4** respectively.

Table 5.1.
Absorbance data for calibration curve of PTX in PBS, pH 7.4 at 218 nm.

SL. No.	Concentration of PTX in PBS, pH 7.4 (µg/ml)	Absorbance values*
1	2	0.0673± 0.021656
2	5	0.1798± 0.031749
3	10	0.3691± 0.034394
4	15	0.5464± 0.039051
5	20	0.7429± 0.036387
6	25	0.9364± 0.038223

* SD means standard deviation

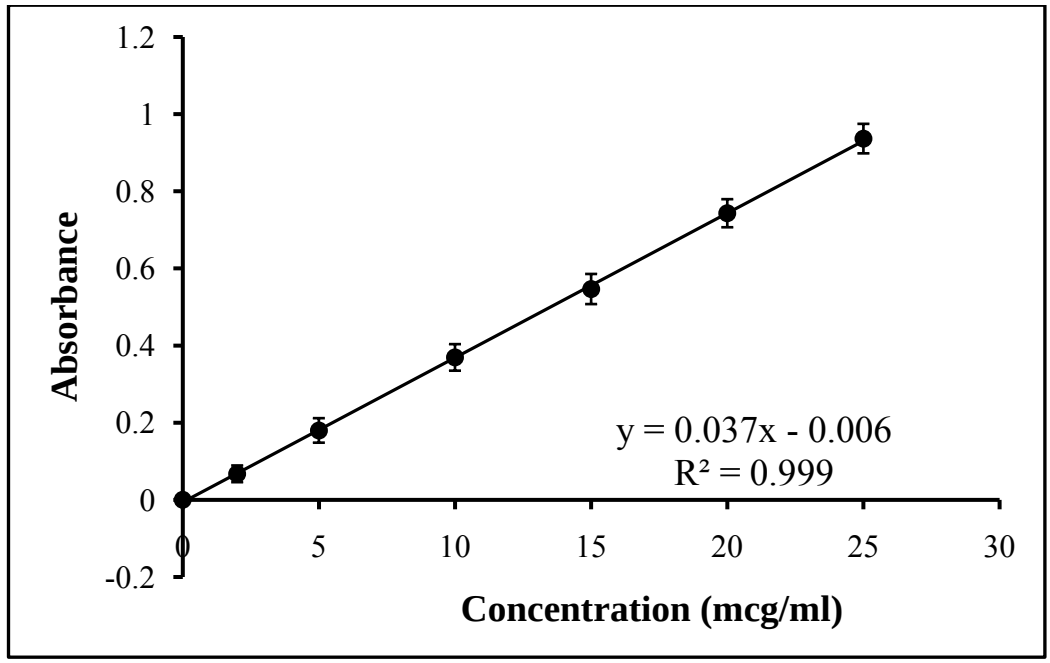

Figure 5.3. Calibration curve of PTX in PBS, pH 7.4 (Data represent mean ± standard deviation, n=3).

Table 5.2.
Absorbance data for calibration curve of PTX in water-acetonitrile mixture (40:60)

SL. No.	Concentration of PTX in water-acetonitrile mixture (µg/ml)	Absorbance values*
1	2	0.0765± 0.008717
2	5	0.1875± 0.018027
3	10	0.3394± 0.026457
4	15	0.5059± 0.021794
5	20	0.6753± 0.024576
6	25	0.8294± 0.031224

* SD means standard deviation

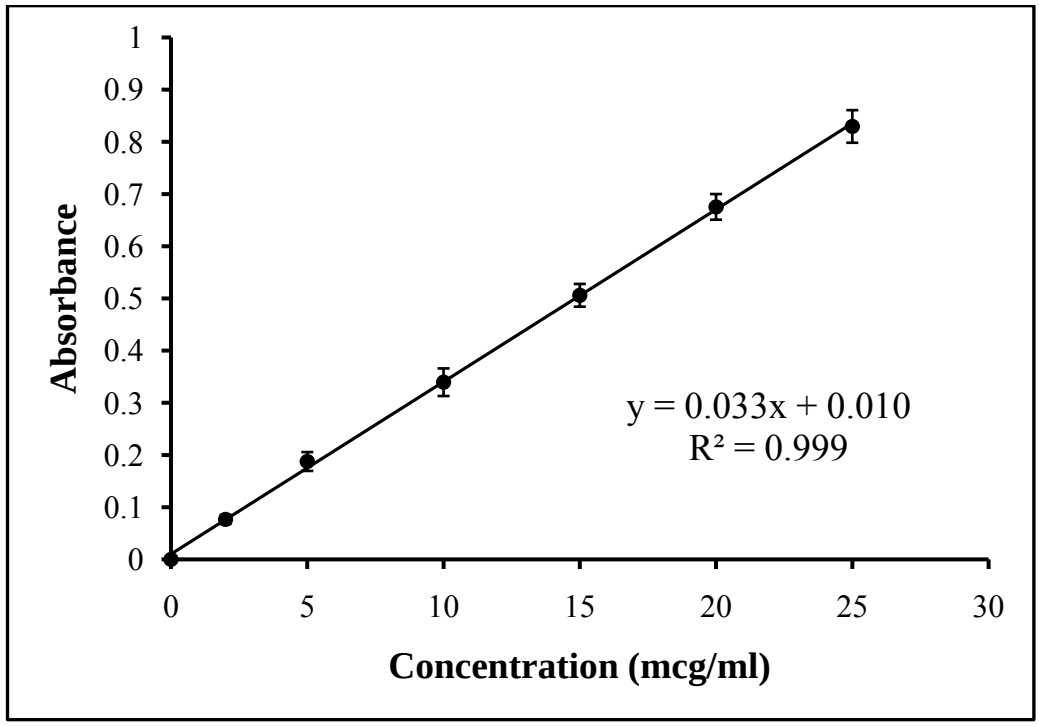

Figure 5.4. Calibration curve of PTX in water: acetonitrile=40:60 (Data represent mean ± standard deviation, n=3).

5.3. Drug-excipients interaction study

FTIR spectroscopy was carried out to investigate the interactions between drug and other excipients **(Satapathy et al., 2016)**. **Figure 5.5 (A–G)** shows the FTIR spectra of drug, all the excipients and formulations (with or without PTX). Pure PTX showed characteristic peaks at 3440 cm^{-1} as N-H stretching vibration and at 2944 cm^{-1} for CH_2 asymmetric and symmetric stretching vibrations. The peak found at 1720 cm^{-1} is assigned to C=O stretching vibration from ester group. C-N stretching and C-O stretching vibrations produced peaks at 1246 cm^{-1} and at 1072 cm^{-1} respectively. Peaks at 980 cm^{-1} and 710 cm^{-1} were for C-H in plane deformation and C-H out-of-plane/C-C=O deformation, respectively. PLGA showed characteristic peaks at 3508 cm^{-1} for O-H, 2998 cm^{-1} for C-H and 1754 cm^{-1} for C-O stretching bands, respectively. PVA produced characteristics peaks at 3450 cm^{-1} for O-H, 2930 cm^{-1} for C-H, 1738 cm^{-1} for C=O stretching bands and 1096 cm^{-1} for C-O stretching band. It was observed that all the characteristic bands of drug, PVA and PLGA were present in their physical mixture. It suggests that there was no chemical interaction between the drug and the excipients. There are no peaks of drug in nanoparticle formulation reveals that the nanoparticles had no free drug on the surface. Small shifting of peaks was found in nanoparticle formulation. Shifting of bands from 1754 to 1756 cm^{-1} and 750 to 752 cm^{-1} for PLGA and that from 1096 cm^{-1} to 1088 cm^{-1} for PVA was observed. Those siftings might be due to the formation of some weak physical bonds such as weak hydrogen bond, van der Waals force of attraction or dipole-dipole interaction.

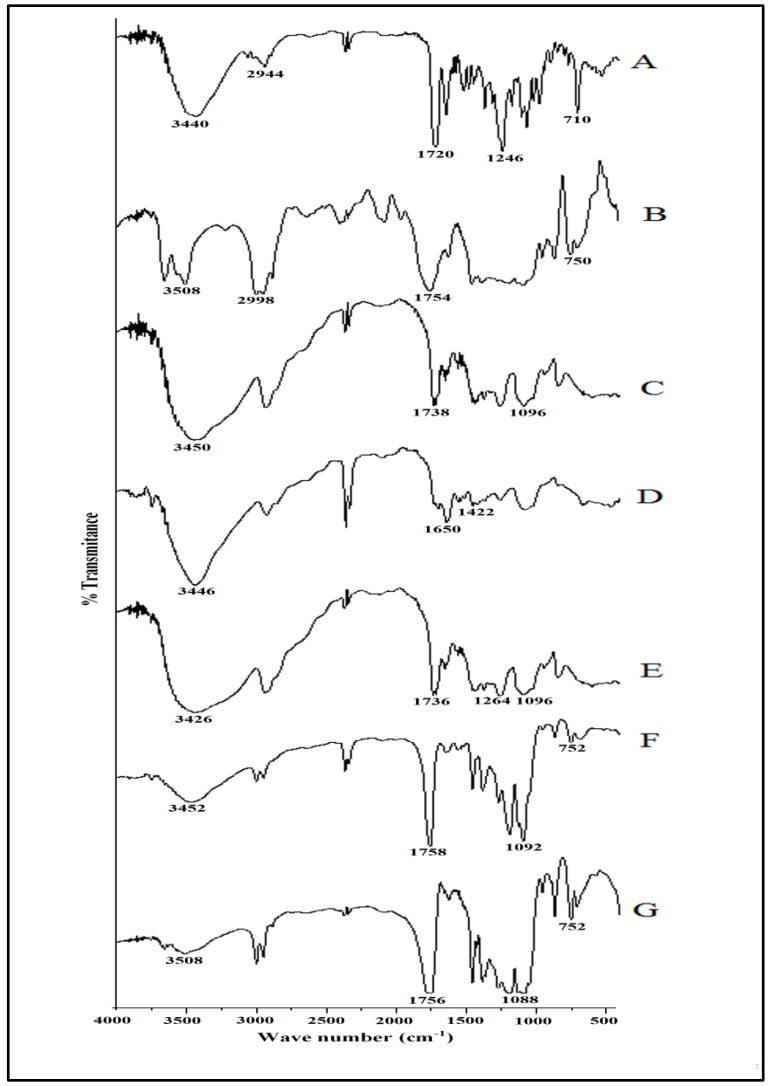

Figure 5.5. FTIR spectrum of paclitaxel (A), PLGA (85:15) (B), PVA (C), mixture of PLGA and PVA (D), mixture of drug, PVA and PLGA (E), blank formulation (F) and formulation NP3 (G).

5.4. DSC study

DSC was performed to confirm the physical state of PTX in the formulation and interaction between the drug and other excipients. The DSC thermogram **(Figure 5.6)** of PTX showed a melting endothermic peak at about 212.25°C which is assigned to the melting temperature of PTX. The drug-loaded nanoparticle formulation also showed an endothermic peak at the

same position, suggesting that drug in the formulation and free-drug was in same physical state. But blank formulation had no peak.

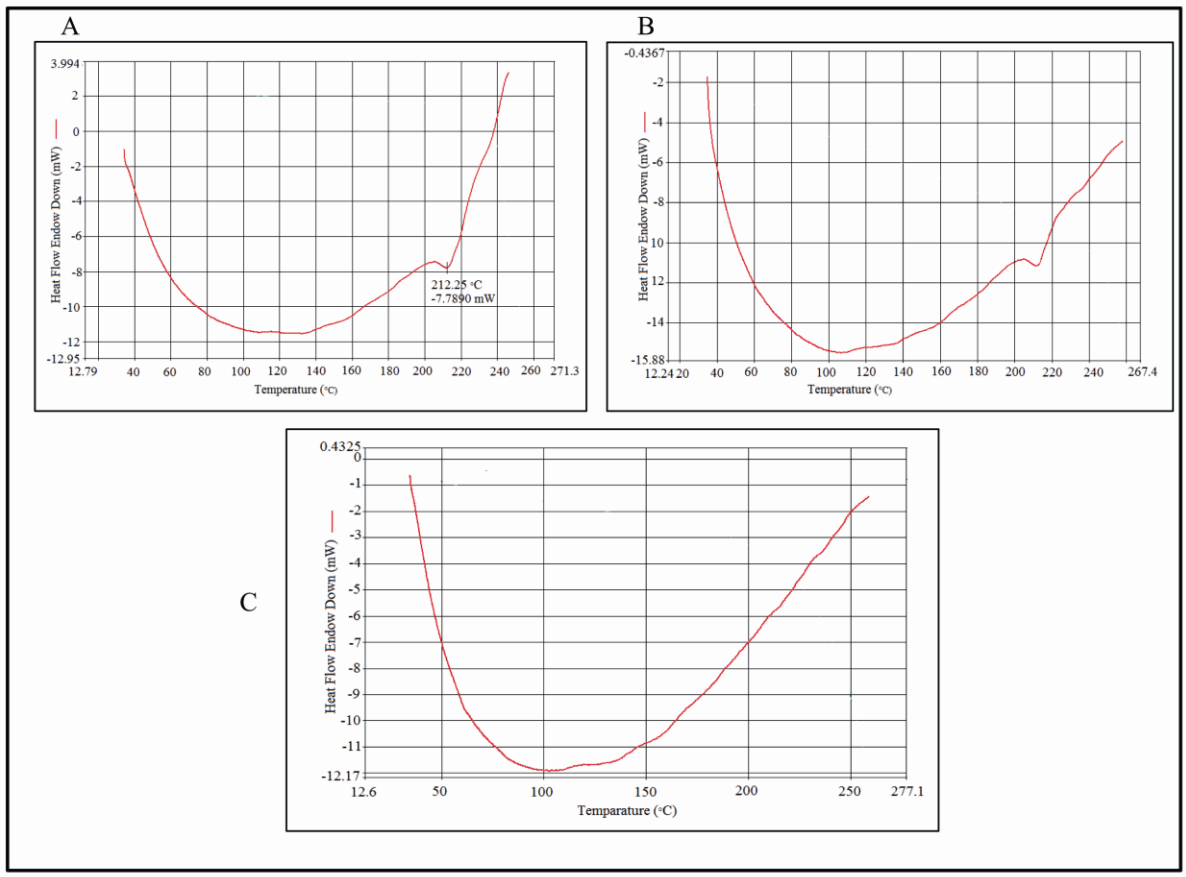

Figure 5.6. Differential scanning calorimetry thermogram of paclitaxel (A), NP3 (B) and blank formulation (C).

5.5. Preparation of nanoparticles

After checking of the compatibility among PTX and other excipients by FTIR spectroscopy and DSC study, various formulations were prepared as shown in **Table 5.3** and it was found that NP3 formulation was the best optimized formulation in terms of final product yield in the process, percentage of drug loading and loading efficiency percentage. This formulation was selected for further *in vitro* characterization and *in vivo* pharmacokinetic study and was reported here.

Table 5.3.
Various compositions, drug loading, loading efficiency and yield percentage of prepared formulations.

Formulation code	Amount of drug (mg)	Amount of PLGA (mg)	Amount of FITC (µl)	Theoretical drug loading (%)	Actual drug loading (%)±SD* (n=3)	Loading efficiency (%)±SD* (n=3)	Yield (%)*
NP1	2.5	240		1.03	0.69±0.11	67.47±10.29	55.22±3.05%
NP2	5	240		2.04	1.58±0.15	77.69±2.42	63.91±5.27%
NP3	10	240		4.00	3.37±0.19	84.25±4.95	72.62±9.96%
FITC-NP3	10	240	100	4.00	3.31±0.15	82.75 ± 5.24	

* SD means standard deviation

5.6. Drug loading and loading efficiency

Increasing amount of drug showed increasing amount of drug loading in the present study. It was found to be saturated at a drug:polymer ratio 1:24 **(Table 5.3)**. Hence, no further formulations have been reported here. The drug loading of NP1, NP2 and NP3 were found to be 0.69±0.11%, 1.58±0.15% and 3.37±0.19%, respectively. Loading efficiencies of the formulations varied from 67.47±10.29% to 84.25±4.95%. NP3 had highest percentage of drug loading and loading efficiency as compared to the other experimental formulations. The yield percentage of NP1, NP2 and NP3 were 55.22±3.05%, 63.91±5.27% and 72.62±9.96% respectively **(Table 5.3)**.

5.7. Particle size and zeta potential

The average particle sizes of different formulations varied from 308.6 nm to 369.5 nm as shown in **Table 5.4** and **Figure 5.7**. The polydispersity indices of different formulations were shown to vary from 0.156 to 0.419 and zeta potential values had a variation between −10.70 and −7.60 mV **(Table 5.4)**. Zeta potential was found to decrease with an increasing amount of drug in the experimental formulation.

Table 5.4.
Particle size, PDI and zeta potential of different formulations.

Formulation code	Mean particle size (nm)[a]	Polydispersity Index[a]	Zeta potential (mV)[a]
NP1	369.5±10.75	0.156±0.046	-7.60±0.19
NP2	317.0±1.84	0.406±0.007	-8.95±0.51
NP3	308.6±6.22	0.419±0.009	-10.70±0.21

[a] Data show mean ± standard deviation (n=3)

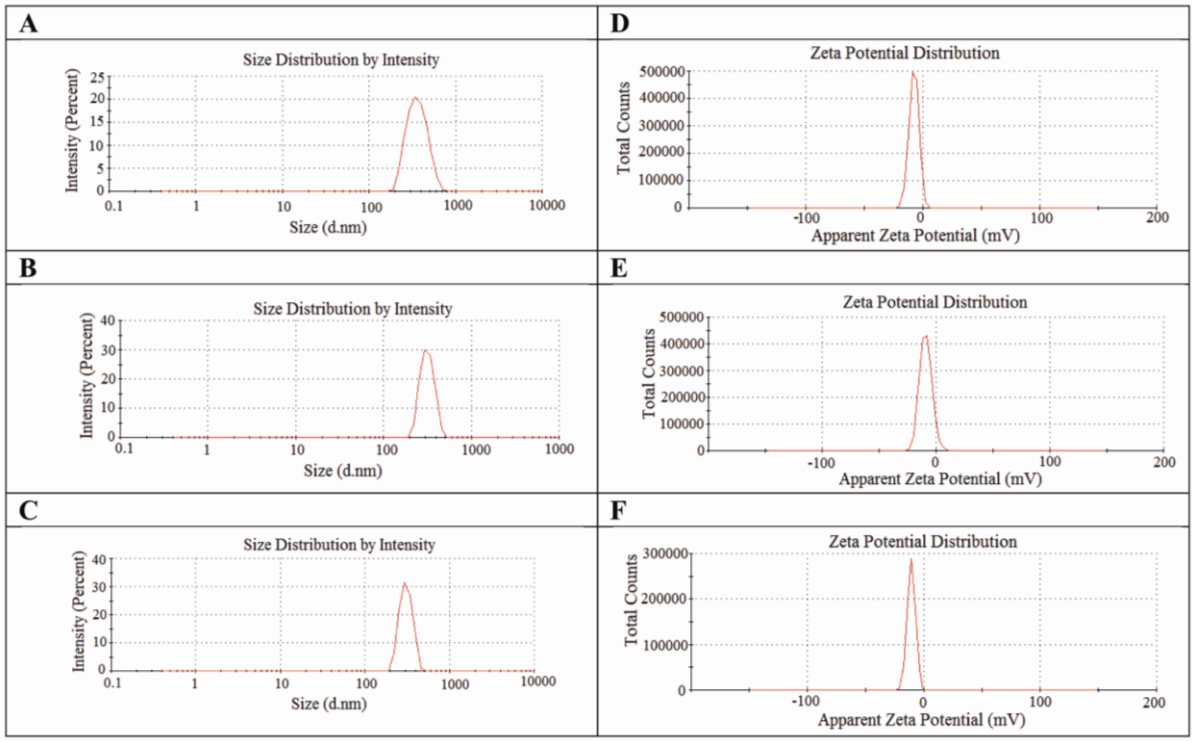

Figure 5.7. Particle size distribution of formulations NP1 (A), NP2 (B) and NP3 (C). Zeta potential of formulations NP1 (D), NP2 (E) and NP3 (F).

5.8. FESEM and TEM study

The morphological characteristics of PTX-nanoparticles were examined with FESEM and TEM. Particles were spherical in shape with orange peel like surface. All the particles were in nanometer size range with a variable distribution pattern **(Figure 5.8)**. In some formulations, some rod shaped PTX-crystals were detected, as PTX owing to its poor

solubility is often difficult to remove. TEM images **(Figure 5.9)** show that drug particles (as seen by black spots) were distributed throughout the formulation.

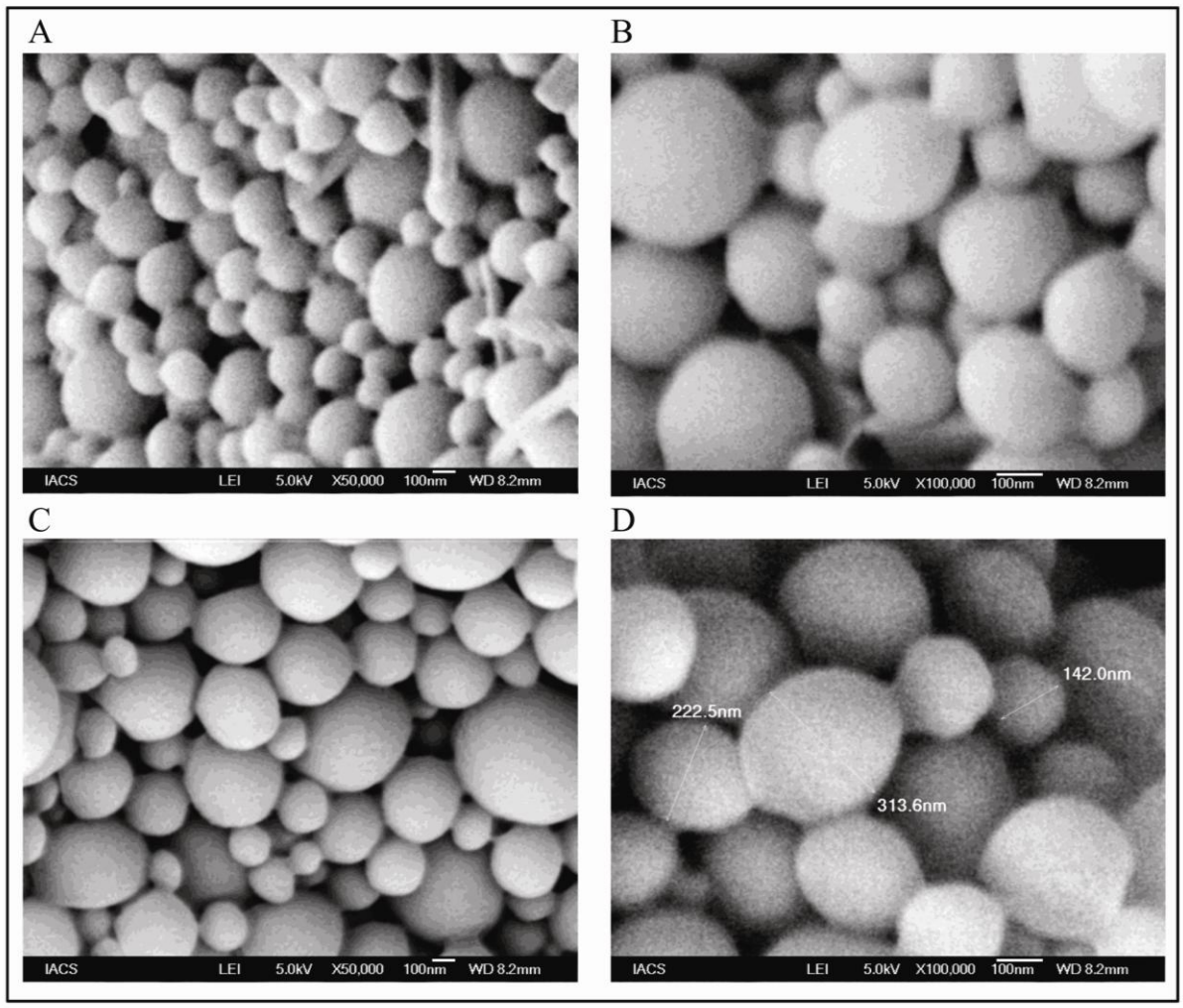

Figure 5.8. FESEM photograph of formulation NP1 at 50,000× (A), formulation NP2 at 100,000× (B), formulation NP3 at 50,000× (C) and formulation NP3 at 100,000× (D).

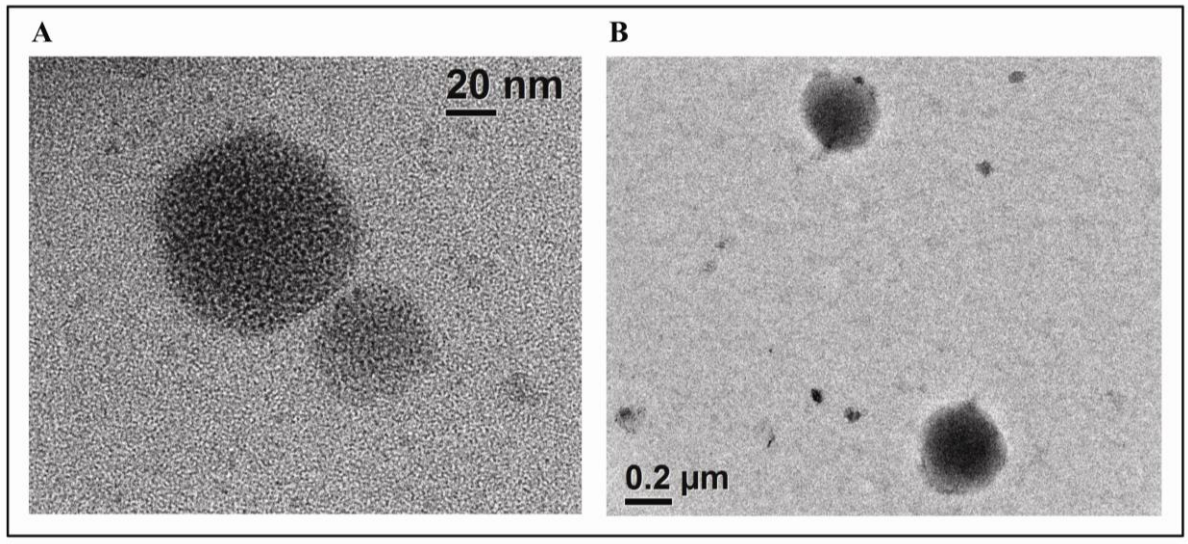

Figure 5.9. Transmission electron microscopic images of the optimized formulation (NP3); small size particles (A) and large size particles (B).

5.9. Drug release and release kinetics

In vitro drug release profile of various formulations shows that the formulations had a biphasic drug release profile as characterized by an initial burst release within 8 h followed by a slow and continuous sustained drug release as shown in **Figure 5.10**. The initial burst release might be due to the dissolution and diffusion of drug that was present closed to the inner surfaces of the nanoparticles followed by sustained release due to the drug diffused from the core of the polymer matrix. Variable particle sizes might play a role into it by varying drug diffusion pathways **(Gratton et al., 2008)**. After 30 days of drug release study, it was observed that cumulative percentages of drug released from NP1, NP2 and NP3 were 89.41±4.46%, 52.61±2.62% and 31.22±1.56% respectively. Drug released from NP3 was comparatively slower than the other two formulations i.e., NP1 and NP2.

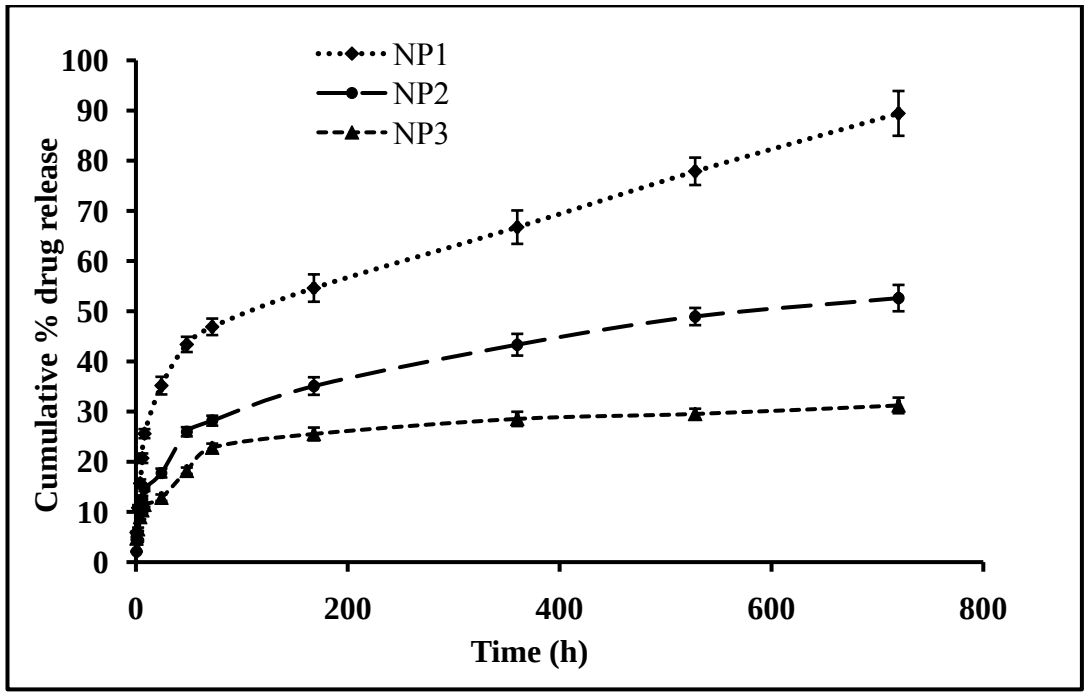

Figure 5.10. *In vitro* release profiles of PTX from NP1, NP2 and NP3 in phosphate buffer, pH 7.4. Data show mean±standard deviation of three different experiments in triplicate.

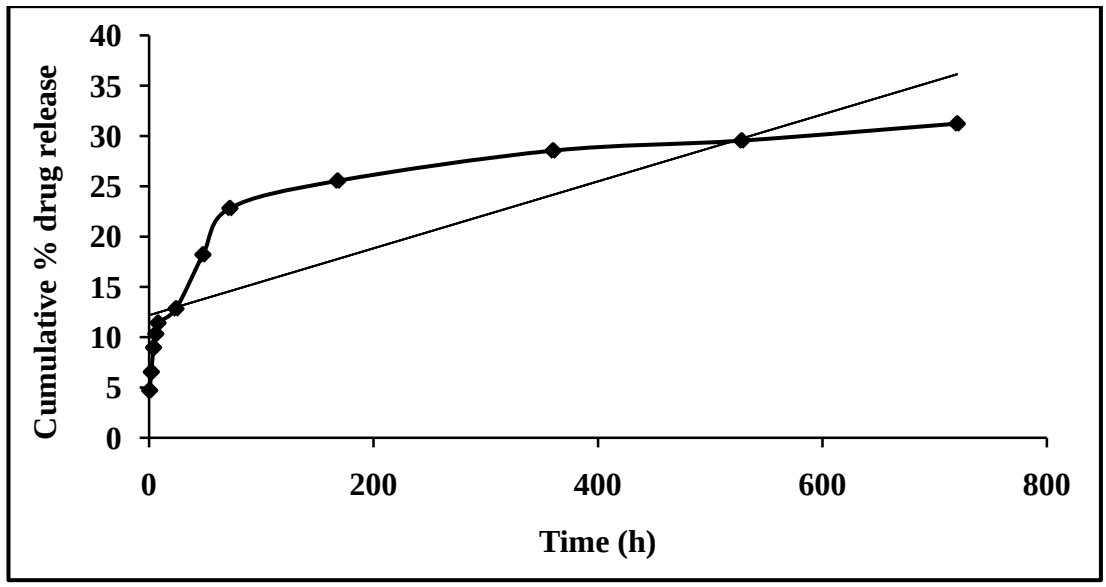

Figure 5.11.1. Zero order kinetics of drug release from the experimental formulation.

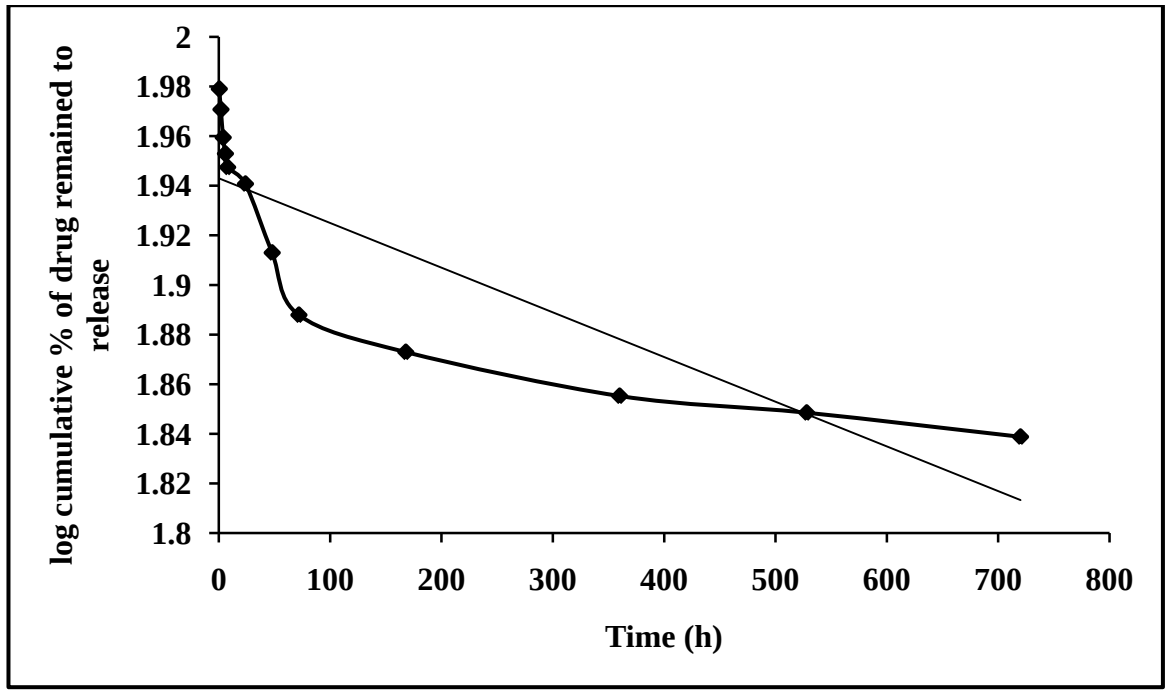

Figure 5.11.2. First order kinetics of drug release from the experimental formulation.

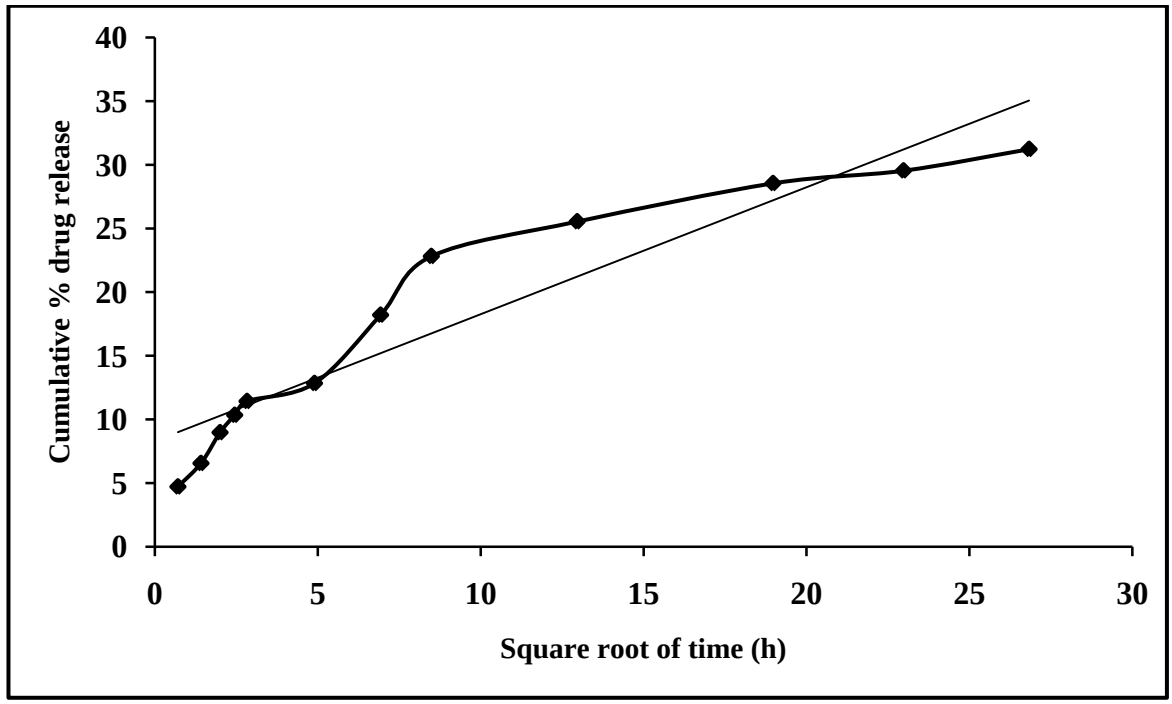

Figure 5.11.3. Higuchi kinetics of drug release from the experimental formulation.

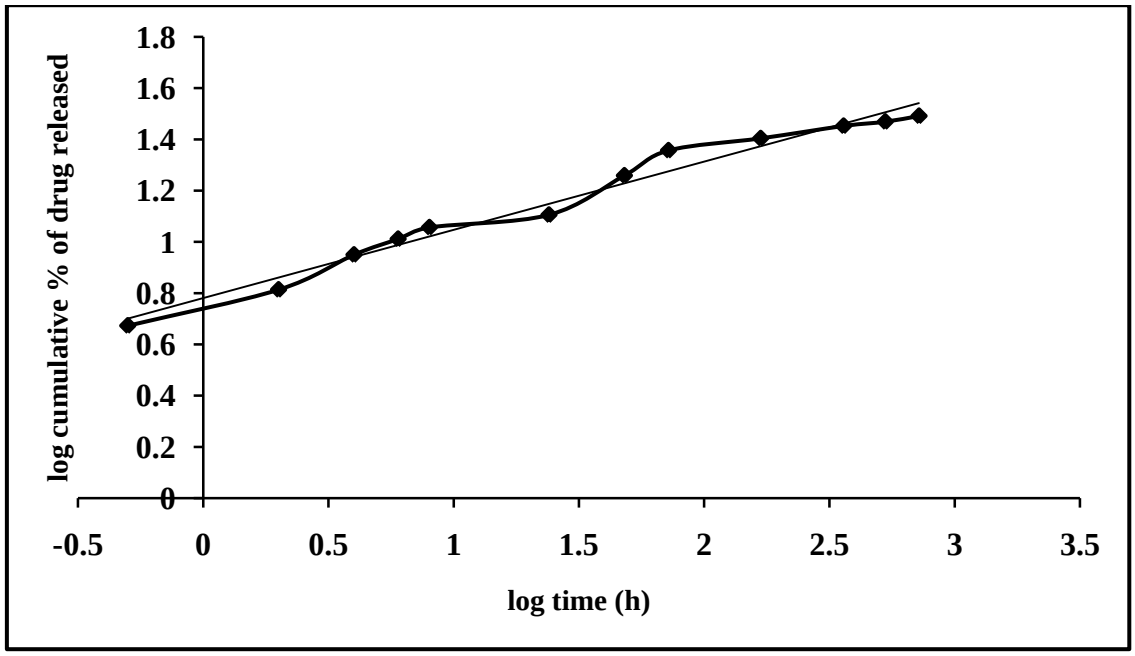

Figure 5.11.4. Korsmeyer-Peppas kinetics of drug release from the experimental formulation.

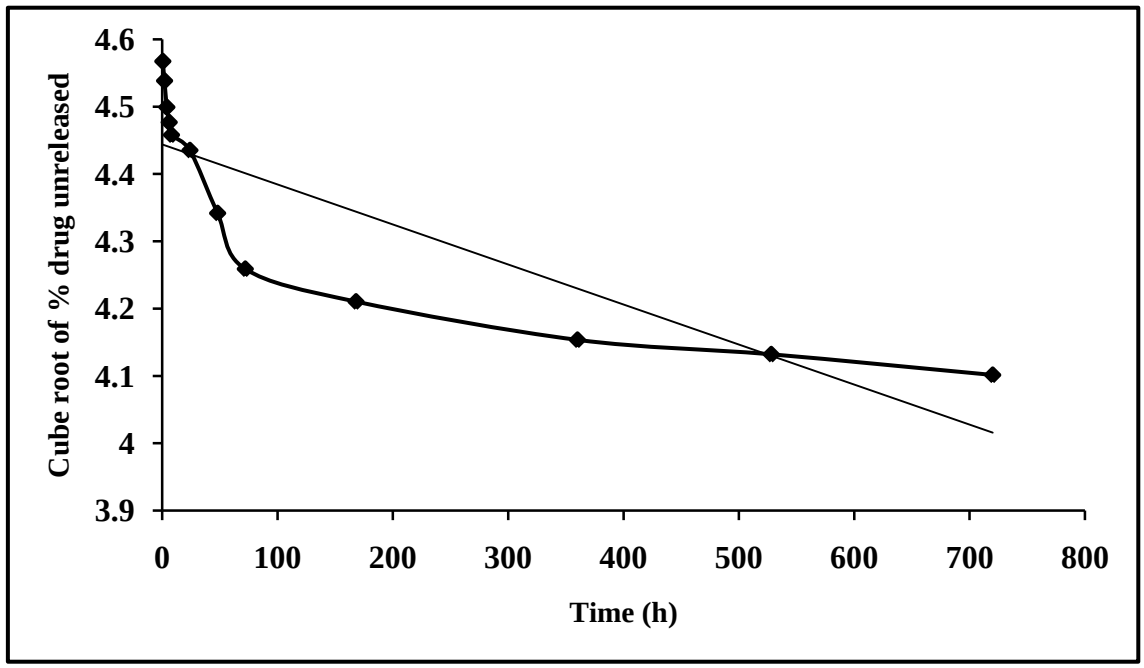

Figure 5.11.5. Hixson-Crowell kinetics of drug release from the experimental formulation.

The different drug release kinetics of PTX from the experimental formulation under study was shown in **Figure 5.11.1-5.11.5**. The correlation coefficient (R^2) and release exponent "n" (wherever applicable) were obtained from various drug release kinetic models tested for experimental formulations **(Table 5.5)**. Drug release data were fitted in different kinetic equations for different formulations. In case of NP1 and NP3, Korsmeyer-Peppas kinetic model (R^2=0.967 and 0.977 respectively) indicated good linearity as compared to the other models whereas NP^2 represented good linearity in Higuchi kinetic model (R^2=0.945).

Table 5.5.
In vitro drug release kinetic equations, R^2 values and drug release exponent "n" of various formulations.

***In vitro* Release Kinetics**	**NP1**	**NP2**	**NP3**
Zero-order Kinetics	y =0.101x+24.70 R^2=0.825	y=0.063x+14.32 R^2=0.804	y=0.033x+12.18 R^2=0.708
First-order Kinetics	y=-0.001x+1.889 R^2=0.957	y=-0.000x+1.932 R^2=0.873	y=-0.000x+1.943 R^2=0.736
Higuchi Kinetics	y=2.905x+14.08 R^2=0.948	y=1.849x+7.450 R^2=0.945	y=0.997x+8.295 R^2=0.887
Korsmeyer-Peppas Kinetics	y=0.349x+0.985 R^2=0.967 n=0.349	y=0.407x+0.645 R^2=0.933 n=0.407	y=0.266x+0.780 R^2=0.977 n=0.266
Hixson-Crowell Kinetics	y=-0.002x+4.241 R^2=0.930	y=-0.001x+4.407 R^2=0.851	y=-0.000x+4.444 R^2=0.727

5.10. Hydrolytic degradation study

The biodegradability of the PLGA-nanoparticles was estimated from the increase in their weight loss following hydrolytic degradation. Hydrolytic stability study demonstrated that pH significantly affects the weight loss. With decreasing pH of the medium the hydrolysis of the formulation increased. After one week study, mass loss at pH 9.2 was 5.66±0.44%, at pH 7.4 was 8.45±0.70%, at pH 5.0 was 11.82±0.99% and at pH 3.0 was 19.62±1.13% **(Figure 5.12)** respectively. There was no significant mass loss of pure PTX observed all over the study (not shown in **Figure 5.12**).

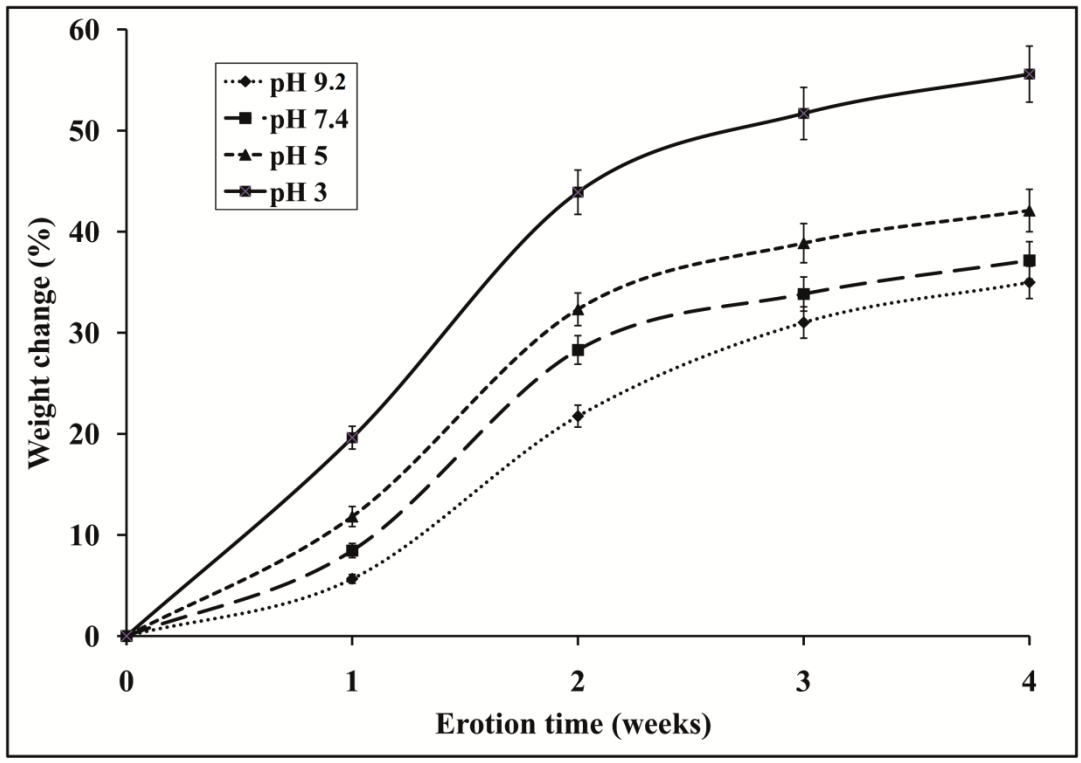

Figure 5.12. Weight change of PLGA nanoparticles at different pH.

5.11. MTT assay

The anti-proliferative effects of free drug, Pacliall®, NP3 and blank formulation were performed by MTT assay using HepG2 cells, Huh-7 cells and normal liver parenchymal cells (Chang liver cells). After 48 h incubation, rate of cell death increased with increasing concentration of NP3 which was comparable with Pacliall® and free drug **(Figure 5.13 (A–C))**. The inhibitory concentration (IC_{50}) values of NP3, Pacliall® and free drug in HepG2 cells were 8.5 nM, 24.0 nM and 26.4 nM, respectively and in Huh-7 cells, the IC_{50} values were 12.2 nM, 27.3 nM and 31.1 nM respectively. The IC_{50} value of NP3 in Huh-7 cells was 1.4 fold more than HepG2 cells. All the treated samples showed dose-dependent cell cytotoxicity. The cytotoxic effect of NP3 in all the cell types was found to be more than those of Pacliall® and free drug. Further, NP3, Pacliall® and free drug had more cytotoxic effect in HepG2 cells and Huh-7 cells as compared to human normal liver parenchymal cells (Chang liver cells). Moreover, there was no effect of the excipients used in the formulation on the cytotoxicity of PTX as there was no cell death detected from blank formulation (without drug).

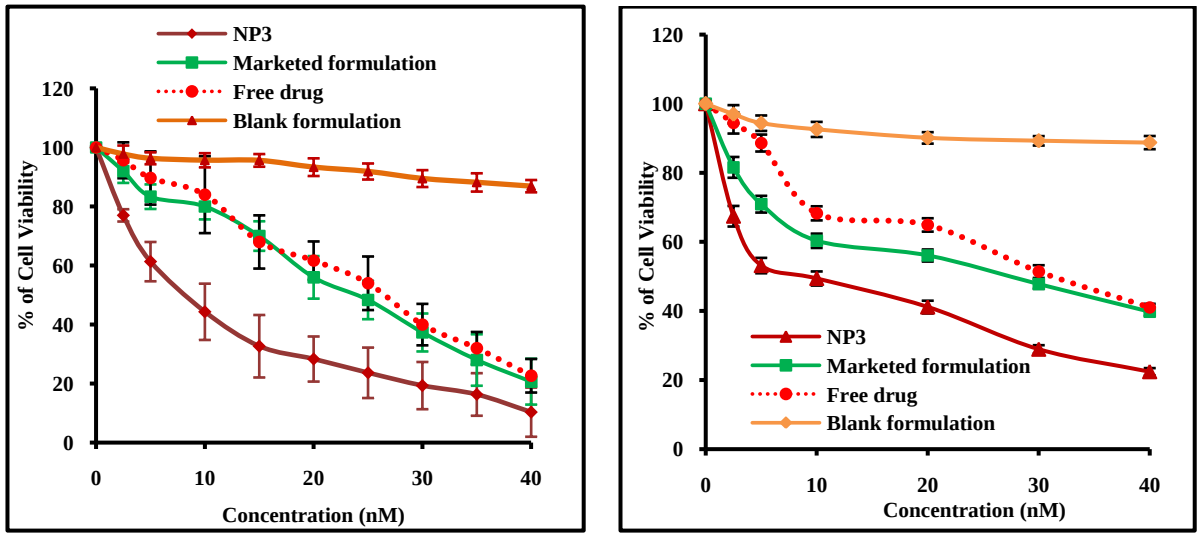

Figure 5.13. Cell viability study by MTT assay of free drug, marketed formulation, NP3 and blank formulation in HepG2 Cells (A), in Huh-7 cells (B) and in Chang Liver cells (C). Data show mean ± standard deviation of three different experiments.

5.12. Cellular uptake study

HepG2 cells were used to observe the cellular uptake of dye containing drug loaded nanoparticle (NP3) using confocal fluorescence microscopy. **Figure 5.14** shows that the intensity of fluorescence was increased in HepG2 cells with increasing incubation time from 1 h to 4 h. The images show that nanoparticles were internalized and distributed well into

cellular cytoplasm, suggesting that PTX-loaded nanoparticles could enter into the hepatic cells.

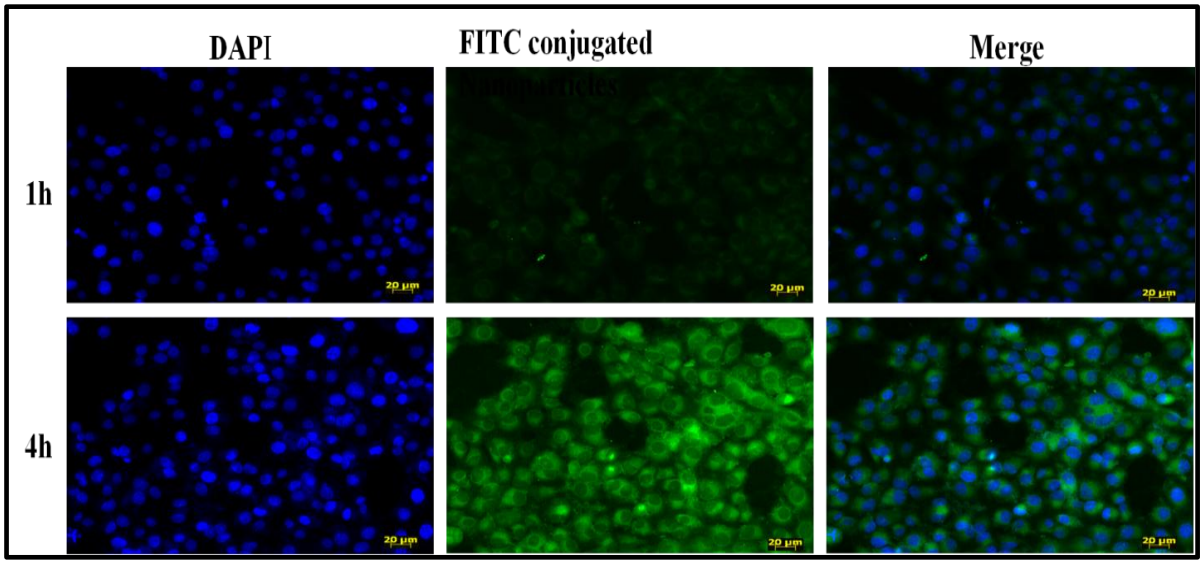

Figure 5.14. Cellular uptake study of NP3 in HepG2 cells for 1 h and 4 h

The data obtained from flow cytometric analysis, it was observed that uptake of the formulation within the HepG2 cells increased in a time dependent manner as median intensity for FITC uptake for controlled, after 1 h and 4 h treatment were found to be 518, 1229 and 2486 respectively **(Figure 5.15 and Table 5.6)**.

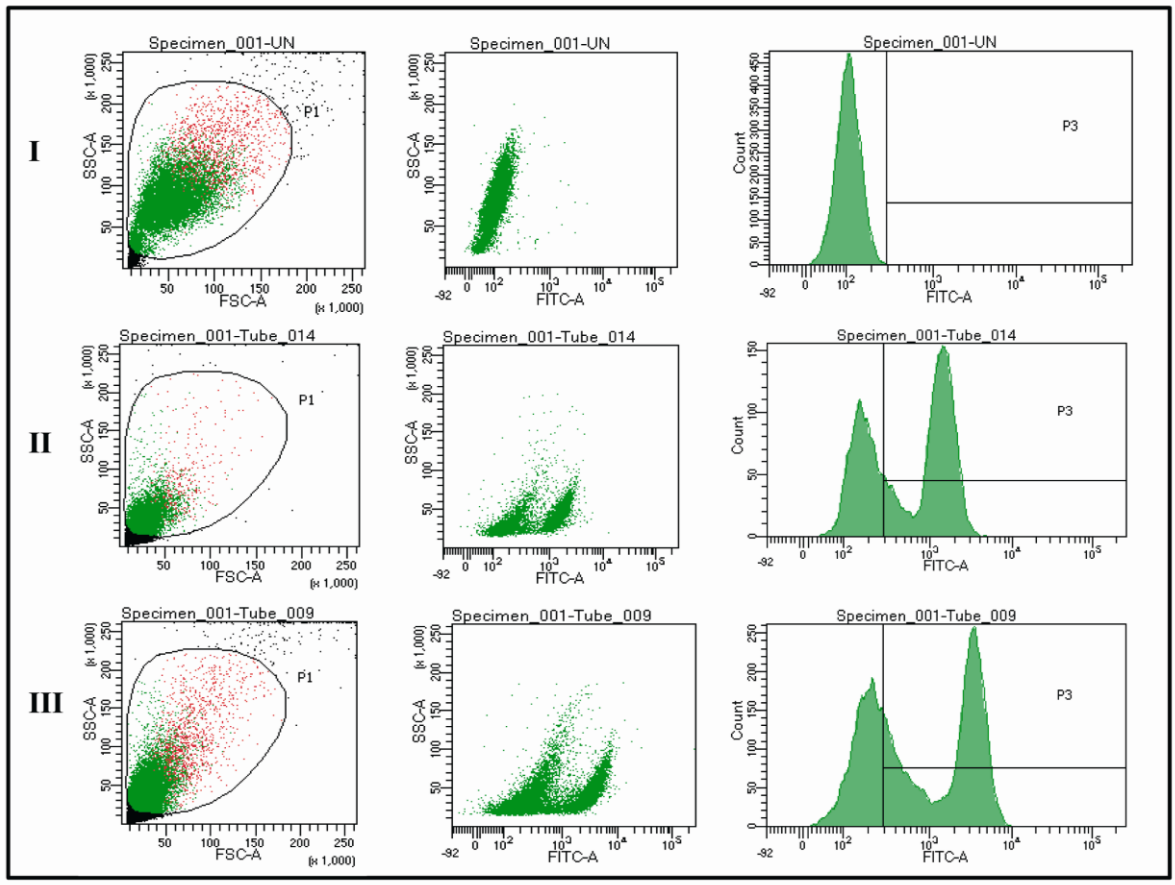

Figure 5.15. Flow cytometric measurement of HepG2 cells incubated with FITC-conjugated nanoparticles at different time points. Control cells (I), cells treated for 1 h (II) and 4 h (III).

Table 5.6. *Median intensity of FITC-conjugated NP3 in HepG2 cells*	
FITC-conjugated NP3 treated groups	**Median intensity of FITC-conjugated NP3 in HepG2 cells**
Control cells	518
After 1 h	1229
After 4 h	2486

5.13. Lipid peroxidation

Lipid peroxidation by free radicals generates TBARS that can be measured by malondialdehyde (MDA) levels. An elevation of MDA concentration was found in HepG2 cells as compared to normal liver cells and control cells. The MDA concentration in HepG2 cell line was 6.33±0.36 nM/mg protein and that in normal liver cells was 5.88±0.39 nM/mg protein. A marked elevation ($p<0.05$) in lipid peroxidation (as assessed by MDA level) in NP3 treated HepG2 cells was observed as compared to NP3 treated normal liver cells (Chang liver cells) **(Figure 5.16)**. NP3 treatment predominantly enhanced lipid peroxidation level both in normal and in HepG2 cells. In HepG2 cells, it was found to show more toxicity as assessed by lipid peroxidation level.

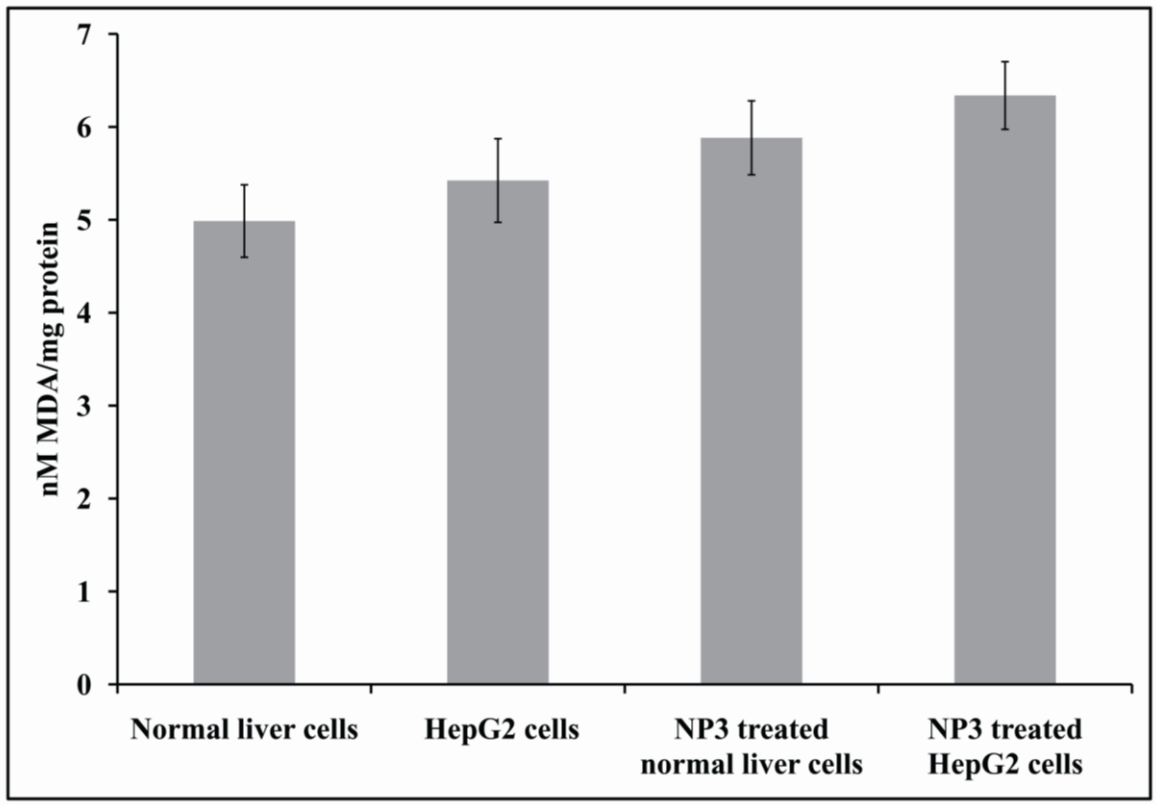

Figure 5.16. MDA level in HepG2 cells and normal liver parenchymal cells. Data show mean±standard deviation of three different experiments.

5.14. Pharmacokinetic study using LC-MS/MS

After intravenous (i.v) administration of single dose of free drug, Pacliall® (marketed formulation) and nanoparticle (NP3), (equivalent dose of 5 mg/kg of PTX) various pharmacokinetic parameters were analyzed using LC-MS/MS and summarized in **Table 5.7**. From the plasma drug concentration-time profile **(Figure 5.17)**, it was found that the plasma drug level of free drug increased rapidly after 0.25 h of i.v. injection than NP3 and Pacliall®. Through-out the study, after 0.5 h, the plasma concentration of NP3 remained comparatively higher than free drug and Pacliall® and then declined slowly. After 48 h, the plasma drug concentration of NP3 was found to be 14.91 fold and 4.58 fold higher than free drug and Pacliall®, respectively. AUC_{0-t} value of NP3 (2915.46±145.54 ng.h/ml) was significantly higher ($p<0.05$) than that for free drug (1272.95±63.54 ng.h/ml) and Pacliall® (2250.84±112.36 ng.h/ml). Plasma half-life ($t_{1/2}$) of NP3 was found to be higher than free drug and Pacliall® (2 fold and 2.25 fold respectively). MRT value of NP3 increased by 3.36 and 1.6 fold, respectively than the value for free drug and Pacliall®. Drug clearance of NP3 decreased by 65.36% and 38.46% as compared to free drug and Pacliall®, respectively.

Table 5.7.
Plasma pharmacokinetic parameters of PTX in rats treated with nanoparticles/marketed formulation/free drug [Dose 5 mg/kg body weight].

Formulation	$t_{1/2}$ (h)	C_{max} (ng/ml)	AUC_{0-t} (ng.h/ml)	$AUMC_{0-t}$ (ng.h^2/ml)	CL (L/h)	MRT (h)	V_{ss} (L)
Nanoparticle	28.48±0.99$^{\#,*}$	951.9±47.5$^{\#}$	2915.46±145.54$^{*,\#}$	32588.88±1486.98$^{*,\#}$	0.80±0.03$^{*,\#}$	11.18±0.56$^{*,\#}$	22.20±0.78$^{*,\#}$
Pacliall®	12.62±0.59	838.1±41.8$^{\$}$	2250.84±112.36$^{\$}$	15530.84±775.29$^{\$}$	1.30±0.05$^{\$}$	6.95±0.35$^{\$}$	11.40±0.40
Free drug	14.22±0.82	1181.4±58.9	1272.95±63.54	4200.73±209.70	2.31±0.08	3.32±0.16	10.61±0.37

Note: Values represent mean ± SD (n=3). Statistical significance was evaluated using one-way ANOVA followed by Tukey *post hoc* test using Origin Pro 8 (OriginLab, Northampton, MA). Differences were considered statistically significant when $p<0.05$ at 95% confidence level.

Abbreviations: $t_{1/2}$, half-life; C_{max}, maximum blood concentration; AUC_{0-t}, the area under the plasma drug concentration–time curve from the time of injection to a determined time point; AUMC, area under the first moment curve; CL, clearance; MRT, mean residence time and V_{ss}, steady state volume of distribution.

$^{\#}$ Indicates statistically significant data when comparison was made between nanoparticle and free drug treated group of rats.

* Indicates statistically significant data when comparison was made between nanoparticle and Pacliall® drug treated group of rats.

$^{\$}$ Indicates statistically significant data when comparison was made between Pacliall® and free drug treated group of rats.

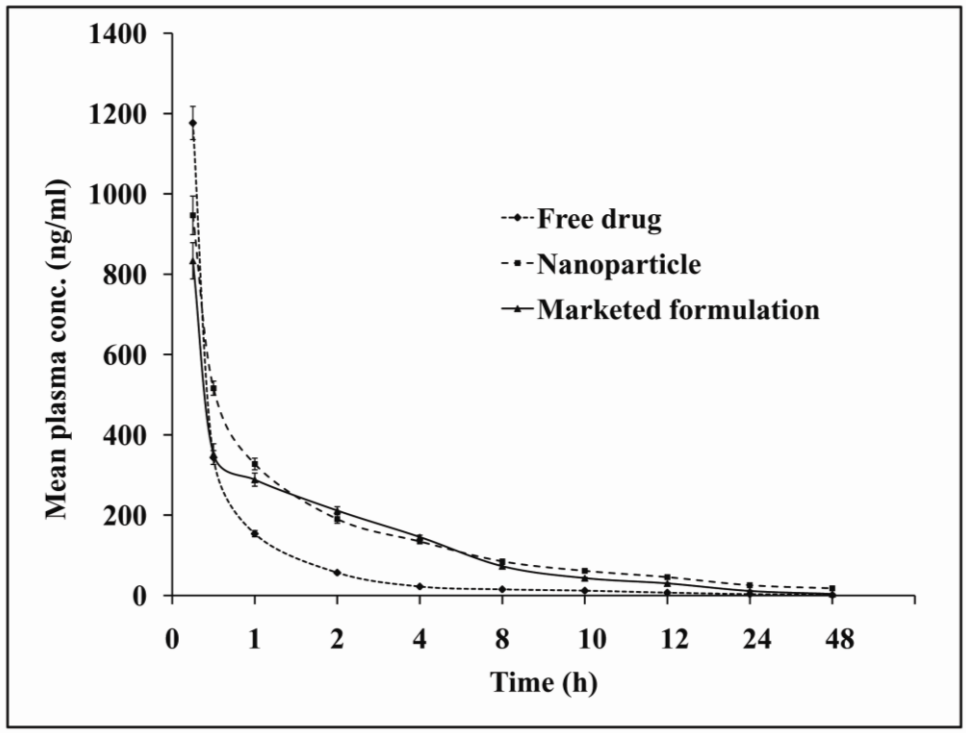

Figure 5.17. Plasma concentration-time profile of PTX after i.v. administration of NP3, Pacliall® and free drug in rats (5 mg/kg). Data show mean±SD (n=3).

Concentration of drug in liver was studied up to 8 h after i.v injection. At 8 h, hepatic drug concentration from NP3 was found to be 12.13 fold and 3.08 fold higher than free drug and Pacliall®, respectively **(Figure 5.18)**. Concentration of NP3 was more than that of free drug/Pacliall® in liver of rats at all the study points except at 0.25 h after injection, where concentration Pacliall® was higher than NP3/free drug. Data suggests that higher amount of drug accumulated in liver after i.v. administration of NP3 as compared to free drug/Pacliall® treated rats.

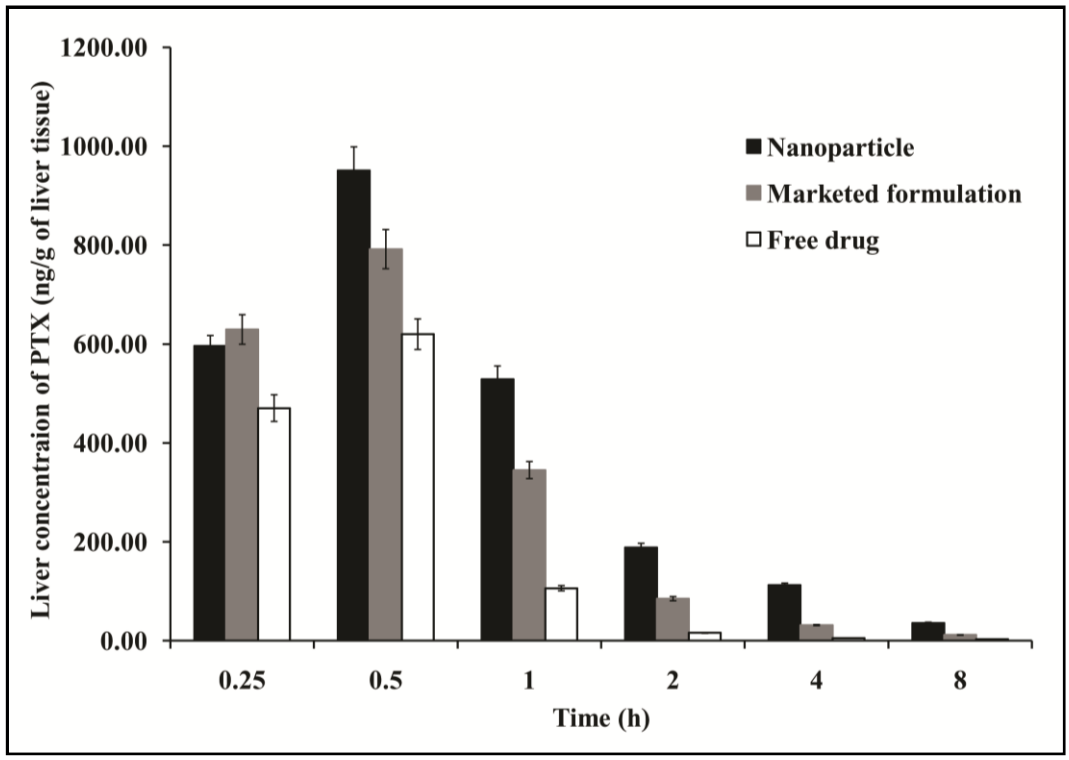

Figure 5.18. Liver concentration of PTX after i.v. administration of NP3, Pacliall® and free drug in rats (5 mg/kg). Data show mean±SD (n=3).

Chapter 6

Discussions

6. DISCUSSIONS

FTIR spectroscopy was used to study the interactions between the drug and the excipients. Presence of characteristic peaks of the drug, PLGA and PVA in the physical mixtures reveals that there were no chemical interactions between the drug and the excipients **(Figure 5.5)**. Though, minor shifting of few peaks was found which might be due to the formation of weak hydrogen bonding, van der Waals forces or dipole-dipole interaction **(Maji et al., 2014)**. Such physical interactions might help for formation of spherical structure and sustained release of drug from the nanoparticles **(Sahana et al., 2010)**. There was no peak of drug observed in nanoparticle formulations, suggesting non availability of free drug on the surface of the nano formulations **(Maji et al., 2014)**. In DSC study, the presence of endothermic peak of drug in nanoparticle formulation **(Figure 5.6)** revealed that the drug was encapsulated and had the same physical state as the free drug. Endothermic peak of the drug was not present in the formulations (without drug) and it suggests the absence of drug in the formulation. The result further confirmed that there was no chemical interaction between the drug and the excipients.

Paclitaxel-loaded nanoparticles were prepared by using emulsification solvent evaporation method. In this work, we have prepared different formulations by gradually increasing the amount of drug and observed the percentage of drug loading and loading efficiency to get optimized formulation. We have initially observed that the percentage of drug loading and loading efficiency increased with increasing amount of drug in the formulations **(Table 5.3)**. But, after a certain amount of drug incorporation, percentage of drug loading and loading efficiency did not increase with increasing amount of drug any further as because polymer matrix has also the limit to accommodate maximum amount of drug (saturation point) in the polymeric network **(Maji et al., 2014)**. Maximum drug loading of the experimental formulations was thus optimized. Thus, out of the various experimental formulations, NP3 was considered as the best formulation in terms of different physicochemical data and has been considered for further investigation. With an increasing amount of drug in formulation, percentage yield also increased. However, percentage yields were little less due to recovery problem. Sticky PLGA was adhered to the homogenizer and the quantities of excipients were

also less. This problem might be minimized if the formulations were prepared in a large quantity.

Submicron size particles were obtained experimentally **(Figure 5.7)**. The sizes of the different formulations varied from 308.6 nm to 369.5 nm **(Table 5.4)**. PDI was used to investigate distribution pattern of nanoparticles. The value reflects size distribution of nanoparticles **(Vaculikova et al., 2016)**. The formulations with a wider range of particle sizes have higher PDI values, while those comprising of evenly sized particles have lower PDI values **(Masarudin et al., 2015)**. In this study, values of PDI (<0.5) indicate that the formulations had a wider distribution pattern within a variable submicron size range.

Zeta potential of various formulations varied from −7.60 to −10.70 mV **(Table 5.4 & Figure 5.7)**. Zeta potential value above +30 mV and/or below −30 mV suggests that the particles remain in a suspended state for longer period of time and avoid rapid agglomeration in suspended state **(Crooke, 2007; Shaw et al., 2017)**. The experimental data suggests that the nanoparticles should be preserved in lyophilized form and reconstituted before use.

FESEM images **(Figure 5.8)** showed that the size of the particles were in below 300 nm with spherical in shape with smooth surfaces. TEM study **(Figure 5.9)** showed that drug distribution occurred throughout the particle.

Cumulative percentage of drug release showed initial rapid release of drug followed by slow release from all the experimental formulations during 30 days (total period of study) **(Figure 5.10)**. Comparatively higher cumulative amount of drug released from NP1 (89.41±4.46%) and NP2 (52.61±2.62%) than NP3 (31.22±1.56%). Small particles below 100 nm range of the formulation might provide faster drug release to meet up immediate need of therapeutic drug level, whereas larger particles might provide more sustained drug release owing to the larger diffusion pathway **(Mukherjee et al., 2008)**. Drug release performance from nanoparticles depends on the presence of larger and smaller particles in a formulation. Although NP3 shows the slowest drug release and had the smallest size in terms of average particle size, higher surface charge (zeta potential) on the particle surface as compared to NP1 and NP2, might retard drug release from the formulation predominantly compared to NP1 and NP2.

In drug release study, we found wide variation in drug release patterns from the three formulations (NP1, NP2 and NP3). NP1 when released about 90% drug, at the same time point NP2 showed about 45% drug release and NP3 showed about 30% drug release. Since, NP2 and NP3 showed predominantly slow drug release patterns as compared to NP1, no further study was conducted as on long-term release study, the formulation may erode and lead to erroneous results.

In vitro drug release kinetic data **(Table 5.5)** revealed that NP1 and NP3 were best fitted with Korsmeyer-Peppas model and NP2 followed Higuchi kinetics. Thus, the release kinetic data revealed that drug release from nanoparticle formulations might follow binary mechanism. To understand drug release mechanism, the drug release data were fitted to Korsmeyer-Peppas model which is related with the function of time for diffusion controlled mechanism **(Shaw et al., 2017)** and depicted by the equation as $M_t/M_a=Kt^n$, where, M_t/M_a is the fraction of drug release, t is time, K is rate constant and n is release exponent. If n=0.85, the release is zero order or case II relaxational release transport. When n is ≤0.43, the release follows Fickian diffusion-controlled drug release and 'n' value between 0.43 and 0.85 indicates that drug release follows an anomalous diffusion (drug diffusion in the hydrated matrix and the polymer chain relaxation). In our study, 'n' values of all the formulations (NP1 and NP3) were <0.43. This suggests that the drug release followed Fickian diffusion mechanism **(Sanna et al., 2011)**.

The variation of degradability at different pH values can be correlated with the effect of pH on hydrophilicity. The polymer at alkaline pH (pH 9.2) kept its non-polar (hydrophobic) character, due to entrapment of hydroxyl ions by the ester groups on the film surface, which lowers their water absorption capacity. As a result, water cannot penetrate into the sample and the weight loss can only be produced by superficial degradation. On the other hand, the acidic pH (pH 3.0) of the media changed the materials from hydrophobic to hydrophilic in character and also catalyzed the hydrolysis of polymer linkages which caused faster degradation of PLGA-nanoparticles **(Sailema-Palate et al., 2016)**.

In vitro cytotoxic activity of experimental nanoparticle (NP3) was assayed by MTT assay using HepG2 cells, Huh-7 cells and normal liver parenchymal cells. IC_{50} values of Pacliall®

and free drug were almost similar in HepG2 cells and Huh-7 cells, although it was predominantly lower for NP3 after 48 h incubation **(Figure 5.13)**. The lower value of IC_{50} was possibly due to a higher cellular uptake of the nanoparticles and thus, more drugs could be taken up by the cells. The drug released from nanoparticles could diffuse into the nuclear compartment and produced effective cell death **(Zeng et al., 2014)**. The percentage viability of normal liver parenchymal cells was more in case of NP3 as compared to Pacliall® and free drug as shown in **Figure 5.13C**. This might be possibly due to low internalization of PTX-PLGA nanoparticles by normal liver cells. The result recommends that NP3 might not be toxic to normal liver parenchymal cells (Chang liver cells). For blank formulation (without drug), the decrease in cell viability of the cultured cell population was not notably significant, suggesting that the excipients of the formulation had no predominant impact on the cell death and these excipients are safe for liver cancer treatment.

Cellular internalization of nanoparticles was observed by confocal fluorescence microscopy **(Figure 5.14)**. Cellular uptake of nanoparticles depends on various factors including size and shape of the nanoparticles, incubation time, temperature etc. In the present study, HepG2 cells were found to internalize NP3 well. The cellular uptake also increased with increasing incubation time from 1 to 4 h, as observed by fluorescence intensity in HepG2 cells as assessed by FACS **(Figure 5.15)**. Higher cellular uptake of nanosize NP3 formulation compared to free drug and marketed formulation as quantified by LC-MS/MS (data not shown) might cause the highest toxicity in HepG2 cells. The present result is well corroborated with previously published observation **(Gratton et al., 2008)**.

MDA is a major end product of peroxidative degradation of the polyunsaturated fatty acid constituents of biological membranes. Oxidative stress is playing an important role in the mechanism of toxicity for a number of nanoparticles through either the excessive generation of reactive oxygen species (ROS) or depletion of cellular antioxidant capacity **(Wise et al., 2010)**. ROS is generally included the superoxide radical ($O_2\cdot$), H_2O_2 and the hydroxyl radical (·OH), which causes damage to cellular components, including DNA and ultimately lead to apoptotic cell death. The MDA concentration in HepG2 cells upon NP3 treatment was 16.88% more than untreated HepG2 cells and 8.48% more than normal liver cells, indicating the generation of much more free radical oxygen and lipid peroxides in HepG2 cells after

NP3 treatment. The results revealed that oxidative stress produced by NP3 in HepG2 cells was predominantly more as compared to normal liver cells.

Plasma and liver pharmacokinetic studies were carried out using NP3, Pacliall® and PTX at an equivalent dose (dose of 5 mg drug/kg body weight in rats). This study showed that plasma concentration of free drug was relatively higher at 0.25 h after injection and it declined sharply after that **(Figure 5.17)**. PTX is very little soluble in water and phosphate buffer. PLGA (85:15) is also very non-polar polymer. Hence, drug release from the formulation was very slow. However, in the live system due to the presence of several enzymes and protein binding and distribution mechanism drug released rather somewhat differently.

Quick distribution of free drug as compared to the NP3 and Pacliall® could be the reason for it. Comparatively higher amount of drug from NP3 was present in plasma all over the study (48 h) and mean residence time was also more for NP3 than free drug and Pacliall®. Sustained drug release and prolonged drug residence in blood from NP3 **(Zhang et al., 2009)** might cause a significantly higher ($p<0.05$) AUC_{0-t} and $AUMC_{0-t}$ values than free drug and Pacliall®. Nanoparticles thus appeared comparatively more bioavailable. Recently, US-FDA has approved a Cremophor® free formulation of albumin-bound PTX NPs (nab-paclitaxel or Abraxane®) for cancer treatment. In this formulation, PTX is formulated within albumin particles to improve the efficacy of the drug and reduce the adverse effects associated with Cremophor®. However, it has been demonstrated that Abraxane® shows a quick elimination of PTX from the blood circulation and does not improve the pharmacokinetics of PTX (Taxol®) **(Sparreboom et al., 2005)**. Moreover, it is a high-cost formulation which might not be easily accessible for every patient, mainly those who are living in low- and middle-income countries **(Bernabeu et al., 2014)**. At the recommended Abraxane® clinical dose, 260 mg/m^2, the mean maximum concentration of paclitaxel which occurred at the end of the infusion was 18,741 ng/ml. The mean total clearance was 15 $L/h/m^2$. The mean volume of distribution was 632 L/m^2. The clearance and volume of distribution of Abraxane® were much higher than the prepared PLGA nanoparticles (clearance was 0.80±0.03 L/h and volume of distribution was 22.20±0.78 L). Abraxane® is more quickly eliminated from the

blood circulation. Thus, the prepared PLGA formulation had better pharmacokinetic properties as compared to nab-paclitaxel.

After intravenous administration of NP3/Pacliall®/free drug in rats, hepatic drug concentration from NP3 was more than the hepatic PTX concentration in free drug/Pacliall® treated rats at all the experimental time points (up to 8 h) except the time point of 0.25 h **(Figure 5.18)**. There was a significant variation ($p<0.05$) of hepatic drug concentration between NP3 and free drug treated rats whereas, the variation is less in rats treated with NP3/Pacliall®. Thus, the developed PTX-loaded PLGA nanoparticles possessed possibly a significant drug delivery potential to liver as compared to the free drug/marketed formulation (Pacliall®). In this work, we have concentrated on the liver only. Though, it is also important to see whether the other organs are affected or not. Literatures show that other organs were also affected upon application of PTX-loaded nanoparticles. But the concentration of the drug (paclitaxel) in other organs was comparatively less than the concentration of the drug in liver. Li et al. **(Li et al., 2011)** measured the PTX levels in liver, spleen, kidney, heart and lung. The researchers reported that the PTX level was 8 fold higher in liver.

Various researchers have conducted studies on paclitaxel-loaded PLGA nanoparticles **(Fonseca et al., 2002; Le Broc-Ryckewaert et al., 2013; Gupta et al., 2014)**. However, the present study is predominantly different from those available reports. We have prepared nanoparticles using multiple emulsion solvent evaporation method. However, the above mentioned researchers prepared nanoparticles completely by different methods. Further, they did not measure the yield value of nanoparticles but, our yield of the formulation was 72.62±9.96%. In the present work, we used HepG2 cells, Huh-7 cells and Chang liver cells. In the reported work, they used other cells for their study. We also performed hydrolytic degradation of PLGA nanoparticles for one month in different pH conditions and the degradation was increased with decreasing pH of the medium. Gupta et al. **(Gupta et al., 2014)** studied the accelerated stability study for three months. The last but not the least, none of the above mentioned studies has performed plasma and liver pharmacokinetic profile of formulation. Our results showed that nanoparticle formulation prolonged the blood level and higher liver uptake than the free drug and marketed formulation.

Non-uniform drug distribution may cause incomplete cancer treatment and drug targeting may be one of the most suitable options to tackle the problem. By targeted drug delivery system drug accumulates in the targeted organ or tissue in a selective way independent of site and method of administration. Thus, drug at the disease site becomes more while its concentration at the non-targeted tissues will be minimum **(Danhier et al., 2010)**. Nanoparticles with targeted ligand such as antibody, antibody fragments, aptamers, polysaccharide, peptide and small biomolecules like folic acid etc. **(Zhong et al., 2014)** are being used to target cells through ligand-receptor interactions. Various ligands used against the receptors of hepatic stellate cells include mannose-6 phosphate, human serum albumin, galactocyte and galactosamine and those of hepatocytes are glycyrrahizin, linoleic acid and apolipoprotein A1 **(Mukherjee et al., 2016)**.

The study shares lots of information of potential interest related to PTX-PLGA nanoparticles. Plasma and hepatic pharmacokinetic data showed that the formulation was superior to free drug and the tested commercial formulation in terms of plasma level, mean residence time, bioavailability, hepatic uptake and clearance. PTX-PLGA nanoparticles had sustained drug release and lower toxicity in contrast to free drug and the marketed formulation providing a potential use of the nanoparticles in liver cancer treatment.

Chapter 7

Summary & Conclusions

7. SUMMARY & CONCLUSIONS

There are many anticancer drugs including PTX are identified for liver cancer treatment. PTX is one of the most useful and effective antineoplastic agents for treatment of liver cancer. It is advantageous to use PTX for the treatment of liver cancer over other drugs owing to its broad spectrum antitumor activity, effectiveness on both solid and disseminated tumors and a unique mechanism of action as it stabilizes the microtubule and selectively disrupts the microtubule dynamics, thus inducing mitotic arrest that leads to cell death. PTX binds with β-tubulin and promotes the assembly of microtubules which prevents microtubular depolymerization and causes cell death. Intravenous infusion of paclitaxel is painful and often causes hypersensitive reactions. Its systemic bioavailability is <8% due to low aqueous solubility (0.3 ± 0.02 g/ml). The low solubility is due to its highly lipophilic nature (log P, 3.96) and bulky polycyclic structure (molecular weight 853 Da). The poor oral bioavailability is also attributed to its significant "first-pass" metabolism by cytochrome P450 in liver and p-glycoprotein mediated effluxing by intestinal cells. Further, clinical formulation of PTX (Taxol®) is used with 1:1 mixture of Cremophore EL (polyethoxylated castor oil) and ethanol due to its low aqueous solubility. The solvent is harmful and shows severe toxic effects such as hypersensitivity reactions, nephrotoxicity and neurotoxicity. Thus, Cremophore EL free formulation of PTX can eliminate the solvent related toxicity, improve stability, bioavailability and present sustained drug release. So, it is important to formulate the paclitaxel to avoid such drawbacks. Colloidal drug carriers especially nanoparticles have gained significant interest in this respect.

In this work, paclitaxel-loaded nanoparticles were prepared by using emulsification solvent evaporation method. Drug-excipients interaction was studied by Fourier Transform Infrared (FT-IR) spectroscopy and data showed that there was no chemical interaction between the drug, PTX and other excipients like Poly(D-L-lactide-co-glycolide) (PLGA) and polyvinyl alcohol (PVA) used for the preparation of nanoparticles. We have prepared different formulations such as NP1, NP2 and NP3 by gradually increasing the amount of drug and observed the percentage of drug loading and loading efficiency to get optimized formulation. Thus, out of the various experimental formulations, NP3 was considered as the best

formulation in terms of different physicochemical data and has been considered for further investigation.

The particle size data showed that the sizes of the different formulations varied from 308.6 nm to 369.5 nm and zeta potential varied from −7.60 to −10.70 mV. The size analysis was further confirmed by FESEM and TEM. FESEM images showed that the size of the particles were in below 300 nm with spherical in shape with smooth surfaces. TEM study showed that drug distribution occurred in the particle throughout. Cumulative percentage of drug release showed initial rapid release of drug followed by slow release from all the experimental formulations during 30 days (total period of study). Comparatively higher cumulative amount of drug released from NP1 and NP2 than NP3. Hydrolytic stability study demonstrated that pH significantly affects the weight loss. With decreasing the pH of the medium the hydrolysis of the formulation increased. The half maximal inhibitory concentration (IC_{50}) values of Pacliall® (marketed formulation) and free drug were almost similar in HepG2 cells and Huh-7 cells, although it was predominantly lower for NP3 after 48 h incubation. The percentage viability of normal liver parenchymal cells was more in case of NP3 as compared to Pacliall® and free drug. Cellular internalization of nanoparticles was observed by confocal fluorescence microscopy. The intensity of fluorescence was increased in HepG2 cells with increasing incubation time from 1 h to 4 h. The nanoparticles were internalized and distributed well into cellular cytoplasm, suggesting that PTX-loaded nanoparticles could enter into the hepatic cells. Flow cytometric analysis also revealed that uptake of the formulation within the HepG2 cells increased in a time dependent manner. The malondialdehyde (MDA) concentration in HepG2 cells upon NP3 treatment was 16.88% more than untreated HepG2 cells and 8.48% more than normal liver cells, indicating the generation of much more free radical oxygen and lipid peroxides in HepG2 cells after NP3 treatment. The results revealed that oxidative stress produced by NP3 in HepG2 cells was predominantly more as compared to normal liver cells. Plasma and liver pharmacokinetic studies were carried out using NP3, Pacliall® and PTX at an equivalent dose (dose of 5 mg drug/kg body weight in rats). This study was performed by using LC-MS/MS. From the plasma drug concentration-time profile, it was found that the plasma drug level of free drug increased rapidly after 0.25 h of i.v. injection than NP3 and Pacliall®. Through-out the study,

after 0.5 h, the plasma concentration of NP3 remained comparatively higher than free drug and Pacliall® and then declined slowly. After 48 h, the plasma drug concentration of NP3 was found to be 14.91 fold and 4.58 fold higher than free drug and Pacliall®, respectively. Concentration of drug in liver was studied up to 8 h after i.v injection. At 8 h, hepatic drug concentration from NP3 was found to be 12.13 fold and 3.08 fold higher than free drug and Pacliall®, respectively. Different pharmacokinetic parameters such as half-life ($t_{1/2}$), maximum blood concentration (C_{max}), area under the concentration-time curve (AUC), mean residence time (MRT), clearance (CL), steady state volume of distribution (V_{ss}), area under the first moment curve (AUMC) of PTX from NP3, Pacliall® and free-drug were calculated, compared and found that there was a significant improvement of these parameters in NP3 treated rats as compared to free-drug treated and Pacliall® groups of rats.

Thus, PTX-loaded PLGA nanoparticles successfully delivered PTX in liver in a sustained manner. *In vitro* study confirmed increased cellular uptake and reduction of IC_{50} upon PTX-PLGA nanoparticle administration as compared to free drug/marketed formulation. The formulation maintained a prolonged blood residence time and higher bioavailability of PTX than free drug/Pacliall®. The experimental biodegradable polymer based nanoparticles may be a potential drug carrier for the treatment of hepatic cancer or other hepatic chronic diseases.

References

REFERENCES

Abdel-Misih SR, Bloomston M. (2010). Liver anatomy. Surgical Clinics 90:643-653.

Acharya SR, Reddy PR. (2016). Brain targeted delivery of paclitaxel using endogenous ligand. Asian J Pharm Sci 11:427-438.

Akbarzadeh A, Rezaei-Sadabady R, Davaran S, et al. (2013). Liposome: classification, preparation, and applications. Nanoscale Res Lett 8:1-9.

Albarran L, Lopez T, Quintana P, et al. (2011). Controlled release of IFC-305 encapsulated in silica nanoparticles for liver cancer synthesized by sol-gel. Colloids Surf A 384:131-136.

Allemann P, Demartines N, Bouzourene H, et al. (2013). Longterm outcome after liver resection for hepatocellular carcinoma larger than 10 cm. World J Surg 37:452-458.

Ansary RH, Awang MB, Rahman MM. (2014). Biodegradable poly (D, L-lactic-co-glycolic acid)-based micro/nanoparticles for sustained release of protein drugs-A review. Trop J Pharm Res 13:1179-1190.

Anselmo AC, Mitragotri S. (2015). A review of clinical translation of inorganic nanoparticles. AAPS J 17:1041-1054.

Asati A, Santra S, Kaittanis C, et al. (2010). Surface-charge-dependent cell localization and cytotoxicity of cerium oxide nanoparticles. ACS Nano 4:5321-5331.

Aygul G, Yerlikaya F, Caban S, et al. (2013). Formulation and *in vitro* evaluation of paclitaxel loaded nanoparticles. Hacettepe Univ J Fac Pharm 33:25-40.

Banquy X, Suarez F, Argaw A, et al. (2009). Effect of mechanical properties of hydrogel nanoparticles on macrophage cell uptake. Soft Matter 5:3984-3991.

Bansal R, Nagorniewicz B, Prakash J. (2016). Clinical advancements in the targeted therapies against liver fibrosis. Mediators Inflamm 7:629-724.

Bao QY, Zhang N, Geng DD, et al. (2014). The enhanced longevity and liver targetability of Paclitaxel by hybrid liposomes encapsulating Paclitaxel-conjugated gold nanoparticles. Int J Pharm 477:408-415.

Bartneck M, Scheyda KM, Warzecha KT, et al. (2015). Fluorescent cell-traceable dexamethasone-loaded liposomes for the treatment of inflammatory liver diseases. Biomaterials 37:367-382.

Battogtokh G, Kang JH, Ko YT. (2015). Long-circulating self-assembled cholesteryl albumin nanoparticles enhance tumor accumulation of hydrophobic anticancer drug. Eur J Pharm Biopharm 96:96-105.

Benyon RC, M. Arthur JP. (2001). Extracellular matrix degradation and the role of hepatic stellate cells. Semin Liver Dis 21:373-384.

Bernabeu E, Helguera G, Legaspi MJ, et al. (2014). Paclitaxel-loaded PCL-TPGS nanoparticles: *in vitro* and *in vivo* performance compared with Abraxane®. Colloids Surf B Biointerfaces 113:43-50.

Bharti R, Dey G, Ojha PK, et al. (2016). Diacerein-mediated inhibition of IL-6/IL-6R signaling induces apoptotic effects on breast cancer. Oncogene 35:3965-3975.

Bosch FX, Josepa R, Mireia D, et al. (2004). Primary liver cancer: worldwide incidence and trends. Gastroenterol 127: S5-S16.

Brewer E, Coleman J, Lowman A. (2011). Emerging technologies of polymeric nanoparticles in cancer drug delivery. J Nanomater 2011:1-10.

Brigger I, Dubernet C, Couvreur P. (2002). Nanoparticles in cancer therapy and diagnosis. Adv Drug Delivery Rev 54:631-651.

Bruix J, Castells A, Bosch J, et al. (1996). Surgical resection of hepatocellular carcinoma in cirrhotic patients: prognostic value of preoperative portal pressure. Gastroenterology 111:1018-1022.

Bruix J, Qin S, Merle P, et al. (2017). Regorafenib for patients with hepatocellular carcinoma who progressed on sorafenib treatment (RESORCE): a randomised, double-blind, placebo-controlled, phase 3 trial. The Lancet 389:56-66.

Bruix J, Sherman M. (2011). Management of hepatocellular carcinoma: an update. Hepatology 53:1020-1022.

Byrne JD, Betancourt T, Brannon-Peppas L. (2008). Active targeting schemes for nanoparticle systems in cancer therapeutics. Adv Drug Deliv Rev 60:1615-1626.

Calne R, Yamanoi A, Oura S, et al. (1993). Liver transplantation for hepatocarcinoma. Surg Today 23:1-3.

Cao N, Cheng D, Zou S, et al. (2011). The synergistic effect of hierarchical assemblies of siRNA and chemotherapeutic drugs co-delivered into hepatic cancer cells. Biomaterials 32:2222-2232.

Carmeliet P, Jain RK. (2000). Angiogenesis in cancer and other diseases. Nature 407:249-257.

Cerqueira BBS, Lasham A, Shelling AN, et al. (2015). Nanoparticle therapeutics: Technologies and methods for overcoming cancer. Eur J Pharm Biopharm 97: 140-151.

Cha C, Fong Y, Jarnagin WR, et al. (2003). Predictors and patterns of recurrence after resection of hepatocellular carcinoma. J Am Coll Surg 197:753-758.

Chen HM, Wang YP, Chen J, et al. (2013). Hydrolytic degradation behavior of poly (L-lactide)/SiO_2 composites. Polym Degrad Stab 98:2672-2679.

Cheng FY, Su CH, Wu PC, et al. (2010). Multifunctional polymeric nanoparticles for combined chemotherapeutic and near-infrared photothermal cancer therapy *in vitro* and *in vivo*. Chem Commun (Camb) 46:3167-3169.

Chikamasa Y, Hirotami M, Kazue A, et al. (1991). Enhancing effect of cetylmannoside on targeting of liposomes to Kupffer cells in rats. Int J Pharm 70:225-233.

Cho HY, Lee CK, Lee YB. (2015). Preparation and evaluation of PEGylated and folate-PEGylated liposomes containing paclitaxel for lymphatic delivery. J Nanomater 16:36.

Choudhury H, Gorain B, Karmakar S, et al. (2014). Improvement of cellular uptake, *in vitro* antitumor activity and sustained release profile with increased bioavailability from a nanoemulsion platform. Int J Pharm 460:131-143.

Chowdhury MH, Satapathy BS, Mondal L, et al. (2013). Effect of streptozotocin-induced hyperglycemia on the progression of hepatocarcinogenesis in rats. Am J Pharmacol Toxicol 8:170-178.

Clavien PA, Lesurtel M, Bossuyt PM, et al. (2012). Recommendations for liver transplantation for hepatocellular carcinoma: an international consensus conference report. Lancet Oncol 13:11-22.

Clerc T, Sbarra V, Botta-Fridlund D, et al. (1995). Bile salt secretion by hepatocytes incubated with bile salts and liposomes or low density lipoproteins. Life Sciences 56:277-286.

Colleoni M, Audisio RA, De Braud F, et al. (1998). Practical considerations in treatment of hepatocellular carcinoma. Drugs 55:367-382.

Costa P, Lobo JMS. (2001). Modeling and comparison of dissolution profiles. Eur J Pharm Sci 13:123-133.

Crissien AM, Frenette C. (2014). Current Management of hepatocellular carcinoma. Gastroenterol Hepatol 10:153-161.

Crooke ST. (2007). Antisense Drug Technology: Principles: Strategies, and Applications, CRC Press, 2007.

Danhier F, Danhier P, De Saedeleer CJ, et al. (2015). Paclitaxel-loaded micelles enhance transvascular permeability and retention of nanomedicines in tumors. ?Int J Pharm 479:399-407.

Danhier F, Feron O, Préat V. (2010). To exploit the tumor microenvironment: passive and active tumor targeting of nanocarriers for anti-cancer drug delivery. J Control Release 148:135-146.

Danhier F, Lecouturier N, Vroman B, et al. (2009). Paclitaxel-loaded PEGylated PLGA-based nanoparticles: *in vitro* and *in vivo* evaluation. J Control Release 133:11-17.

Dash S, Murthy PN, Nath L, et al. (2010). Kinetic modeling on drug release from controlled drug delivery systems. Acta Pol Pharm Drug Res 67:217-223.

De Souza PC, Ranjan A, Towner RA. (2015). Nanoformulations for therapy of pancreatic and liver cancers. Nanomedicine 10:1515-1534.

Ding Y, Zhou YY, Chen H, et al. (2013). The performance of thiol terminated PEG-paclitaxel-conjugated gold nanoparticles. Biomaterials 34:10217-10227.

Di-Wen S, Pan GZ, Hao L, et al. (2016). Improved antitumor activity of epirubicin-loaded CXCR4-targeted polymeric nanoparticles in liver cancers. Int J Pharm 500:54-61.

Eley JG, Pujari VD, McLane J. (2004). Poly(lactide-co-glycolide) nanoparticles containing coumarin-6 for suppository delivery: *in vitro* release profile and *in vivo* tissue distribution. Drug Dlivery 11:255-261.

El-Marakby EM, Hathout RM, Taha I, et al. (2017). A novel serum-stable liver targeted cytotoxic system using valerate-conjugated chitosan nanoparticles surface decorated with glycyrrhizin. Int J Pharm 525:123-138.

Elsabahy M, Heo GS, Lim SM, et al. (2015). Polymeric Nanostructures for Imaging and Therapy. Chem Rev 115:10967-11011.

Fessi H, Puisieux F, Devissaguet JP, et al. (1989). Nanocapsule formation by interfacial polymer deposition following solvent displacement. Int J Pharm 55:R1-R4.

Fonseca C, Simoes S, Gaspar R. (2002). Paclitaxel-loaded PLGA nanoparticles: preparation, physicochemical characterization and *in vitro* anti-tumoral activity. J Control Release 83:273-286.

Francis MF, Cristea M, Winnik FM. (2004). Polymeric micelles for oral drug delivery: why and how. Pure Appl Chem 76:1321-1335.

Fu J, Wang H. (2018). Precision diagnosis and treatment of liver cancer in China. Cancer let 412:283-288.

G Storm, Belliot SO, T Daemen, et al. (1995). Surface modification of nanoparticles to oppose uptake by the mononuclear phagocyte system. Adv Drug Deliv Rev 17:31-48.

Gao DY, Lin TT, Sung YC, et al. (2015). CXCR4-Targeted Lipid-Coated PLGA Nanoparticles Deliver Sorafenib and Overcome Acquired Drug Resistance in Liver Cancer. Biomaterials 67:194-203.

Ghibellini G, Leslie EM, Brouwer KL. (2006). Methods to evaluate biliary excretion of drugs in humans: an updated review. Mol Pharm 3:198-211.

Ghosh S, Mondal L, Chakraborty S, et al. (2017). Early stage HIV management and reduction of stavudine-induced hepatotoxicity in rats by experimentally developed biodegradable nanoparticles. AAPS Pharm Sci Tech 18:697-709.

Giner-Casares JJ, Henriksen-Lacey M, Coronado-Puchau M, et al. (2016). Inorganic nanoparticles for biomedicine: where materials scientists meet medical research. Mater Today 19:19-28.

Gratton SE, Ropp PA, Pohlhaus PD, et al. (2008). The effect of particle design on cellular internalization pathways. Proc Natl Acad Sci USA 105:11613-11618.

Greish K. (2007). Enhanced permeability and retention of macromolecular drugs in solid tumors: a royal gate for targeted anticancer nanomedicines. J Drug Target 15:457-464.

Greupink R, Bakker HI, Reker-Smit C, et al. (2005). Studies on the targeted delivery of the antifibrogenic compound mycophenolic acid to the hepatic stellate cell. Int J Hepatol 43:884-892.

Guan M, Zhou Y, Zhu QL, et al. (2012). N-trimethyl chitosan nanoparticle-encapsulated lactosyl-norcantharidin for liver cancer therapy with high targeting efficacy. Nanomed Nanotech Biol Med 8:1172-1181.

Guo X, Szoka FC. (2003). Chemical approaches to triggerable lipid vesicles for drug and gene delivery. Acc Chem Res 36:335-341.

Gupta PN, Jain S, Nehate C, et al. (2014). Development and evaluation of paclitaxel loaded PLGA: poloxamer blend nanoparticles for cancer chemotherapy. Int J Biol Macromol 69:393-399.

Hendi A. (2011). Silver nanoparticles mediate differential responses in some of liver and kidney functions during skin wound healing. J King Saud Univ Sci 23:47-52.

Heurtault B, Saulnier P, Pech B, et al. (2002). A novel phase inversion-based process for the preparation of lipid nanocarriers. Pharm Res 19:875-880.

Hillaireau H, Couvreur P. (2009). Nanocarriers' entry into the cell: relevance to drug delivery. Cell Mol Life Sci 66:2873-2896.

Hoekstra LT, de Graaf W, Nibourg GA, et al. (2013). Physiological and biochemical basis of clinical liver function tests. Ann Surg 257:27-36.

http://www.who.int/mediacentre/factsheets/fs297/en/

Hu CMJ, Zhang L. (2009). Therapeutic nanoparticles to combat cancer drug resistance. Curr Drug Metab 10:836-841.

Huynh NT, Passirani C, Saulnier P, et al. (2009). Lipid nanocapsules: a new platform for nanomedicine. Int J Pharm 379:201-209.

Hwang S, Lee YJ, Kim KH, et al. (2015). The impact of tumor size on long-term survival outcomes after resection of solitary hepatocellular carcinoma: single-institution experience with 2558 patients. J Gastrointest Surg 19:1281-1290.

Ibraheem D, Iqbal M, Agusti G, et al. (2014). Effects of process parameters on the colloidal properties of polycaprolactone microparticles prepared by double emulsion like process. Colloids Surf A Physicochem Eng Asp 445:79-91.

Jain GK, Pathan SA, Akhter S, et al. (2010). Mechanistic study of hydrolytic erosion and drug release behavior of PLGA nanoparticles: influence of chitosan. Polym Degrad Stab 95:2360-2366.

James AM, Ambrose EJ, Lowick JH. (1956). Differences between the electrical charge carried by normal and homologous tumour cells. Nature 177:576-577.

Janát-Amsbury MM, Ray A, Peterson CM, et al. (2011). Geometry and surface characteristics of gold nanoparticles influence their biodistribution and uptake by macrophages. Eur J Pharm Biopharm 77: 417-423.

Jemal A, Freddie B, Melissa MC, et al. (2011). Global cancer statistics, CA: Cancer J Clin 61:69-90.

Jeon SI, Lee JH, Andrade JD, et al. (1991). Protein surface interactions in the presence of polyethylene oxide. I. Simplified theory. J Colloid Interface Sci 142:149-158.

Jimenez Calvente C, Sehgal A, Popov Y, et al. (2015). Specific hepatic delivery of procollagen alpha1(I) small interfering RNA in lipid-like nanoparticles resolves liver fibrosis. Hepatology 62:1285-1297.

Cho K, Wang X, Nie S, et al. (2008). Therapeutic nanoparticles for drug delivery in cancer. Clin Cancer Res 14:1310-1316.

Kang JH, Oishi J, Kim JH, et al. (2010). Hepatoma-targeted gene delivery using a tumor cell-specific gene regulation system combined with a human liver cell-specific bionanocapsule. Nanomed Nanotech Biol Med 6:583-589.

Krasnici S, Werner A, Eichhorn ME, et al. (2003). Effect of the surface charge of liposomes on their uptake by angiogenic tumor vessels. Int J Cancer 105:561-567.

Lacoeuille F, Hindre F, Moal F, et al. (2007). *In vivo* evaluation of lipid nanocapsules as a promising colloidal carrier for paclitaxel. Int J of Pharm 344:143-149.

Le Broc-Ryckewaert D, Carpentier R, Lipka E, et al. (2013). Development of innovative paclitaxel-loaded small PLGA nanoparticles: study of their antiproliferative activity and their molecular interactions on prostatic cancer cells. Int J Pharm 454:712-719.

Li L, Tang F, Liu H, et al. (2010). In vivo delivery of silica nanorattle encapsulated docetaxel for liver cancer therapy with low toxicity and high efficacy. ACS Nano 4:6874-6882.

Li M, Zhang W, Wang B, et al. (2016). Ligand-based targeted therapy: a novel strategy for hepatocellular carcinoma. Int J Nanomed 11:5645-5669.

Li R, Eun JS, Lee MK. (2011). Pharmacokinetics and biodistribution of paclitaxel loaded in pegylated solid lipid nanoparticles after intravenous administration. Arch Pharm Res 34:331-337.

Lin TT, Gao DY, Liu YC, et al. (2016). Development and characterization of sorafenib-loaded PLGA nanoparticles for the systemic treatment of liver fibrosis. J Control Release 221:62-70.

Liu L, Chen H, Wang M, et al. (2014). Combination therapy of sorafenib and TACE for unresectable HCC: a systematic review and meta-analysis. PLoS One 9:e91124.

Liu Q, Li R, Zhu Z, et al. (2012). Enhanced antitumor efficacy, biodistribution and penetration of docetaxel-loaded biodegradable nanoparticles. Int J Pharm 430:350-358.

Liu Q, Li R, Zhu Z, et al. (2012). Enhanced antitumor efficacy, biodistribution and penetration of docetaxel-loaded biodegradable nanoparticles. Int J Pharm 430:350-358.

Llovet JM, Ducreux M, Lencioni R, et al. (2012). European Association for the Study of the Liver European Organisation for Research and Treatment of Cancer: EASL-EORTC clinical practice guidelines: management of hepatocellular carcinoma. J Hepatol 56:908-943.

Loutfy SA, El-Din HMA, Elberry MH, et al. (2016). Synthesis, characterization and cytotoxic evaluation of chitosan nanoparticles: *in vitro* liver cancer model. Adv Nat Sci Nanosci Nanotechnol 7:035008.

Lu J, Li Z, Zink JI, et al. (2012). *In vivo* tumor suppression efficacy of mesoporous silica nanoparticles-based drug-delivery system: enhanced efficacy by folate modification. Nanomedicine 8:212-20.

Lv PP, Wei W, Yue H, et al. (2011). Porous quaternized chitosan nanoparticles containing paclitaxel nanocrystals improved therapeutic efficacy in non-small cell lung cancer after oral administration. Biomacromolecules 12:4230-4239.

Ma X, Hui H, Jin Y, et al. (2016). Enhanced immunotherapy of SM5-1 in hepatocellular carcinoma by conjugating with gold nanoparticles and its *in vivo* bioluminescence tomographic evaluation. Biomaterials 87:46-56.

Maeda H. (2001). The enhanced permeability and retention (EPR) effect in tumor vasculature: the key role of tumor-selective macromolecular drug targeting. Adv Enzyme Regul 41:189-207.

Maeng JH, Lee DH, Jung KH, et al. (2010). Multifunctional doxorubicin loaded superparamagnetic iron oxide nanoparticles for chemotherapy and magnetic resonance imaging in liver cancer. Biomaterials 31:4995-5006.

Maia MS, Bicudo SD, Sicherle CC, et al. (2010). Lipid peroxidation and generation of hydrogen peroxide in frozen thawed ram semen cryopreserved in extenders with antioxidants. Anim Reprod Sci 122:118-123.

Maji R, Dey NS, Satapathy BS, et al. (2014). Preparation and characterization of tamoxifen citrate loaded nanoparticles for breast cancer therapy. Int J Nanomedicine 9:3107.

Mandal D, Ojha PK, Nandy BC, et al. (2010). Effect of carriers on solid dispersions of simvastatin (Sim): physico-chemical characterizations and dissolution studies. Der Pharm Lett 2:47-56.

Marinina J, Shenderova A, Mallery SR, et al. (2000). Stabilization of vinca alkaloids encapsulated in poly (lactide-co-glycolide) microspheres. Pharm Res 17:677-683.

Masarudin MJ, Cutts SM, Evison BJ, et al. (2015). Factors determining the stability, size distribution, and cellular accumulation of small, monodisperse chitosan nanoparticles as candidate vectors for anticancer drug delivery:application to the passive encapsulation of [14C]-doxorubicin. Nanotechnol Sci Appl 8:67-80.

Matsumura Y, Maeda H. (1986). A new concept for macromolecular therapeutics in cancer chemotherapy: mechanism of tumoritropic accumulation of proteins and the antitumor agent smancs. Cancer Res 46:6387-6392.

Mazzaferro V, Bhoori S, Sposito C, et al. (2011). Milan criteria in liver transplantation for hepatocellular carcinoma: an evidence-based analysis of 15 years of experience. Liver Transpl 17:S44-S57.

Mazzaferro V, Regalia E, Doci R, et al. (1996). Liver transplantation for the treatment of small hepatocellular carcinomas in patients with cirrhosis. N Engl J Med 334:693-699.

Mazzaferro V. (2007). Results of liver transplantation: with or with-out Milan criteria? Liver Transpl 13:S44-S47.

Melgert BN, Olinga P, Van Der Laan J, et al. (2001). Targeting dexamethasone to Kupffer cells: effects on liver inflammation and fibrosis in rats. Hepatology 34:719-728.

Meng WC, Pan Y, Zhao X. (2015). Epirubicin-gold nanoparticles suppress hepatocellular carcinoma xenograft growth in nude mice. J Biomed Res 29:486.

Merkel TJ, Jones SW, Herlihy KP, et al. (2011). Using mechanobiological mimicry of red blood cells to extend circulation times of hydrogel microparticles. Proc Natl Acad Sci USA 108:586-591.

Mishra N, Yadav NP, Rai VK, et al. (2013). Efficient hepatic delivery of drugs: novel strategies and their significance. Biomed Res Int 2013.

Morille M, Passirani C, Bonneval EL, et al. (2009). Galactosylated DNA lipid nanocapsules for efficient hepatocyte targeting. Int J Pharm 379:293-300.

Mosafer J, Abnous K, Tafaghodi M, et al. (2017). *In vitro* and *in vivo* evaluation of anti-nucleolin-targeted magnetic PLGA nanoparticles loaded with doxorubicin as a theranostic agent for enhanced targeted cancer imaging and therapy. Eur J Pharm Biopharm 113:60-74.

Movassaghian S, Merkel OM, Torchilin VP. (2015). Applications of polymer micelles for imaging and drug delivery. Wiley Interdiscip Rev Nanomed Nanobiotechnol 7:691-707.

Mudshinge SR, Deore AB, Patil S, et al. (2011). Nanoparticles: emerging carriers for drug delivery. Saudi Pharm J 19:129-141.

Mukherjee B, Chakraborty S, L. Mondal, B.S. Satapathy, S. Sengupta, L. Dutta, A. Choudhury, D. Mandal, Multifunctional drug nanocarriers facilitate more specific entry of therapeutic payload into tumors and control multiple drug resistance in cancer, Nanobiomaterials in Cancer Therapy (2016) 203-225.

Mukherjee B, Chakraborty S, Mondal L, et al. (2016). Multifunctional drug nanocarriers facilitate more specific entry of therapeutic payload into tumors and control multiple drug resistance in cancer. Nanobiomaterials in Cancer Therapy 203-25.

Mukherjee B, Ghosh MK, Hossain CM. (2012). Chemically Induced Hepatocellular Carcinoma and Stages of Development with Biochemical and Genetic Modulation: A Special Reference to Insulin-Like-Growth Factor II and Raf Gene Signaling. HEPATOCELLULAR CARCINOMA - BASIC RESEARCH Edited by Wan-Yee Lau.

Mukherjee B, Santra K, Pattnaik G, et al. (2008). Preparation, characterization and *in-vitro* evaluation of sustained release protein-loaded nanoparticles based on biodegradable polymers. Int J Nanomedicine 3:487.

Nag M, Gajbhiye V, Kesharwani P, et al. (2016). Transferrin functionalized chitosan-PEG nanoparticles for targeted delivery of paclitaxel to cancer cells. Colloids Surf B Biointerfaces 148:363-70.

Nie S, Xing Y, Kim GJ, et al. (2007). Nanotechnology applications in cancer. Annu Rev Biomed Eng 9:257-288.

Panja S, Dey G, Bharti R, et al. (2016). Metal ion ornamented ultrafast light-sensitive nanogel for potential *in vivo* cancer therapy. Chem Mater 28:8598-8610.

Paul W, Sharma CP. (2010). Inorganic nanoparticles for targeted drug delivery. Biointegration of Medical Implant Materials 1:204-236.

Pelicano H, Martin DS, Xu RH, et al. (2006). Glycolysis inhibition for anticancer treatment. Oncogene 25:4633-4646.

Pond SM, Tozer TN. (1984). First-pass elimination basic concepts and clinical consequences. Clin Pharmacokinet 9:1-25.

Priyadarshini K, Keerthi AU. (2012). Paclitaxel against cancer: a short review. Med chem 2:139-141.

Qi L, Xu Z, Chen M. (2007). *In vitro* and *in vivo* suppression of hepatocellular carcinoma growth by chitosan nanoparticles. Eur J Cancer 43:184-193.

Qi WW, Yu H, Guo H, et al. (2015). Doxorubicin-loaded Glycyrrhetinic Acid-modified Recombinant Human Serum Albumin Nanoparticles for Targeting Liver Tumor Chemotherapy. Mol Pharmaceutics 12:675-683.

Qin JM, Yin PH, Li Q, et al. (2012). Anti-tumor effects of brucine immuno-nanoparticles on hepatocellular carcinoma. Int J Nanomedicine 7:369-379.

Ran S, Downes A, Thorpe PE. (2002). Increased exposure of anionic phospholipids on the surface of tumor blood vessels. Cancer Res 62:6132-6140.

Raza A, Sood GK. (2014). Hepatocellular carcinoma review: Current treatment, and evidence-based medicine. World J Gastroenterol 20: 4115-4127.

Reddy LH, Couvreur P. (2011). Nanotechnology for therapy and imaging of liver diseases. J Hepatol 55:1461-1466.

Rockey DC. (2001). Hepatic blood flow regulation by stellate cells in normal and injured liver. Semin Liver Dis 21:337-349.

Ruan G, Feng SS, Li QT. (2002). Effects of material hydrophobicity on physical properties of polymeric microspheres formed by double emulsion process. J Control Release 84:151-160.

Ryu JH, Koo H, Sun IC, et al. (2012). Tumor-targeting multi-functional nanoparticles for theragnosis: new paradigm for cancer therapy. Adv Drug Deliv Rev 64:1447-1458.

Sachdeva MS. (1998). Drug targeting systems for cancer chemotherapy. Expert Opin Investig Drugs 7:1849-1864.

Sahana B, Santra K, Basu S, et al. (2010). Development of biodegradable polymer based tamoxifen citrate loaded nanoparticles and effect of some manufacturing process parameters on them: a physicochemical and *in-vitro* evaluation. Int J Nanomedicine 5:621-630.

Sailema-Palate GP, Vidaurre A, Campillo-Fernández AJ, et al. (2016). A comparative study on poly(?-caprolactone) film degradation at extreme pH values. Polym Degrad Stab 130:118-125.

Sanna V, Roggio AM, Posadino AM, et al. (2011). Novel docetaxel-loaded nanoparticles based on poly (lactide-co-caprolactone) and poly (lactide-co-glycolide-co-caprolactone) for prostate cancer treatment: formulation, characterization, and cytotoxicity studies. Nanoscale Res Lett 6:260.

Satapathy BS, Mukherjee B, Baishya R, et al. (2016). Lipid nanocarrier-based transport of docetaxel across the blood brain barrier. RSC Adv 6:85261-85274.

Schuppan D, Ruehl M, Somasundaram R, et al. (2001). Matrix as a modulator of hepatic fibrogenesis. Semin Liver Dis 21:351-372.

Scripture CD, William FD, Alex S. (2006). Peripheral neuropathy induced by paclitaxel: recent insights and future perspectives. Curr Neuropharmacol 4:165-172.

Sha BY, Gao W, Wang S, et al. (2011). Cytotoxicity of titanium dioxide nanoparticles differs in four liver cells from human and rat. Compos Part B 42:2136-2144.

Sharma G, Valenta DT, Altman Y, et al. (2010). Polymer particle shape independently influences binding and internalization by macrophages. J Control Release 147:408-412.

Shaw TK, Mandal D, Dey G, et al. (2017). Successful delivery of docetaxel to rat brain using experimentally developed nanoliposome: a treatment strategy for brain tumor. Drug Deliv 24:346-357.

Siegel SL, Miller KD, Jemal A. (2018). Cancer statistics, 2018. CA: CA Cancer J Clin 68:7-30.

Sipai ABM, Vandana Y, Mamatha Y, et al. (2012). Liposomes: an overview. J Pharm Sci Innov 1:13-21.

Sitzmann JV, Order SE, Klein JL, et al. (1987). Conversion by new treatment modalities of nonresectable to resectable hepatocellular cancer. J Clin Oncol 5:1566-1573.

Sitzmann JV. (1995). Conversion of unreseetable to resectable liver cancer: An approach and follow-up study. World J Surg 19:790-794.

Sparreboom A, Scripture CD, Trieu V, et al. (2005). Comparative preclinical and clinical pharmacokinetics of a cremophor-free, nanoparticle albumin-bound paclitaxel (ABI-007) and paclitaxel formulated in cremophor (taxol). Clin Cancer Res 11:4136-4143.

Surendran SP, Thomas RG, Moon MJ, et al. (2017). Nanoparticles for the treatment of liver fibrosis. Int. J. Nanomed 12:6997-7006.

Tallury P, Kar S, Bamrungsap S, et al. (2009). Ultra-small water-dispersible fluorescent chitosan nanoparticles: synthesis, characterization and specific targeting. Chem Commun 17:2347-2349.

Tang ZZ. (2006). The meaning and approach to carry out liver metastasis and recurrence research. Chin J Gen Surg 21:761.

Thomas MB, Zhu AX. (2005). Hepatocellular carcinoma: the need for progress. J Clin Oncol 23:2892-2899.

Tian Q, Zhang CN, Wang XH, et al. (2010). Glycyrrhetinic acid-modified chitosan/poly(ethylene glycol) nanoparticles for liver-targeted delivery. Biomaterials 31:4748-4756.

Toh MR, Chiu GNC. (2013). Liposomes as sterile preparations and limitations of sterilisation techniques in liposomal manufacturing. Asian J Pharm Sci 8:88-95.

Tomuleasa C, Soritau O, Orza A, et al. (2012). Gold nanoparticles conjugated with cisplatin/doxorubicin/capecitabine lower the chemoresistance of hepatocellular carcinoma-derived cancer cells. J Gastrointestin Liver Dis 21:1-10.

Torchilin VP, Trubetskoy VS. (1995). Which polymers can make nanoparticulate drug carriers long-circulating? Adv Drug Deliv Rev 16:141-155.

Trojan J, Zangos S, Schnitzbauer AA. (2016). Diagnostics and Treatment of Hepatocellular Carcinoma in 2016: Standards and Developments. Visc Med 32:116-120.

Vaculikova E, Cernikova A, Placha D, et al. (2016). Preparation of hydrochlorothiazide nanoparticles for solubility enhancement. Molecules 21:1005.

Wang H, Cheng G, Du Y, et al. (2013). Hypersensitivity reaction studies of a polyethoxylated castor oil free liposomes based alternative paclitaxel formulation. Mol Med Rep 7:947-952.

Wang H, Thorling CA, Liang X, et al. (2015). Diagnostic imaging and therapeutic application of nanoparticles targeting the liver. J Mater Chem B 3:939-958.

Wang JL, Tang GP, Shen J, et al. (2012). A gene nanocomplex conjugated with monoclonal antibodies for targeted therapy of hepatocellular carcinoma. Biomaterials 33:4597-4607.

Wang L, Yao J, Zhang X, et al. (2018). Delivery of paclitaxel using nanoparticles composed of poly(ethylene oxide)-b-poly(butylene oxide) (PEO-PBO). Colloids Surf B Biointerfaces 161:464-470.

Wang X, Gu X, Wang H, et al. (2018). Enhanced delivery of doxorubicin to the liver through selfassembled nanoparticles formed via conjugation of glycyrrhetinic acid to the hydroxyl group of hyaluronic acid. Carbohydr Polym 195:170-179.

Wang X, Song L, Li N, et al. (2013). Pharmacokinetics and biodistribution study of paclitaxel liposome in Sprague-Dawley rats and beagle dogs by liquid chromatography-tandem mass spectrometry. Drug Res 63:603-606.

Wang Y, Jiang G, Qiu T, et al. (2012). Preparation and evaluation of paclitaxel-loaded nanoparticles incorporated with galactose-carrying polymer for hepatocytes targeted delivery. Drug Dev Ind Pharm 38:1039-1046.

Wise JP, Goodale BC, Wise SS, et al. (2010). Silver nanospheres are cytotoxic and genotoxic to fish cells. Aquat Toxicol 97:34-41.

Wu MC. (2009). Surgical treatment of primary liver cancer. Chin J Gen Surg 3:1-3.

Xie H, Wang H, An W, et al. (2014). The efficacy of radiofrequency ablation combined with transcatheter arterial chemoembolization for primary hepatocellular carcinoma in a cohort of 487 patients. PLoS One 9:e89081.

Xu Z, Chen L, Gu W, et al. (2009). The performance of docetaxel-loaded solid lipid nanoparticles targeted to hepatocellular carcinoma. Biomaterials 30:226-232.

Yatvin MB, Kreutz W, Horwitz BA, et al. (1980). pH-sensitive liposomes: possible clinical implications. Science 210:1253-1255.

Yezhelyev MV, Gao X, Xing Y, et al. (2006). Emerging use of nanoparticles in diagnosis and treatment of breast cancer. The lancet oncology 7:657-667.

Yin C, Evason KJ, Asahina K, et al. (2013). Hepatic stellate cells in liver development, regeneration and cancer. J Clin Invest 123:1902-1910.

You JO, Auguste DT. (2009). Nanocarrier cross-linking density and pH sensitivity regulate intracellular gene transfer. Nano letters 9:4467-4473.

Yu B, Hsu SH, Zhou C, et al. (2012). Lipid nanoparticles for hepatic delivery of small interfering RNA. Biomaterials 33:5924-5934.

Zamboni CG, Kozielski KL, Vaughan HJ, et al. (2017). Polymeric nanoparticles as cancer-specific DNA delivery vectors to human hepatocellular carcinoma. J Control Release 263:18-28.

Zeng N, Hu Q, Liu Z, et al. (2012). Preparation and characterization of paclitaxel-loaded DSPE-PEG-liquid crystalline nanoparticles (LCNPs) for improved bioavailability. Int J Pharm 424:58-66.

Zeng X, Morgenstern R, Nyström AM. (2014). Nanoparticle-directed sub-cellular localization of doxorubicin and the sensitization breast cancer cells by circumventing GST-mediated drug resistance. Biomaterials 35:1227-1239.

Zhang H, Huang N, Yang G, et al. (2017). Bufalin-loaded bovine serum albumin nanoparticles demonstrated improved anti-tumor activity against hepatocellular carcinoma: preparation, characterization, pharmacokinetics and tissue distribution. Oncotarget 8:63311-63323.

Zhang X, Guo S, Fan R, et al. (2012). Dual-functional liposome for tumor targeting and overcoming multidrug resistance in hepatocellular carcinoma cells. Biomaterials 33:7103-7114.

Zhang X, Sun P, Bi R, et al. (2009). Targeted delivery of levofloxacin-liposomes for the treatment of pulmonary inflammation. J Drug Target 17:399-407.

Zhang Z, Liao G, Nagai T, et al. (1996). Mitoxantrone polybutyl cyanoacrylate nanoparticles as an anti-neoplastic targeting drug delivery system. Int J Pharm 139:1-8.

Zhong Y, Meng F, Deng C, et al. (2014). Ligand-directed active tumor-targeting polymeric nanoparticles for cancer chemotherapy. Biomacromolecules 15:1955-1969.

Zhou Q, Ching AKK, Leung WKC, et al. (2011). Novel therapeutic potential in targeting microtubules by nanoparticle albumin-bound paclitaxel in hepatocellular carcinoma. Int J Oncol 38:721-731.

Appendix

International Journal of Biological Macromolecules 112 (2018) 818–830

Contents lists available at ScienceDirect

International Journal of Biological Macromolecules

journal homepage: http://www.elsevier.com/locate/ijbiomac

Preferential hepatic uptake of paclitaxel-loaded poly-(D-L-lactide-*co*-glycolide) nanoparticles — A possibility for hepatic drug targeting: Pharmacokinetics and biodistribution

Dipika Mandal [a], Tapan Kumar Shaw [a], Goutam Dey [b], Murari Mohan Pal [a], Biswajit Mukherjee [a,*], Amal Kumar Bandyopadhyay [a], Mahitosh Mandal [b]

[a] Department of Pharmaceutical Technology, Jadavpur University, Kolkata, West Bengal, India
[b] School of Medical Science and Technology, Indian Institute of Technology Kharagpur, Kharagpur, West Bengal, India

ARTICLE INFO

Article history:
Received 16 September 2017
Received in revised form 12 January 2018
Accepted 2 February 2018
Available online 5 February 2018

Keywords:
Poly-(D-L-lactide-*co*-glycolide) nanoparticles
Paclitaxel
Liver cancer
HepG2 cells
Cytotoxicity
Pharmacokinetics

ABSTRACT

Liver cancer is a leading cause of death related to cancer worldwide. Poly(D-L-lactide-*co*-glycolide) (PLGA) nanoparticles provide prolonged blood residence time and sustained drug release, desirable for cancer treatment. To achieve this, we have developed paclitaxel-loaded PLGA nanoparticles by emulsification solvent evaporation method and evaluated by *in vitro* and *in vivo* studies. The results obtained from *in vitro* study showed that drug loading efficiency was 84.25% with an initial burst release followed by sustained drug release. Cellular uptake and *in vitro* cytotoxicity of the formulated nanoparticles using HepG2, Huh-7 cancer cells and Chang liver cells were also investigated. The formulated nanoparticles showed more cytotoxic effect at lower concentration and were internalized well by HepG2 cells compared to free-drug and marketed formulation. Prolonged half-life and higher plasma and liver drug concentrations of the formulated nanoparticles were observed as compared to free drug and marketed formulation in rats. Thus, paclitaxel-loaded polymeric nanoparticle has shown its potential for the treatment of liver cancer.

© 2018 Elsevier B.V. All rights reserved.

1. Introduction

Cancer, one of the most devastating diseases having a tremendous morbidity and mortality impact in the developing world, caused nearly 8.8 million deaths in 2015 [1]. In 2018, 1,735,350 new cancer cases and 609,640 cancer deaths are expected to occur in the United States [2]. Globally, 1 in 6 deaths is due to cancer. Among all the cancers, liver cancer is common and second-leading cause of cancer deaths after lung cancer [1]. Liver cancer more commonly occurs in sub-Saharan Africa and Southeast Asia than in the US. Men are more susceptible than woman in case of liver cancer [3]. The main causes of liver cancer are chronic infection with hepatitis B virus (HBV), hepatitis C virus (HCV) and alcoholic cirrhosis [4]. Except surgery, chemotherapy is the main treatment for liver cancer. Its clinical application is restricted due to some limitations such as side-effects like non-specific dose-limiting organ toxicities, short circulating half-life, poor solubility, stability and pharmacokinetic properties and development of drug resistance [5]. Thus, there is an urgent need to develop some alternative approach to treat liver cancer which can nullify the existing drawbacks. Recently, polymeric nanoparticles, a novel drug delivery system, may be a promising approach for beginning of new era as chemotherapeutic agent to treat liver cancer. The main advantages of polymeric nanoparticles include increase in water solubility, reduction of side-effects and toxicity, improvement of pharmacokinetic properties and tissue distribution through the leaky neovasculature and premature lymphatic system of tumor cells, improvement of anti-tumor efficacy of anticancer agents [6–8]. Poly-(D-L-lactide-*co*-glycolide) (PLGA) is very useful to develop drug nanocarrier for cancer therapy owing to its high stability, outstanding biocompatibility, biodegradability and low immunogenicity. The United State Food and drug administration (US-FDA) has approved PLGA as harmless for application as pharmaceutical excipients. It has ability for passive targeting of novel drug delivery system with enhanced permeability and retention effect (EPR) [9–12]. Recently, there are many chemotherapeutic agents which are identified as anticancer drugs. Among these drugs, some are available in the market as formulated drugs and some of them are in the clinical trials. Sorafenib, an oral multiple kinase inhibitor, is approved by US-FDA for advanced liver cancer treatment. Another oral multi-kinase inhibitor, regorafenib has also been shown to improve overall survival of advanced liver cancer patients after a phase 3 trial [13]. In 2017, regorafenib has been approved by FDA due to the efficacy and safety. Other liver cancer targeted drugs that have been evaluated in clinical trials include sunitinib and linifanib (multi-targeted tyrosine kinase inhibitor), erlotinib and

* Corresponding author.
E-mail address: biswajit.mukherjee@jadavpuruniversity.in (B. Mukherjee).

https://doi.org/10.1016/j.ijbiomac.2018.02.021
0141-8130/© 2018 Elsevier B.V. All rights reserved.

gefitinib (inhibitors for epidermal growth factor receptor), brivanib (selective inhibitor of fibroblastic growth factor receptor and vascular endothelial growth factor), tivantinib (oral Met receptor tyrosine kinase inhibitor), everolimus (inhibitor of mammalian target of rapamycin) and bevacizumab (humanized monoclonal antibody against vascular endothelial growth factor) [14].

Paclitaxel (PTX) is a powerful anticancer chemotherapeutic agent [15]. PTX is one of the most useful and effective antineoplastic agents for treatment of liver cancer [16]. It is advantageous to use PTX for the treatment of liver cancer over other drugs owing to its broad spectrum antitumor activity, effectiveness on both solid and disseminated tumors and a unique mechanism of action as it stabilizes the microtubule and selectively disrupts the microtubule dynamics, thus inducing mitotic arrest that leads to cell death. PTX binds with β-tubulin and promotes the assembly of microtubules which prevents microtubular depolymerization and causes cell death [17]. It shows activity against several cancers such as advanced ovarian cancer, breast cancer, lung cancer and liver cancer [18,19]. Intravenous infusion of paclitaxel is painful and often causes hypersensitive reactions [20]. Its systemic bioavailability is <8% due to low aqueous solubility (0.3 ± 0.02 g/mL). The low solubility is due to its highly lipophilic nature (log P, 3.96) and bulky polycyclic structure (molecular weight 853 Da). The poor oral bioavailability is also attributed to its significant "first-pass" metabolism by cytochrome P450 in liver and *p*-glycoprotein mediated effluxing by intestinal cells [21]. So, it is important to formulate the paclitaxel to avoid such drawbacks. In the recent years, the use of biodegradable nanomaterials has gained impressive attention to bypass those properties for efficacious treatment [22].

Clinical formulation of PTX (Taxol®) is used with 1:1 mixture of Cremophore EL (polyethoxylated castor oil) and ethanol due to its low aqueous solubility. The solvent is harmful and shows severe toxic effects such as hypersensitivity reactions, nephrotoxicity and neurotoxicity [23–25]. Thus, Cremophore EL free formulation of PTX can eliminate the solvent related toxicity, improve stability, bioavailability and present sustained drug release [26]. Till now, several Cremophore EL free formulations of paclitaxel examples, liposome [27], emulsion [28], cyclodextrin [29], microsphere [30] and polymeric nanoparticles [24] have been developed as alternate delivery system.

However, PTX is always chosen to design in an advanced delivery system to minimize the side-effects and to explain its biomedical action.

The aim of the present study is to develop paclitaxel-loaded poly-(D-L-lactide-*co*-glycolide) nanoparticles for intravenous administration of PTX for prolonged drug release and sustained drug action to successfully treat hepatocellular tumor.

2. Materials and methods

2.1. Materials

Paclitaxel (99.95%) was gifted by Fresenius Kabi Oncology Ltd. (Kolkata, India). PLGA (MW 50,000–75,000; poly-D-L-lactide-*co*-glycolide ratio 85:15) was purchased from Sigma-Aldrich Co (Bengaluru, India) and polyvinyl alcohol (PVA, MW 125,000) was procured from S.D. Fine Chem. Pvt. Ltd. (Mumbai, India). Dichloromethane (DCM) was procured from Merck. Fluorescein isothiocyanate 98% (FITC) was purchased from HiMedia Lab. Dulbecco's Modified Eagle's Medium (DMEM) containing fetal bovine serum (FBS) and antibiotics (1% penicillin streptomycin) were purchased from HiMedia Laboratories Pvt. Ltd. (Mumbai, India). 40,6- Diamidino-2-phenylindole (DAPI) and tetrazolium dye 3-(4,5-dimethylthiazol-2-yl)-2,5-diphenyltetrazolium bromide (MTT) were purchased from Sigma-Aldrich. Human liver hepatocellular carcinoma HepG2 cells were procured from National Center for Cell Science (NCCS, Pune, India). Marketed formulation of paclitaxel (Pacliall® injection 100 mg vial) was purchased from Panacea Biotec Limited, Mumbai, India. All other chemicals and reagents used were of analytical reagent grade.

2.2. Preparation of paclitaxel-loaded nanoparticles

Paclitaxel-loaded PLGA nanoparticles were prepared using multiple-emulsion solvent evaporation method [31,32]. In the first step, 2.5% (*w*/*v*) and 1.5% (w/v) aqueous solutions of PVA were prepared separately. After that, an organic solution of drug and PLGA was prepared in dichloromethane (2 ml). The amounts of drug and polymer used for various formulations were shown in Table 1. Previously prepared 0.5 ml of 2.5% PVA solution was added drop-wise into the drug-polymer mixture and homogenized at 20,000 rpm with a high speed homogenizer (IKA Laboratory Equipment, Model T10B Ultra-Turrax, Staufen, Germany) for 5 min at room temperature and primary emulsion was formed (water-in-oil). This primary emulsion was then added drop-wise into 75 ml of 1.5% PVA solution with constant homogenization at 20,000 rpm for 8 min. PVA is a well-known hydrophilic polymer usually acts as stabilizer [33]. Although PVA has hydrophilic –OH group, it has also a nonpolar vinyl part. Thus, it reduces the surface tension between the aqueous part and the nonpolar non-aqueous part, where vinyl group remains towards non-polar part and OH-group faces towards aqueous part. Thus, it stabilizes primary emulsion. The resulting mixture was stirred overnight using a magnetic stirrer for removal of organic solvent. The nanoparticles were then separated by centrifugation using a cold centrifuge (3K30 Sigma Lab Centrifuge, Merrington Hall Farm, Shrewsbury, UK) at 15,000 rpm for 45 min and washed three times with double distilled water at the same speed for removal of free drug and PVA. The separated nanoparticles were poured in a petridish and kept it at −40 °C overnight. Then the frozen nanoparticles were lyophilized using freeze dryer (Laboratory Freeze Dryer, Instrumentation India Ltd., Kolkata, India) for 8 h. This method has been well-standardized with PVA as stabilizer. In this method, no other cryoprotectant (such as sucrose) was required. Cryoprotectants (such as sucrose, lactose, manitol) mostly function because of the presence of number of poly hydroxyl group. In PVA, there is also the presence of number of hydroxyl group, owing to which it could have acted as cryoprotectant by itself. Finally, the product was collected and kept in an air tight container at 4 °C. We have prepared nanoparticle formulation without drug using the same procedure as discussed above.

FITC containing nanoparticles were also prepared to visualize the distribution of nanoparticles in the cancer cells. FITC-stock solution was prepared by dissolving FITC in ethanol:chloroform (1:3 ratio). During emulsification, 100 μl of this solution was added into the organic phase of drug-polymer mixture and all other steps were same as mentioned above.

2.3. Drug-excipients interaction study by Fourier transform infrared spectroscopy (FTIR)

FTIR (Perkin-Elmer RX-1, USA) was carried out to observe infrared spectra of pure drug (paclitaxel), PLGA, PVA, their physical mixture, blank formulation and prepared nanoparticles. During analysis, sample was mixed with potassium bromide in the ratio of 1:100 and compressed into pellets using a hydraulic press at 5.5 metric ton pressure. The pellets were scanned with FTIR spectroscope in a range of 4000–400 cm^{-1}.

2.4. Differential scanning calorimetry (DSC) study

The physical state of PTX and PTX in PTX-loaded PLGA nanoparticles were investigated by differential scanning calorimetry (Jade DSC, Perkin Elmer, Japan). The samples were weighed from 1.18 to 2.784 mg and heated at a scanning rate of 10 °C min^{-1} under dry nitrogen flow at 20 ml/min over a temperature range of 32 °C to 310 °C [34].

Table 1
Various compositions and yield percentage of prepared formulations.

Formulation code	Amount of drug (mg)	Amount of PLGA (mg)	Amount of FITC (μl)	Theoretical drug loading (%)	Actual drug loading (%) ± SD[a] (n = 3)	Loading efficiency (%) ± SD[a] (n = 3)	Yield (%)[a] ± SD (n = 3)
NP1	2.5	240		1.03	0.69 ± 0.11	67.47 ± 10.29	55.22 ± 3.05%
NP2	5	240		2.04	1.58 ± 0.15	77.69 ± 2.42	63.91 ± 5.27%
NP3	10	240		4.00	3.37 ± 0.19	84.25 ± 4.95	72.62 ± 9.96%
FITC-NP3	10	240	100	4.00	3.31 ± 0.15	82.75 ± 5.24	

[a] SD means standard deviation.

2.5. Physicochemical characterization of nanoparticles

2.5.1. Drug loading and loading efficiency

Drug loading was carried out to identify the amount of drug entrapped in the experimental formulations. The required amount of nanoparticles (2 mg) was suspended with 2 ml of water-acetonitrile mixture (40:60 v/v). The mixture was vortexed for 5 min followed by shaking in an incubator shaker for 3–4 h at 37 °C. Finally, it was centrifuged at 10,000 rpm for 5 min and the supernatant was collected. After appropriate dilution, the absorbance was measured spectrophotometrically at 218 nm. The same procedure was also followed for blank formulation and absorbance was measured. The actual amount of drug present in nanoparticles was calculated from the difference between the absorbance of nanoparticle formulation and blank formulation. The percentage of actual drug loading and loading efficiency were calculated using the following equations:

$$\text{Percentage of actual drug loading} = \frac{\text{Amount of drug present in nanoparticles}}{\text{Weight of nanoparticle sample analysed}} \times 100$$

$$\text{Percentage of loading efficiency} = \frac{\text{Actual drug loading}}{\text{Theoretical drug loading}} \times 100$$

2.5.2. Yield percentage

The amount of nanoparticles obtained was determined with respect to the total amount of raw materials used for the formulation. The lyophilized nanoparticles were weighed and the percentage yield of the formulations was calculated by using the following formula:

$$\text{Percentage yield} = \frac{\text{Amount of nanoparticles obtained}}{\text{Total amount of drug and polymer used}} \times 100$$

2.5.3. Particle size, size distribution and zeta potential

The particle size distribution of nanoparticles is important to understand size range of the particles. Zeta potential is the measurement of surface charges of nanoparticles which implies the stability of colloidal dispersion. Average particle size, size distribution and zeta potential of paclitaxel-loaded PLGA nanoparticles were studied by dynamic light scattering technique (Zetasizer Nano ZS90, Malvern Instrument, Malvern, UK). The analysis was performed at 25 °C with scattering angle of 90°. Samples were dispersed with Milli-Q water before observation [32].

2.5.4. Surface morphology by field emission scanning electron microscopy (FESEM)

Surface morphology of the nanoparticles was analyzed using field emission scanning electron microscope (Model-JSM-6700F; JEOL, Tokyo, Japan). The samples were coated with platinum under vacuum for 6 min before observation [35].

2.5.5. Transmission electron microscopy (TEM)

Drug distribution and internal morphology of nanoparticles were determined by transmission electron microscope (FEI type FP5018/40 Tecnai G2 Spirit Bio twin, Praha, Czech Republic). Small amount of nanoparticles were uniformly distributed in Milli-Q water and a drop was placed on a carbon coated grid. The grid was then air-dried overnight and examined using TEM.

2.6. In vitro drug release and release kinetics

In vitro drug release study was carried out in phosphate-buffered saline (PBS), pH 7.4 containing 0.5% sodium lauryl sulfate [36] to check the release of the drug from the formulations. To see the drug release, we have taken 5 mg of the prepared nanoparticles in a microcentrifuge tube containing 2 ml of release medium. The tube was placed in an incubator shaker at 37 °C. At different time intervals (0.5, 2, 4, 6, 8, 24, 48, 72, 168, 360, 528 and 720 h), the tube was removed from incubator shaker followed by centrifuged at 15000 rpm for 10 min. The supernatant portion of the sample was collected from the tube. The tube was again filled up with 2 ml of fresh medium and the nanoparticles were resuspended and incubated under the same condition as mentioned above. The absorbance of the supernatant of the collected sample was measured using a UV spectrophotometer at 218 nm. The concentration of the drug was calculated from the calibration curve. The same procedure was repeated in three times to check the reproducibility.

We have used different mathematical models such as zero order, first order, Higuchi, Korsmeyer-Peppas, and Hixon Crowell model to evaluate *in vitro* drug release kinetic patterns using drug release data. The best kinetic model was selected based on the highest correlation coefficient (R^2) values, calculated by using Microsoft Excel software [37,38].

2.7. Hydrolytic stability study

Required amount (10 mg) of NP3 and pure PTX were taken separately in 2 ml buffer of different pH (3.0, 5.0, 7.4 and 9.0) to measure the hydrolytic degradation of nanoparticles as compared with pure drug. Buffers used were citrate buffer pH 3 and 5, phosphate buffered saline pH 7.4 and sodium bicarbonate buffer pH 9. The solutions were kept in an incubator at 37 ± 2 °C with mild shaking. After the scheduled time intervals that is, 7th day, 14th day, 21st day and 28th day, the samples were removed from incubator, centrifuged and washed two times with double distilled water and dried in speed vac for 30 min and then mass of nanoparticles was measured. The incubation medium was completely replaced with fresh medium. For determination of mass loss, the weight of each sample was carefully measured before the hydrolytic degradation measurement. After drying, the weight of the samples was taken to evaluate the change of weight. The weight change was calculated according to the following formula [39,40]:

$$\text{Weight change}\% = \frac{W_0 - W_t}{W_0} \times 100$$

where, W_0 and W_t represent the initial weight and the weight at time t respectively.

2.8. Cancer cell culture and culture condition

Human liver hepatocellular carcinoma HepG2/Huh-7 cells were cultured in Dulbecco's Modified Eagle's Medium (DMEM) containing fetal bovine serum (FBS) and antibiotics (1% penicillin streptomycin). Normal Chang liver cells were cultured similarly in Minimum Essential Medium (MEM) medium. Cancer cells were maintained at 37 °C in CO_2 incubator. The atmosphere inside the incubator was kept humidified. Cells were grown in T-25 culture flask and taken for further experiments.

2.9. (4,5-Dimethylthiazol-2-yl)-2,5-diphenyltetrazolium bromide assay (MTT assay)

MTT assay was performed in cancer cells [41] to evaluate anti-proliferative potential of free drug, marketed formulation of paclitaxel (Pacliall®) and NP3 (selected as the best experimental formulation upon physicochemical evaluation). We have now performed MTT assay using multiple cell lines, HepG2 cells and Huh-7 cells and further, in normal cell type (Chang liver cells). Human liver cancer (HepG2, Huh-7) cells and normal cell type (Chang liver cells) were cultured, collected and resuspended in complete DMEM medium (for HepG2, Huh-7) and MEM (Chang liver cells) medium. 2.0×10^3 cells were seeded in each well of 96 well plates. After overnight incubation, complete medium was removed and incomplete medium containing free paclitaxel/Pacliall®/NP3 (Dose dependent treatment) was added in each well. After 48 h of incubation, drug containing medium was discarded and MTT solution (1 mg/ml) was added. After 4 h of incubation, MTT solution was discarded and 100 μl DMSO was added. After 20 min, optical density was measured at 560 nm by plate reader (Biorad, Hercules, CA, USA).

2.10. Cellular uptake assay

Cellular uptake study was performed according to earlier reported method [42] to evaluate the entry of NP3 inside HepG2 cancer cells. Briefly, cells were cultured on sterile lysine-coated cover slips. After attaining the 50–60% confluence, cells were starved with incomplete medium. Cells were then treated with low doses of FITC conjugated NP3 for 1 h and 4 h. Then, cells were incubated in 4% formalin solution followed by washing with sterile PBS and staining with DAPI. Florescent images were captured by using Zeiss Observer microscope (Carl Zeiss, Oberkochen, Germany) at 20× magnification. For quantitative uptake, HepG2 cells were grown in 13 mm petridish at a concentration 10^6 cells/well for a period of 24 h. After that, FITC conjugated paclitaxel-loaded nanoparticle was added and the cells were incubated with the formulation for different time periods such as 1 h and 4 h. Then the cells were collected by trypsinization and suspended in PBS for analysis by flow cytometry (FACS Canto II cell sorter, BD Biosciences, San Jose, CA) using FACS Diva Software (BD Biosciences) to measure cellular uptake of nanoparticles. Cells without treatment were considered as control.

2.11. Lipid peroxidation

Lipid peroxidation in HepG2 cells and normal liver cells (Chang liver cells) was estimated by the method available [43]. Malondialdehyde (MDA), a product of lipid peroxidation was determined spectrophotometrically by using Thiobarbituric Acid-Reactive Substances (TBARS). Lysate supernatant (0.2 ml) was mixed with 0.8 ml of phosphate buffered saline (pH 7.4) followed by 0.025 ml of butylated hydroxyl toluene solution (8.8 g l^{-1}) and 0.5 ml of 30% trichloroacetic acid. The mixture was incubated at 37 °C for 1 h. From the above solution 1 ml was mixed with 0.25 ml of 1% thiobarbituric acid in 0.05 N NaOH and 0.075 ml of 0.1 M EDTA. The solution was vortexed and heated on a water-bath at 95 °C for 20 min and then cooled under tap water. The absorbance of the mixture was read at 532 nm and the calculated lipid peroxidation value was expressed in nM MDA/h/mg protein using a molar extinction coefficient of 1.56×105/M/cm [44].

2.12. In vivo study

2.12.1. Plasma and liver pharmacokinetic study

Pharmacokinetic studies were performed using Sprague-Dawley rats (male) with an average body weight 150 ± 20 g to investigate various pharmacokinetic parameters of drug in plasma and to determine hepatic drug concentration upon i.v. administration from NP3, marketed formulation (Pacliall®) and free drug suspension. The study protocol was approved by Institutional Animal Ethical Committee (IAEC), Jadavpur University, Kolkata and the study was conducted following the IAEC guideline. The animals were housed and maintained under standard laboratory conditions as mentioned below. The temperature and relative humidity (RH) were maintained at 25 ± 2 °C and 55 ± 5%, respectively. The animals were maintained in 12 h light and dark cycle [45]. The animals were fasted for 12 h with free access of water before sacrifice. The animals were divided into four groups. First group of animals was treated with nanoparticle formulation (NP3), the second group of animals received commercial paclitaxel formulation and animals of the third group received free drug suspension. Doses were calculated as equivalent dose of 5 mg/kg body weight of rat [46]. The fourth group of animals received no treatment and was considered as control group. The animals of group A-C were treated with the experimental formulations (NP3), Pacliall® and free drug containing equivalent amount of drug by intravenous injection in tail vein. After the scheduled time intervals (15 min, 30 min, 1 h, 2 h, 4 h, 8 h, 10 h, 12 h, 24 h and 48 h), the animals were anaesthetized and sacrificed. Around 0.5 ml of blood was collected by terminal heart puncture of the animals and placed in microcentrifuge tube containing small amount of EDTA solution. Plasma was separated immediately using centrifugation at 5000 rpm for 6 min at 4 °C. We have also collected the liver of corresponding animals at the same time intervals. The plasma and liver organs were preserved in −80 °C until analysis. The concentrations of PTX upon treatment of NP3, marketed formulation (Pacliall®) and free drug suspension were estimated by tandem liquid chromatography-mass spectroscopy (LC-MS/MS) [47].

2.12.2. Sample analysis by LC-MS/MS

PTX stock solution was prepared by serial dilution with HPLC grade methanol. Calibration control (CC) and quality control (QC) samples were prepared by spiking the working stock solutions in blank plasma. Here, protein precipitation technique was used to extract the CC, QC and PTX from the study samples. Protein of plasma sample (100 μl) was precipitated with 300 μl ice cold 50:50 acetonitrile-methanol mixture containing 200 ng/ml docetaxel as internal standard (IS). The mixture was vortex-mixed for 10 min, centrifuged at 10,000 rpm at 4 °C for 5 min. Supernatant (100 μl) was mixed with 100 μl of water and loaded into LC-MS/MS (LC: Shimadzu Model 20AC, MS: AB-SCIEX, Model: API4000, Software: Analyst 1.6). Analytes were eluted using YMC Triat C18 column (30×2.1 mm, 5 μ) and gradient elution technique of two mobile phases (mobile phase A: 0.1% formic acid in water and mobile phase B: 0.1% formic acid in methanol-acetonitrile-water mixture (45:45:10)) was conducted with injection volume 20 μl, flow rate 0.8 ml/min and total run time 3.0 min. Liver samples were weighed and diluted with four times water, homogenized and processed following the above mentioned protein precipitation technique using liver homogenate. Plasma data were plotted against time and various pharmacokinetic parameters such as maximum plasma concentration (C_{max}), area under curve to the last measurable concentration (AUC_{0-t}), half-life ($t_{1/2}$), clearance, steady state volume of distribution (V_{ss}) and mean residence time (MRT) were determined by WinNonlin software (Certara, Princeton, NJ). Further, hepatic drug concentration was also determined.

2.13. Statistical analysis

All the experimental works were carried out at least three times for checking reproducibility. Data was expressed as the mean ± standard deviation (SD). Statistical significance was evaluated using one-way ANOVA followed by Tukey *post hoc* test using Origin Pro 8 software (Origin Lab, Northampton, MA). Differences were considered statistically significant when $p < 0.05$ at 95% confidence level.

3. Results

3.1. FTIR study

FTIR spectroscopy was carried out to investigate the interactions between drug and other excipients [48]. Fig. 1 (A–G) shows the FTIR spectra of drug, all the excipients and formulations (with or without PTX). Pure PTX showed characteristic peaks at 3440 cm^{-1} as N—H stretching vibration and at 2944 cm^{-1} for CH_2 asymmetric and symmetric stretching vibrations. The peak found at 1720 $cm^{-1}$is assigned to C═O stretching vibration from ester group. C—N stretching and C—O stretching vibrations produced peaks at 1246 $cm^{-1}$and at 1072 cm^{-1} respectively. Peaks at 980 cm^{-1} and 710 cm^{-1} were for C—H in-plane deformation and C—H out-of-plane/C—C═O deformation, respectively. PLGA showed characteristic peaks at 3508 cm^{-1} for O—H, 2998 cm^{-1} for C—H and 1754 cm^{-1} for C—O stretching bands, respectively. PVA produced characteristics peaks at 3450 cm^{-1} for O—H, 2930 cm^{-1} for C—H, 1738 cm^{-1} for C═O stretching bands and 1096 cm^{-1} for C—O stretching band. It was observed that all the characteristic bands of drug, PVA and PLGA were present in their physical mixture. It suggests that there was no chemical interaction between the drug and the excipients. Missing of the peaks of drug in nanoparticle formulation reveals that the nanoparticles had no free drug on the surface. Small shifting of peaks was found in nanoparticle formulation. Shifting of bands from 1754 to 1756 cm^{-1} and 750 to 752 cm^{-1} for PLGA and that from 1096 cm^{-1} to 1088 cm^{-1} for PVA was observed. Those siftings might be due to the formation of some weak physical bonds such as weak hydrogen bond, van der Waals force of attraction or dipole-dipole interaction.

3.2. DSC study

DSC was performed to confirm the physical state of PTX in the formulation and interaction between the drug and other excipients. The DSC thermogram (Fig. S1) of PTX showed a melting endothermic peak at about 212.25 °C which is assigned to the melting temperature of PTX. The drug-loaded nanoparticle formulation also showed an endothermic peak at the same position, suggesting that drug in the formulation and free-drug was in same physical state. But blank formulation had no peak.

3.3. Drug loading and loading efficiency

Increasing amount of drug showed increasing amount of drug loading in the present study. It was found to be saturated at a drug: polymer ratio 1:24 (Table 1). Hence no further formulations have been reported here. The drug loading of NP1, NP2 and NP3 were found to be 0.69 ± 0.11%, 1.58 ± 0.15% and 3.37 ± 0.19%, respectively. Loading efficiencies of the formulations varied from 67.47 ± 10.29% to 84.25 ± 4.95%. NP3 had highest percentage of drug loading and loading efficiency as compared to the other experimental formulations. The yield percentage of NP1, NP2 and NP3 were 55.22 ± 3.05%, 63.91 ± 5.27% and 72.62 ± 9.96% respectively (Table 1).

3.4. Particle size and zeta potential

The average particle sizes of different formulations varied from 308 nm to 369.5 nm as shown in Table 2 and Fig. S2. The polydispersity indices of different formulations were shown to vary from 0.156 to 0.419 and zeta potential values had a variation between −10.70 and −7.60 mV (Table 2). Zeta potential was found to decrease with an increasing amount of drug in the experimental formulation.

3.5. FESEM and TEM study

The morphological characteristics of PTX-nanoparticles were examined with FESEM and TEM. Particles were spherical in shape with orange peel like surface. All the particles were in nanometer size range with a variable distribution pattern (Fig. 2). In some formulations, some rod shaped PTX-crystals were detected, as PTX owing to its poor solubility is often difficult to remove. TEM images (Fig. 3) show that drug particles (as seen by black spots) were distributed throughout the formulation.

3.6. Drug release and release kinetics

In vitro drug release profile of various formulations shows that the formulations had a biphasic drug release profile as characterized by an initial burst release within 8 h followed by a slow and continuous sustained drug release as shown in Fig. 4 (A). The initial burst release might be due to the dissolution and diffusion of drug that was present closed to the inner surfaces of the nanoparticles followed by sustained release due to the drug diffused from the core of the polymer matrix. Variable particle sizes might play a role into it by varying drug diffusion pathways [49]. After 30 days of drug release study, it was observed that cumulative percentages of drug released from NP1, NP2 and NP3 were 89.41 ± 4.46%, 52.61 ± 2.62% and 31.22 ± 1.56% respectively. Drug released from NP3 was comparatively slower than the other two formulations *i.e.*, NP1 and NP2.

The correlation coefficient (R^2) and release exponent "n" (wherever applicable) were obtained from various drug release kinetic models tested for experimental formulations (Table 3). Drug release data were fitted in different kinetic equations for different formulations. In case of NP1 and NP3, Korsmeyer-Peppas kinetic model ($R^2 = 0.967$ and 0.977 respectively) indicated good linearity as compared to the other models whereas NP2 represented good linearity in Higuchi kinetic model ($R^2 = 0.945$).

3.7. Hydrolytic degradation study

The biodegradability of the PLGA-nanoparticles was estimated from the increase in their weight loss following hydrolytic degradation. Hydrolytic stability study demonstrated that pH significantly affects the weight loss. With decreasing pH of the medium the hydrolysis of the formulation increased. After one week study, mass loss at pH 9 was 5.66 ± 0.44%, at pH 7.4 was 8.45 ± 0.70%, at pH 5 was 11.82 ± 0.99% and at pH 3 was 19.62 ± 1.13% (Fig. 4B) respectively. There was no significant mass loss of pure PTX observed all over the study (not shown in Fig. 4B).

3.8. MTT assay

The anti-proliferative effects of free drug, Pacliall®, NP3 and blank formulation were performed by MTT assay using HepG2 cells, Huh-7 cells and normal liver parenchymal cells (Chang liver cells). After 48 h incubation, rate of cell death increased with increasing concentration of NP3 which was comparable with Pacliall® and free drug (Fig. 5 (A–C)). The inhibitory concentration (IC_{50}) values of NP3, Pacliall® and free drug in HepG2 cells were 8.5 nM, 24.0 nM and 26.4 nM, respectively and in Huh-7 cells, the IC_{50} values were 12.2 nM, 27.3 nM and 31.1 nM

respectively. The IC_{50} value of NP3 in Huh-7 cells was 1.4 fold more than HepG2 cells. All the treated samples showed dose-dependent cell cytotoxicity. The cytotoxic effect of NP3 in all the cell types was found to be more than those of Pacliall® and free drug. Further, NP3, Pacliall® and free drug had more cytotoxic effect in HepG2 cells and Huh-7 cells as compared to human normal liver parenchymal cells (Chang liver cells). Moreover, there was no effect of the excipients used in the formulation on the cytotoxicity of PTX as there was no cell death detected from blank formulation (without drug).

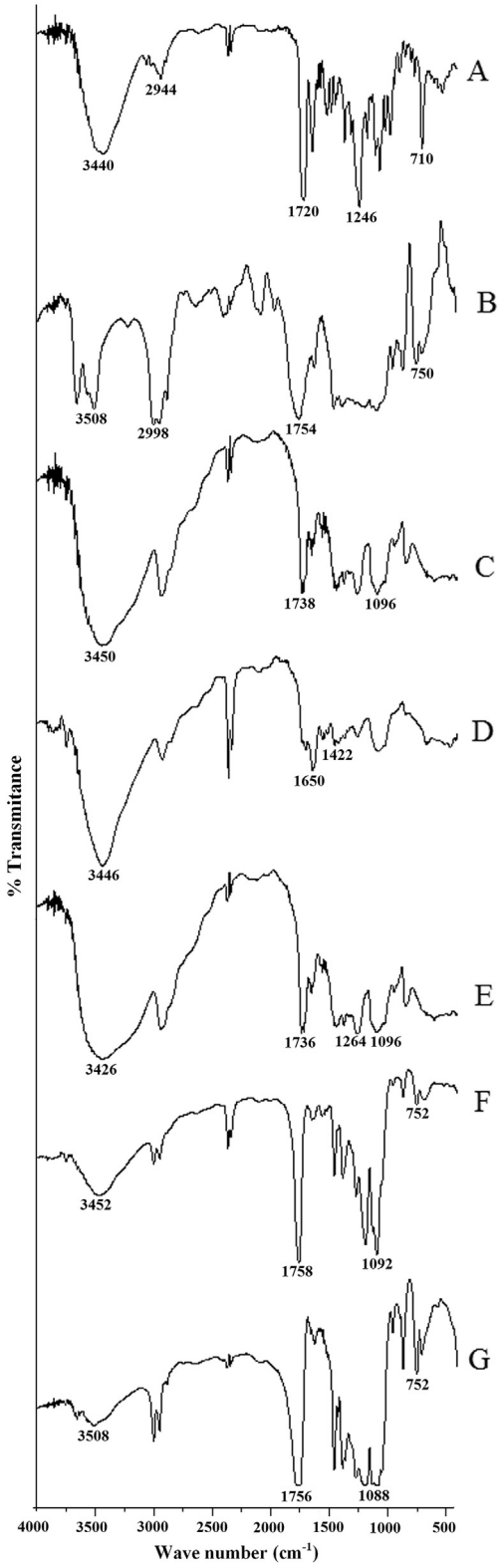

Fig. 1. FTIR spectrum of paclitaxel (A), PLGA (85:15) (B), PVA (C), mixture of PLGA and PVA (D), mixture of drug, PVA and PLGA (E), blank formulation (F) and formulation NP3 (G).

Table 2
Particle size, PDI and zeta potential of different formulations.

Formulation code	Mean particle size (nm)[a]	Polydispersity index[a]	Zeta potential (mV)[a]
NP1	369.5 ± 10.75	0.156 ± 0.046	−7.60 ± 0.19
NP2	317.0 ± 1.84	0.406 ± 0.007	−8.95 ± 0.51
NP3	308.6 ± 6.22	0.419 ± 0.009	−10.70 ± 0.21

[a] Data show mean ± standard deviation (n = 3).

3.9. Cellular uptake study

HepG2 cells were used to observe the cellular uptake of dye containing drug loaded nanoparticle (NP3) using confocal fluorescence microscopy. Fig. 5D shows that the intensity of fluorescence was increased in HepG2 cells with increasing incubation time from 1 h to 4 h. The images show that nanoparticles were internalized and distributed well into cellular cytoplasm, suggesting that PTX-loaded nanoparticles could enter into the hepatic cells. The data obtained from flow cytometric analysis, it was observed that uptake of the formulation within the HepG2 cells increased in a time dependent manner as median intensity for FITC uptake for controlled, after 1 h and 4 h treatment were found to be 518, 1229 and 2486 respectively (Fig. 6).

3.10. Lipid peroxidation

Lipid peroxidation by free radicals generates TBARS that can be measured by malondialdehyde (MDA) levels. An elevation of MDA concentration was found in HepG2 cells as compared to normal liver cells and control cells. The MDA concentration in HepG2 cell line was 6.33 ± 0.36 nM/mg protein and that in normal liver cells was 5.88 ± 0.39 nM/mg protein. A marked elevation ($p < 0.05$) in lipid peroxidation (as assessed by MDA level) in NP3 treated HepG2 cells was observed as compared to NP3 treated normal liver cells (Chang liver cells) (Fig. 7). NP3 treatment predominantly enhanced lipid peroxidation level both in normal and in HepG2 cells. In HepG2 cells, it was found to show more toxicity as assessed by lipid peroxidation level.

3.11. Pharmacokinetic study using LC-MS/MS

After intravenous (i.v) administration of single dose of free drug, Pacliall® (marketed formulation) and nanoparticle (NP3), (equivalent dose of 5 mg/kg of PTX) various pharmacokinetic parameters were analyzed using LC-MS/MS and summarized in Table 4. From the plasma drug concentration-time profile (Fig. 8), it was found that the plasma drug level of free drug increased rapidly after 0.25 h of i.v. injection than NP3 and Pacliall®. Through-out the study, after 0.5 h, the plasma concentration of NP3 remained comparatively higher than free drug and Pacliall® and then declined slowly. After 48 h, the plasma drug concentration of NP3 was found to be 14.91 fold and 4.58 fold higher than free drug and Pacliall®, respectively. AUC_{0-t} value of NP3 (2915.46 ± 145.54) was significantly higher ($p < 0.05$) than that for free drug (1272.95 ± 63.54) and Pacliall® (2250.84 ± 112.36). Plasma half-life ($t_{1/2}$) of NP3 was found to be higher than free drug and Pacliall® (2 fold and 2.25 fold respectively). MRT value of NP3 increased by 3.36 and 1.6 fold, respectively than the value for free drug and Pacliall®. Drug clearance of NP3 decreased by 65.36% and 38.46% as compared to free drug and Pacliall®, respectively.

Concentration of drug in liver was studied up to 8 h after i.v injection. At 8 h, hepatic drug concentration from NP3 was found to be 12.13 fold and 3.08 fold higher than free drug and Pacliall®, respectively (Fig. 9).

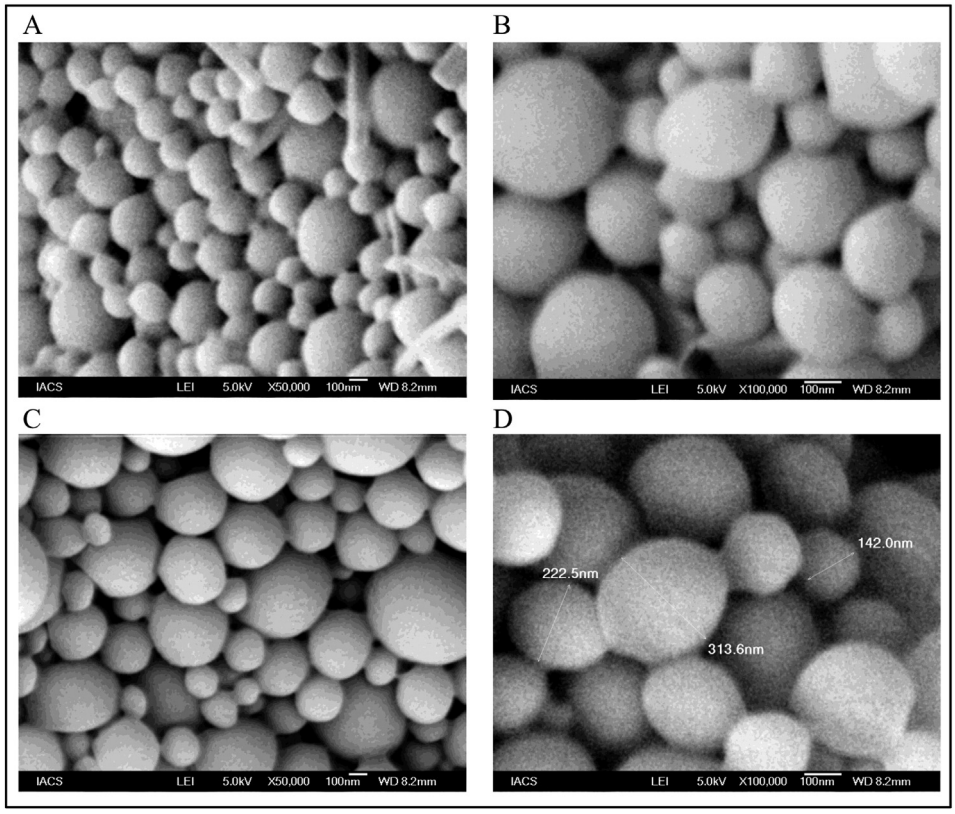

Fig. 2. FESEM photograph of formulation NP1 at 50,000× (A), formulation NP2 at 100,000× (B), formulation NP3 at 50,000× (C) and formulation NP3 at 100,000× (D).

Concentration of NP3 was more than that of free drug/Pacliall® in liver of rats at all the study points except at 0.25 h after injection, where concentration Pacliall® was higher than NP3/free drug. Data suggest that higher amount of drug accumulated in liver after i.v. administration of NP3 as compared to free drug/Pacliall® treated rats.

4. Discussion

FTIR spectroscopy was used to study the interactions between the drug and the excipients. Presence of characteristic peaks of the drug, PLGA and PVA in the physical mixtures reveals that there was no chemical interaction between the drug and the excipients (Fig. 1). Though, minor shifting of few peaks was found which might be due to the formation of weak hydrogen bonding, van der Waals forces or dipole-dipole interaction [32]. Such physical interactions might help for formation of spherical structure and sustained release of drug from the nanoparticles [50]. There was no peak of drug observed in nanoparticle formulation, suggesting non availability of free drug on the surface of the nano formulations [32]. In DSC study, the presence of endothermic peak of drug in nanoparticle formulation (Fig. S1) revealed that the drug was encapsulated and had the same physical state as the free drug. Endothermic peak of the drug was not present in the formulations (without drug) and it suggests the absence of drug in the formulation. The result further confirmed that there was no chemical interaction between the drug and the excipients.

Paclitaxel-loaded nanoparticles were prepared by using emulsification solvent evaporation method. In this work, we have prepared different formulations by gradually increasing the amount of drug and observed the percentage of drug loading and loading efficiency to get optimized formulation. We have initially observed that the percentage

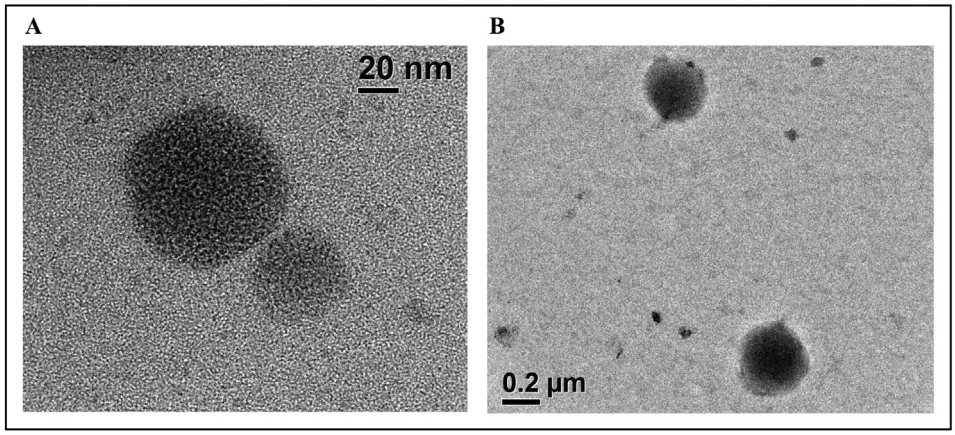

Fig. 3. Transmission electron microscopic images of the optimized formulation (NP3); small size particles (A) and large size particles (B).

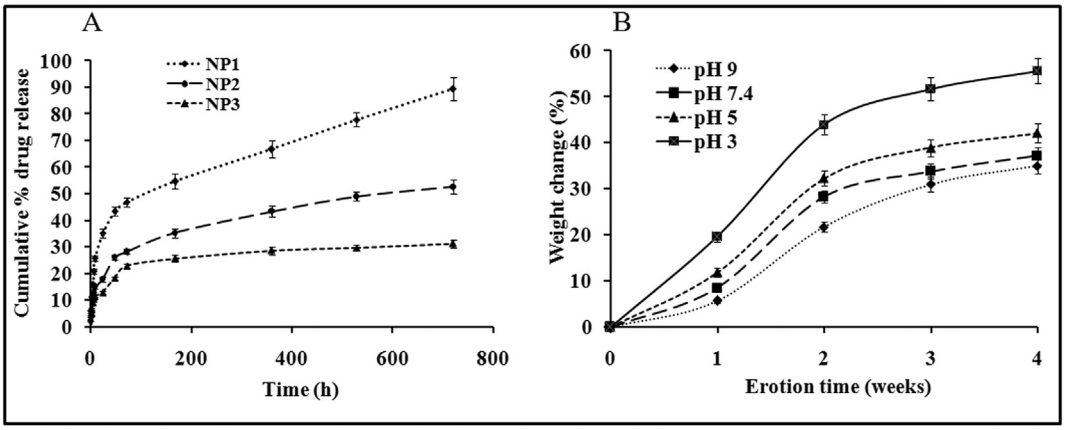

Fig. 4. *In vitro* release profiles of PTX from NP1, NP2 and NP3 in phosphate buffer, pH 7.4. Data show mean ± standard deviation of three different experiments in triplicate (A), Weight change of PLGA nanoparticles at different pH (B).

of drug loading and loading efficiency increased with increasing amount of drug in the formulations (Table 1). But, after a certain amount of drug incorporation, percentage of drug loading and loading efficiency did not increase with increasing amount of drug any further as because polymer matrix has also the limit to accommodate maximum amount of drug (saturation point) in the polymeric network [32]. Maximum drug loading of the experimental formulations was thus optimized. Thus, out of the various experimental formulations, NP3 was considered as the best formulation in terms of different physicochemical data and has been considered for further investigation. With an increasing amount of drug in formulation, percentage yield also increased. However, percentage yields were little less due to recovery problem. Sticky PLGA was adhered to the homogenizer and the quantities of excipients were also less. This problem might be minimized if the formulations were prepared in a large quantity.

Submicron size particles were obtained experimentally (Fig. S2). The sizes of the different formulations varied from 308.6 nm to 369.5 nm (Table 2). PDI was used to investigate distribution pattern of nanoparticles. The value reflects size distribution of nanoparticles [51]. The formulations with a wider range of particle sizes have higher PDI values, while those comprising of evenly sized particles have lower PDI values [52]. In this study, values of PDI (<0.5) indicate that the formulations had a wider distribution pattern within a variable submicron size range.

Zeta potential of various formulations varied from −7.60 to −10.70 mV (Table 2) (Fig. S2). Zeta potential value above +30 mV and/or below −30 mV suggests that the particles remain in a suspended state for longer period of time and avoid rapid agglomeration in suspended state [53,54]. The experimental data suggest that the nanoparticles should be preserved in lyophilized form and reconstituted before use.

Table 3
In vitro drug release kinetic equations, R^2 values and drug release exponent 'n' of various formulations.

In vitro release kinetics	NP1	NP2	NP3
Zero-order kinetics	$y = 0.101\times + 24.70$ $R^2 = 0.825$	$y = 0.063\times + 14.32$ $R^2 = 0.804$	$y = 0.033\times + 12.18$ $R^2 = 0.708$
First-order kinetics	$y = -0.001\times + 1.889$ $R^2 = 0.957$	$y = -0.000\times + 1.932$ $R^2 = 0.873$	$y = -0.000\times + 1.943$ $R^2 = 0.736$
Higuchi kinetics	$y = 2.905\times + 14.08$ $R^2 = 0.948$	$y = 1.849\times + 7.450$ $R^2 = 0.945$	$y = 0.997\times + 8.295$ $R^2 = 0.887$
Korsmeyer-Peppas kinetics	$y = 0.349\times + 0.985$ $R^2 = 0.967$ $n = 0.349$	$y = 0.407\times + 0.645$ $R^2 = 0.933$ $n = 0.407$	$y = 0.266\times + 0.780$ $R^2 = 0.977$ $n = 0.266$
Hixson-Crowell kinetics	$y = -0.002\times + 4.241$ $R^2 = 0.930$	$y = -0.001\times + 4.407$ $R^2 = 0.851$	$y = -0.000\times + 4.444$ $R^2 = 0.727$

FESEM images (Fig. 2) showed that the size of the particles were in below 300 nm with spherical in shape with smooth surfaces. TEM study (Fig. 3) showed that drug distribution occurred in the particle throughout.

Cumulative percentage of drug release showed initial rapid release of drug followed by slow release from all the experimental formulations during 30 days (total period of study) (Fig.4 (A)). Comparatively higher cumulative amount of drug released from NP1 (89.41 ± 4.46%) and NP2 (52.61 ± 2.62%) than NP3 (31.22 ± 1.56%). Small particles below 100 nm range of the formulation might provide faster drug release to meet up immediate need of therapeutic drug level, whereas larger particles might provide more sustained drug release owing to the larger diffusion pathway [55]. Drug release performance from nanoparticles depends on the presence of larger and smaller particles in a formulation. Although NP3 shows the slowest drug release and had the smallest size in terms of average particle size, higher surface charge (zeta potential) on the particle surface as compared to NP1 and NP2, might retard drug release from the formulation predominantly compared to NP1 and NP2.

In drug release study, we found wide variation in drug release patterns from the three formulations (NP1, NP2 and NP3). NP1 when released about 90% drug, at the same time point NP2 showed about 45% drug release and NP3 showed about 30% drug release. Since, NP2 and NP3 showed predominantly slow drug release patterns as compared to NP1, no further study was conducted as on long-term release study, the formulation may erode and lead to erroneous results.

In vitro drug release kinetic data (Table 3) revealed that NP1 and NP3 were best fitted with Korsmeyer-Peppas model and NP2 followed Higuchi kinetics. Thus, the release kinetic data revealed that drug release from nanoparticle formulations might follow binary mechanism. To understand drug release mechanism, the drug release data were fitted to Korsmeyer-Peppas model which is related with the function of time for diffusion controlled mechanism [54] and depicted by the equation as $M_t/M_a = Kt^n$, where M_t/M_a is the fraction of drug release, t is time, K is rate constant and n is release exponent. If n = 0.85, the release is zero order or case II relaxational release transport. When n is ≤0.43, the release follows Fickian diffusion-controlled drug release and 'n' value between 0.43 and 0.85 indicates that drug release follows an anomalous diffusion (drug diffusion in the hydrated matrix and the polymer chain relaxation). In our study, 'n' values of all the formulations (NP1 and NP3) were <0.43. This suggests that the drug release followed Fickian diffusion mechanism [56].

The variation of degradability at different pH values can be correlated with the effect of pH on hydrophilicity. The polymer at alkaline pH (pH 9) kept its non-polar (hydrophobic) character, due to entrapment of hydroxyl ions by the ester groups on the film surface, which

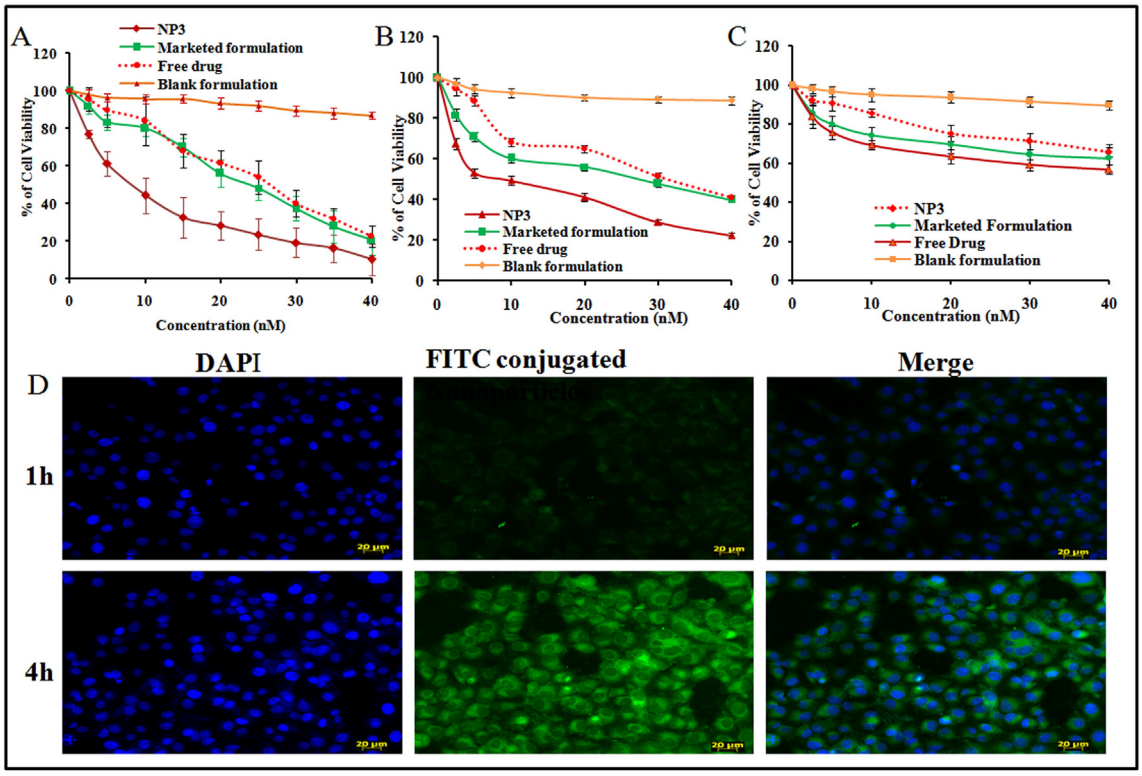

Fig. 5. Cell viability study by MTT assay of free drug, marketed formulation and NP3 in HepG2 Cells (A), in Huh-7 cells (B) and in Chang Liver cells (C). Data show mean ± standard deviation of three different experiments. Cellular uptake study of NP3 in HepG2 cells for 1 h and 4 h (D).

lowers their water absorption capacity. As a result, water cannot penetrate into the sample and the weight loss can only be produced by superficial degradation. On the other hand, the acidic pH (pH 3) of the media changed the materials from hydrophobic to hydrophilic in character and also catalyzed the hydrolysis of polymer linkages which caused faster degradation of PLGA-nanoparticles [57].

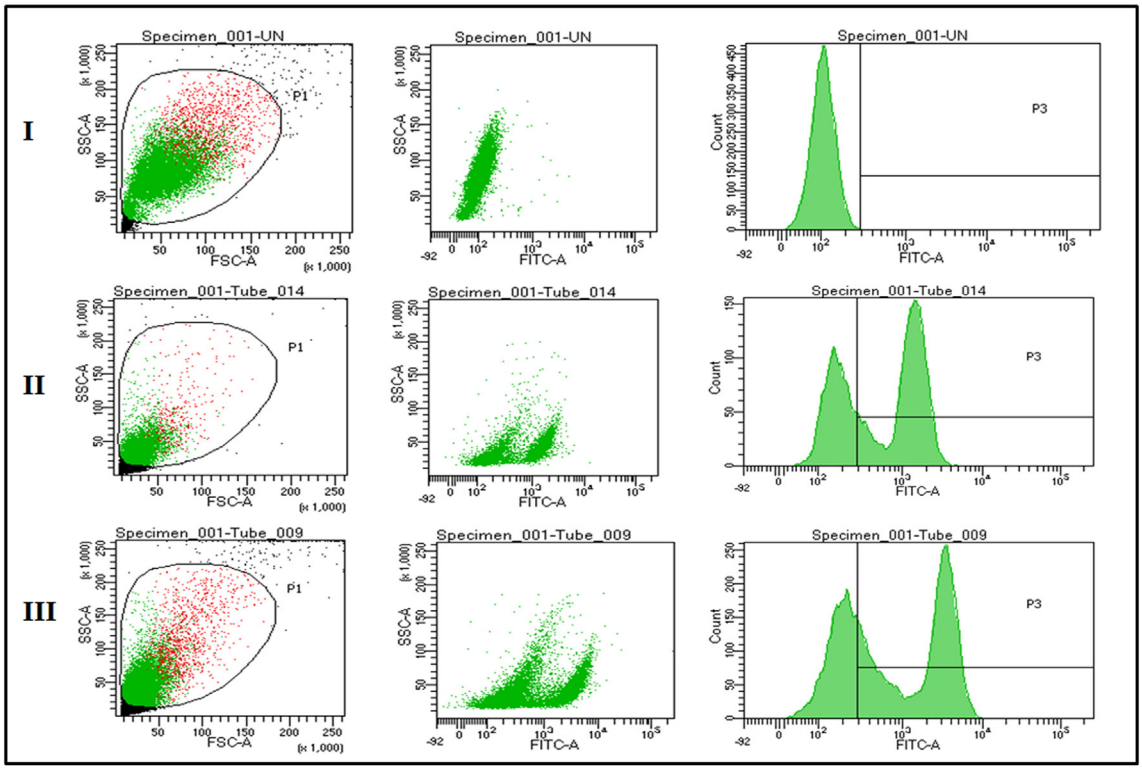

Fig. 6. Flow cytometric measurement of HepG2 cells incubated with FITC-conjugated nanoparticles at different time points. Control (I), at 1h (II), and at 4h (III)

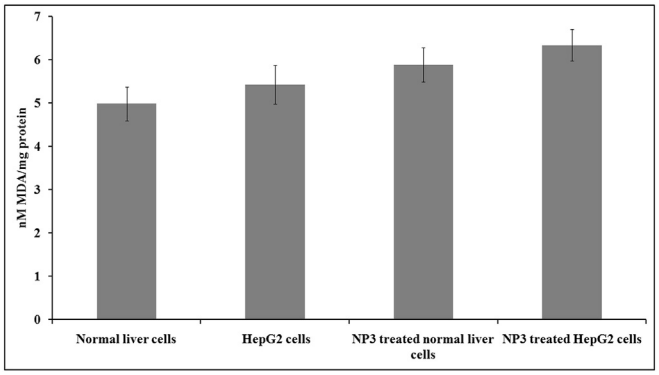

Fig. 7. MDA level in HepG2 cells and normal liver parenchymal cells. Data show mean ± standard deviation of three different experiments.

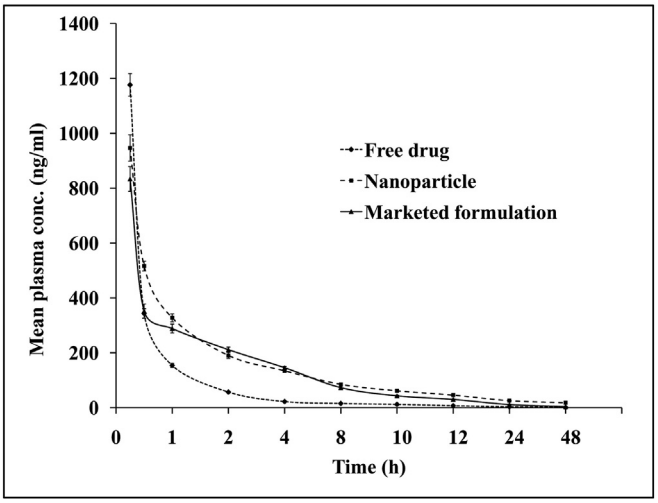

Fig. 8. Plasma concentration-time profile of PTX after i.v. administration of NP3, Pacliall® and free drug in rats (5 mg/kg). Data show mean ± SD (n = 3).

In vitro cytotoxic activity of experimental nanoparticle (NP3) was assayed by MTT assay using HepG2 cells, Huh-7 cells and normal liver parenchymal cells. IC_{50} values of Pacliall® and free drug were almost similar in HepG2 cells and Huh-7 cells, although it was predominantly lower for NP3 after 48 h incubation (Fig. 5A and B). The lower value of IC_{50} was possibly due to a higher cellular uptake of the nanoparticles and thus, more drugs could be taken up by the cells. The drug released from nanoparticles could diffuse into the nuclear compartment and produced effective cell death [58]. The percentage viability of normal liver parenchymal cells was more in case of NP3 as compared to Pacliall® and free drug as shown in Fig. 5C. This might be possibly due to low internalization of PTX-PLGA nanoparticles by normal liver cells. The result recommends that NP3 might not be toxic to normal liver parenchymal cells (Chang liver cells). For blank formulation (without drug), the decrease in cell viability of the cultured cell population was not notably significant, suggesting that the excipients of the formulation had no predominant impact on the cell death and these excipients are safe for liver cancer treatment.

Cellular internalization of nanoparticles was observed by confocal fluorescence microscopy (Fig. 5D). Cellular uptake of nanoparticles depends on various factors including size and shape of the nanoparticles, incubation time, temperature *etc*. In the present study, HepG2 cells were found to internalize NP3 well. The cellular uptake also increased with increasing incubation time from 1 to 4 h, as observed by fluorescence intensity in HepG2 cells as assessed by FACS (Fig. 6). Higher cellular uptake of nanosize NP3 formulation compared to free drug and marketed formulation as quantified by LC-MS/MS (data not shown) might cause the highest toxicity in HepG2 cells. The present result is well corroborated with previously published observation [49].

MDA is a major end product of peroxidative degradation of the polyunsaturated fatty acid constituents of biological membranes. Oxidative stress is playing an important role in the mechanism of toxicity for a number of nanoparticles through either the excessive generation of reactive oxygen species (ROS) or depletion of cellular antioxidant capacity [59]. ROS is generally included the superoxide radical ($O_2\cdot$), H_2O_2, and the hydroxyl radical ($\cdot OH$), which cause damage to cellular components, including DNA and ultimately lead to apoptotic cell death. The MDA concentration in HepG2 cells upon NP3 treatment was 16.88% more than untreated HepG2 cells and 8.48% more than normal liver cells, indicating the generation of much more free radical oxygen and lipid peroxides in HepG2 cells after NP3 treatment. The results revealed that oxidative stress produced by NP3 in HepG2 cells was predominantly more as compared to normal liver cells.

Plasma and liver pharmacokinetic studies were carried out using NP3, Pacliall® and PTX at an equivalent dose (dose of 5 mg drug/kg body weight in rats). This study showed that plasma concentration of free drug was relatively higher at 0.25 h after injection and it declined sharply after that (Fig. 8). PTX is very little soluble in water and phosphate buffer. PLGA (85:15) is also very non-polar polymer. Hence, drug release from the formulation was very slow. However, in the live system due to the presence of several enzymes and protein binding and distribution mechanism drug released rather somewhat differently.

Quick distribution of free drug as compared to the NP3 and Pacliall® could be the reason for it. Comparatively higher amount of drug from NP3 was present in plasma all over the study (48 h) and mean residence time was also more for NP3 than free drug and Pacliall®. Sustained drug release and prolonged drug residence in blood from NP3 [60] might cause a significantly higher ($p < 0.05$) $AUC_{0\text{-}t}$ and $AUMC_{0\text{-}t}$ values than free drug and Pacliall®. Nanoparticles thus appeared comparatively more bioavailable. Recently, US-FDA has approved a Cremophor® free formulation of albumin-bound PTX NPs (nab-paclitaxel or Abraxane®) for cancer treatment. In this formulation, PTX is formulated within

Table 4
Plasma pharmacokinetic parameters of PTX in rats treated with nanoparticles/marketed formulation/free drug [dose 5 mg of drug/kg body weight].

Formulation	$t_{1/2}$ (h)	C_{max} (ng/ml)	$AUC_{0\text{-}t}$ (ng·h/ml)	$AUMC_{0\text{-}t}$ (ng·h^2/ml)	CL (L/h)	MRT (h)	V_{ss} (L)
Nanoparticle	28.48 ± 0.99[#,*]	951.9 ± 47.5[#]	2915.46 ± 145.54[*,#]	32,588.88 ± 1486.98[*,#]	0.80 ± 0.03[*,#]	11.18 ± 0.56[*,#]	22.20 ± 0.78[*,#]
Pacliall®	12.62 ± 0.59	838.1 ± 41.8[$]	2250.84 ± 112.36[$]	15,530.84 ± 775.29[$]	1.30 ± 0.05[$]	6.95 ± 0.35[$]	11.40 ± 0.40
Free drug	14.22 ± 0.82	1181.4 ± 58.9	1272.95 ± 63.54	4200.73 ± 209.70	2.31 ± 0.08	3.32 ± 0.16	10.61 ± 0.37

Note: values represent mean ± SD (n = 3). Statistical significance was evaluated using one-way ANOVA followed by Tukey *post hoc* test using Origin Pro 8 (OriginLab, Northampton, MA). Differences were considered statistically significant when $p < 0.05$ at 95% confidence level.
Abbreviations: $t_{1/2}$, half-life; C_{max}, maximum blood concentration; $AUC_{0\text{-}t}$, the area under the plasma drug concentration–time curve from the time of injection to a determined time point; AUMC, area under the first moment curve; CL, clearance; MRT, mean residence time and V_{ss}, steady state volume of distribution.
[#] Indicates statistically significant data when comparison was made between nanoparticle and free drug treated group of rats.
[*] Indicates statistically significant data when comparison was made between nanoparticle and Pacliall® drug treated group of rats.
[$] Indicates statistically significant data when comparison was made between Pacliall® and free drug treated group of rats.

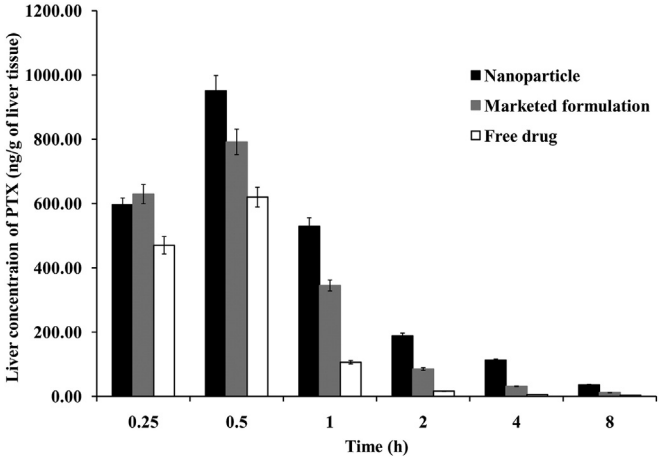

Fig. 9. Liver concentration of PTX after i.v. administration of NP3, Pacliall® and free drug in rats (5 mg/kg). Data show mean ± SD (n = 3).

albumin particles to improve the efficacy of the drug and reduce the adverse effects associated with Cremophor®. However, it has been demonstrated that Abraxane® shows a quick elimination of PTX from the blood circulation and does not improve the pharmacokinetics of PTX (Taxol®) [61]. Moreover, it is a high-cost formulation which might not be easily accessible for every patient, mainly those who are living in low- and middle-income countries [62]. At the recommended Abraxane® clinical dose, 260 mg/m^2, the mean maximum concentration of paclitaxel which occurred at the end of the infusion was 18,741 ng/mL. The mean total clearance was 15 L/h/m^2. The mean volume of distribution was 632 L/m^2. The clearance and volume of distribution of Abraxane® were much higher than the prepared PLGA nanoparticles (clearance was 0.80 ± 0.03 L/h and volume of distribution was 22.20 ± 0.78 L). Abraxane® is more quickly eliminated from the blood circulation. Thus, the prepared PLGA formulation had better pharmacokinetic properties as compared to nab-paclitaxel.

After intravenous administration of NP3/Pacliall®/free drug in rats, hepatic drug concentration from NP3 was more than the hepatic PTX concentration in free drug/Pacliall® treated rats at all the experimental time points (up to 8 h) except the time point of 0.25 h (Fig. 9). There was a significant variation ($p < 0.05$) of hepatic drug concentration between NP3 and free drug treated rats whereas, the variation is less in rats treated with NP3/Pacliall®. Thus, the developed PTX-loaded PLGA nanoparticles possessed possibly a significant drug delivery potential to liver as compared to the free drug/marketed formulation (Pacliall®). In this work, we have concentrated on the liver only. Though, it is also important to see whether the other organs are affected or not. Literatures show that other organs were also affected upon application of PTX loaded nanoparticles. But the concentration of the drug (paclitaxel) in other organs was comparatively less than the concentration of the drug in liver. R. Li et al. [63] measured the PTX levels in liver, spleen, kidney, heart and lung. The researchers reported that the PTX level was 8 fold higher in liver.

Various researchers have conducted studies on paclitaxel-loaded PLGA nanoparticles [64–66]. However, the present study is predominantly different from those available reports (Table S1). We have prepared nanoparticles using multiple emulsion solvent evaporation method. However, the above mentioned researchers prepared nanoparticles completely by different methods. Further, they did not measure the yield value of nanoparticles but, our yield of the formulation was 72.62 ± 9.96%. In the present work, we used HepG2 cells, Huh-7 cells and Chang liver cells. In the reported work they used other cells for their study. We also performed hydrolytic degradation of PLGA nanoparticles for one month in different pH conditions and the degradation was increased with decreasing pH of the medium. Gupta et al. [66] studied the accelerated stability study for three months. The last but not the least, none of the above mentioned studies have performed plasma and liver pharmacokinetic profile of formulation. Our results showed that nanoparticle formulation prolonged the blood level and higher liver uptake than the free drug and marketed formulation.

Non-uniform drug distribution may cause incomplete cancer treatment and drug targeting may be one of the most suitable options to tackle the problem. By targeted drug delivery system drug accumulates in the targeted organ or tissue in a selective way independent of site and method of administration. Thus, drug at the disease site becomes more while its concentration at the non-targeted tissues will be minimum [67]. Nanoparticles with targeted ligand such as antibody, antibody fragments, aptamers, polysaccharide, peptide and small biomolecules like folic acid *etc.* [68] are being used to target cells through ligand-receptor interactions. Various ligands used against the receptors of hepatic stellate cells include mannose-6 phosphate, human serum albumin, galactocyte and galactosamine and those of hepatocytes are glycyrrahizin, linoleic acid and apolipoprotein A1 [69].

The study shares lots of information of potential interest related to PTX-PLGA nanoparticles. Plasma and hepatic pharmacokinetic data showed that the formulation was superior to free drug and the tested commercial formulation in terms of plasma level, mean residence time, bioavailability, hepatic uptake and clearance. PTX-PLGA nanoparticles had sustained drug release and lower toxicity in contrast to free drug and the marketed formulation providing a potential use of the nanoparticles in liver cancer treatment.

5. Conclusion

In conclusion, PTX-loaded PLGA nanoparticles successfully delivered PTX in liver in a sustained manner. *In vitro* study confirmed increased cellular uptake and reduction of IC_{50} upon PTX-PLGA nanoparticle administration as compared to free drug/marketed formulation. The formulation maintained a prolonged blood residence time and higher bioavailability of PTX than free drug/Pacliall®. The experimental biodegradable polymer based nanoparticles may be a potential drug carrier for the treatment of hepatic cancer or other hepatic chronic diseases. Further studies are required.

Acknowledgement

The authors are thankful to the University Grants Commission (UGC), New Delhi, Government of India (grant no. F1-17.1/2011-12/RGNF-SC-WES-466/(SA-III/Website)) for financial support to complete this work.

Appendix A. Supplementary data

Supplementary data to this article can be found online at https://doi.org/10.1016/j.ijbiomac.2018.02.021.

References

[1] http://www.who.int/mediacentre/factsheets/fs297/en/.
[2] S.L. Siegel, K.D. Miller, A. Jemal, Cancer statistics, CA Cancer J. Clin. (2018) 2018, https://doi.org/10.3322/caac.21442 (Epub ahead of print).
[3] A. Jemal, B. Freddie, M.C. Melissa, F. Jacques, W. Elizabeth, F. David, Global cancer statistics, CA Cancer J. Clin. 61 (2011) 69–90.
[4] F.X. Bosch, R. Josepa, D. Mireia, C. Ramon, Primary liver cancer: worldwide incidence and trends, Gastroenterologia 127 (2004) S5–S16.
[5] N. Mukesh, G. Virendra, K. Prashant, K.J. Narendra, Transferrin functionalized chitosan-PEG nanoparticles for targeted delivery of paclitaxel to cancer cells, Colloids Surf., B. 148 (2016) 363–370.
[6] J.H. Ryu, H. Koo, I.C. Sun, S.H. Yuk, K. Choi, K. Kim, I.C. Kwon, Tumor-targeting multifunctional nanoparticles for theragnosis: new paradigm for cancer therapy, Adv. Drug Deliv. Rev. 64 (2012) 1447–1458.
[7] K. Greish, Enhanced permeability and retention of macromolecular drugs in solid tumors: a royal gate for targeted anticancer nanomedicines, J. Drug Target. 15 (2007) 457–464.

[8] J. Lu, Z. Li, J.I. Zink, F. Tamanoi, *In vivo* tumor suppression efficacy of mesoporous silica nanoparticles-based drug-delivery system: enhanced efficacy by folate modification, Nanomedicine 8 (2012) 212–220.
[9] S. Taurin, H. Nehoff, K. Greish, Anticancer nanomedicine and tumor vascular permeability: where is the missing link? J. Control. Release 164 (2012) 265–275.
[10] F. Danhier, E. Ansorena, J.M. Silva, R. Coco, A. Le Breton, V. Preat, PLGA-based nanoparticles: an overview of biomedical applications, J. Control. Release 161 (2012) 505–522.
[11] H. Maeda, Macromolecular therapeutics in cancer treatment: the EPR effect and beyond, J. Control. Release 164 (2012) 138–144.
[12] S. Acharya, S.K. Sahoo, PLGA nanoparticles containing various anticancer agents and tumour delivery by EPR effect, Adv. Drug Deliv. Rev. 63 (2011) 170–183.
[13] J. Bruix, S. Qin, P. Merle, A. Granito, Y.H. Huang, G. Bodoky, M. Pracht, O. Yokosuka, O. Rosmorduc, V. Breder, R. Gerolami, Regorafenib for patients with hepatocellular carcinoma who progressed on sorafenib treatment (RESORCE): a randomised, double-blind, placebo-controlled, phase 3 trial, Lancet 389 (2017) 56–66.
[14] J. Fu, H. Wang, Precision diagnosis and treatment of liver cancer in China, Cancer Lett. 412 (2018) 283–288.
[15] A.M. Barbuti, Z.S. Chen, Paclitaxel through the ages of anticancer therapy: exploring its role in chemoresistance and radiation therapy, Cancer 7 (2015) 2360–2371.
[16] E. Bernabeu, M. Cagel, E. Lagomarsino, M. Moretton, D.A. Chiappetta, Paclitaxel: what has been done and the challenges remain ahead, Int. J. Pharm. 526 (2017) 474–495.
[17] K. Priyadarshini, A.U. Keerthi, Paclitaxel against cancer: a short review, Med. Chem. 2 (2012) 139–141.
[18] H.Y. Cho, C.K. Lee, Y.B. Lee, Preparation and evaluation of PEGylated and folate-PEGylated liposomes containing paclitaxel for lymphatic delivery, J. Nanomater. 16 (2015) 36.
[19] F. Danhier, P. Danhier, C.J. De Saedeleer, A.C. Fruytier, N. Schleich, A. des Rieux, P. Sonveaux, B. Gallez, V. Préat, Paclitaxel-loaded micelles enhance transvascular permeability and retention of nanomedicines in tumors, Int. J. Pharm. 479 (2015) 399–407.
[20] H. Wang, G. Cheng, Y. Du, L. Ye, W. Chen, L. Zhang, T. Wang, J. Tian, F. Fu, Hypersensitivity reaction studies of a polyethoxylated castor oil free liposomes based alternative paclitaxel formulation, Mol. Med. Rep. 7 (2013) 947–952.
[21] C.D. Scripture, F.D. William, S. Alex, Peripheral neuropathy induced by paclitaxel: recent insights and future perspectives, Curr. Neuropharmacol. 4 (2006) 165–172.
[22] A. Raza, G.K. Sood, Hepatocellular carcinoma review: current treatment, and evidence-based medicine, World J. Gastroenterol. 20 (2014) 4115–4127.
[23] G. Battogtokh, J.H. Kang, Y.T. Ko, Long-circulating self-assembled cholesteryl albumin nanoparticles enhance tumor accumulation of hydrophobic anticancer drug, Eur. J. Pharm. Biopharm. 96 (2015) 96–105.
[24] F. Danhier, N. Lecouturier, B. Vroman, C. Jérôme, J. Marchand-Brynaert, O. Feron, V. Préat, Paclitaxel-loaded PEGylated PLGA-based nanoparticles: *in vitro* and *in vivo* evaluation, J. Control. Release 133 (2009) 11–17.
[25] P.P. Lv, W. Wei, H. Yue, T.Y. Yang, L.-Y. Wang, G.H. Ma, Porous quaternized chitosan nanoparticles containing paclitaxel nanocrystals improved therapeutic efficacy in non-small cell lung cancer after oral administration, Biomacromolecules 12 (2011) 4230–4239.
[26] G. Aygül, F. Yerlikaya, S. Caban, İ. Vural, Y. Çapan, Formulation and *in vitro* evaluation of paclitaxel loaded nanoparticles, Hacettepe Univ. J. Fac. Pharm. 33 (2013) 25–40.
[27] P. Utreja, S. Jain, S. Yadav, K.L. Khandhuja, A.K. Tiwary, Efficacy and toxicological studies of cremophor EL free alternative paclitaxel formulation, Curr. Drug Saf. 6 (2011) 329–338.
[28] Y. Wang, K.C. Wu, B.X. Zhao, X. Zhao, X. Wang, S. Chen, S.F. Nie, W.S. Pan, X. Zhang, Q. Zhang, A novel paclitaxel microemulsion containing a reduced amount of Cremophor EL: pharmacokinetics, biodistribution, and *in vivo* antitumor efficacy and safety, Biomed. Res. Int. 2011 (2011).
[29] M. Shah, V. Shah, A. Ghosh, Z. Zhang, T. Minko, Molecular inclusion complexes of β-cyclodextrin derivatives enhance aqueous solubility and cellular internalization of paclitaxel: preformulation and *in vitro* assessments, J. Pharm. Pharmacol. (2) (2015) 8.
[30] J. Shiny, T. Ramchander, P. Goverdhan, M. Habibuddin, J.V. Aukunuru, Development and evaluation of a novel biodegradable sustained release microsphere formulation of paclitaxel intended to treat breast cancer, Int. J. Pharm. Investig. 3 (2013) 119.
[31] J. Mosafer, K. Abnous, M. Tafaghodi, A. Mokhtarzadeh, M. Ramezani, *In vitro* and *in vivo* evaluation of anti-nucleolin-targeted magnetic PLGA nanoparticles loaded with doxorubicin as a theranostic agent for enhanced targeted cancer imaging and therapy, Eur. J. Pharm. Biopharm. 113 (2017) 60–74.
[32] R. Maji, N.S. Dey, B.S. Satapathy, B. Mukherjee, S. Mondal, Preparation and characterization of tamoxifen citrate loaded nanoparticles for breast cancer therapy, Int. J. Nanomedicine 9 (2014) 3107.
[33] D. Ibraheem, M. Iqbal, G. Agusti, H. Fessi, A. Elaissari, Effects of process parameters on the colloidal properties of polycaprolactone microparticles prepared by double emulsion like process, Colloids Surf. A Physicochem. Eng. Asp. 445 (2014) 79–91.
[34] D. Mandal, P.K. Ojha, B.C. Nandy, L.K. Ghosh, Effect of carriers on solid dispersions of simvastatin (Sim): physico-chemical characterizations and dissolution studies, Der. Pharm. Lett. 2 (2010) 47–56.
[35] S. Ghosh, L. Mondal, S. Chakraborty, B. Mukherjee, Early stage HIV management and reduction of stavudine-induced hepatotoxicity in rats by experimentally developed biodegradable nanoparticles, AAPS Pharm. Sci. Tech. 18 (2017) 697–709.
[36] S.R. Acharya, P.R. Reddy, Brain targeted delivery of paclitaxel using endogenous ligand, Asian J. Pharm. Sci. 11 (2016) 427–438.
[37] P. Costa, J.M.S. Lobo, Modeling and comparison of dissolution profiles, Eur. J. Pharm. Sci. 13 (2001) 123–133.
[38] S. Dash, P.N. Murthy, L. Nath, P. Chowdhury, Kinetic modeling on drug release from controlled drug delivery systems, Acta Pol. Pharm. Drug Res. 67 (2010) 217–223.
[39] G.K. Jain, S.A. Pathan, S. Akhter, N. Ahmad, N. Jain, S. Talegaonkar, R.K. Khar, F.J. Ahmad, Mechanistic study of hydrolytic erosion and drug release behaviour of PLGA nanoparticles: influence of chitosan, Polym. Degrad. Stab. 95 (2010) 2360–2366.
[40] H.M. Chen, Y.P. Wang, J. Chen, J.H. Yang, N. Zhang, T. Huang, Y. Wang, Hydrolytic degradation behavior of poly (L-lactide)/SiO 2 composites, Polym. Degrad. Stab. 98 (2013) 2672–2679.
[41] R. Bharti, G. Dey, P.K. Ojha, S. Rajput, S.K. Jaganathan, R. Sen, M. Mandal, Diacerein-mediated inhibition of IL-6/IL-6R signaling induces apoptotic effects on breast cancer, Oncogene 35 (2016) 3965–3975.
[42] S. Panja, G. Dey, R. Bharti, P. Mandal, M. Mandal, S. Chattopadhyay, Metal ion ornamented ultrafast light-sensitive nanogel for potential *in vivo* cancer therapy, Chem. Mater. 28 (2016) 8598–8610.
[43] M.S. Maia, S.D. Bicudo, C.C. Sicherle, L. Rodello, I.C. Gallego, Lipid peroxidation and generation of hydrogen peroxide in frozen thawed ram semen cryopreserved in extenders with antioxidants, Anim. Reprod. Sci. 122 (2010) 118–123.
[44] M.H. Chowdhury, B.S. Satapathy, L. Mondal, S. Chakraborty, B. Mukherjee, Effect of streptozotocin-induced hyperglycemia on the progression of hepatocarcinogenesis in rats, Am. J. Pharmacol. Toxicol. 8 (2013) 170–178.
[45] H. Choudhury, B. Gorain, S. Karmakar, E. Biswas, G. Dey, R. Barik, M. Mandal, T.K. Pal, Improvement of cellular uptake, *in vitro* antitumor activity and sustained release profile with increased bioavailability from a nanoemulsion platform, Int. J. Pharm. 460 (2014) 131–143.
[46] X. Wang, L. Song, N. Li, Z. Qiu, S. Zhou, C. Li, J. Zhao, H. Song, X. Chen, Pharmacokinetics and biodistribution study of paclitaxel liposome in Sprague-Dawley rats and beagle dogs by liquid chromatography-tandem mass spectrometry, Drug Res. 63 (2013) 603–606.
[47] N. Zeng, Q. Hu, Z. Liu, X. Gao, R. Hu, Q. Song, G. Gu, H. Xia, L. Yao, Z. Pang, X. Jiang, Preparation and characterization of paclitaxel-loaded DSPE-PEG-liquid crystalline nanoparticles (LCNPs) for improved bioavailability, Int. J. Pharm. 424 (2012) 58–66.
[48] B.S. Satapathy, B. Mukherjee, R. Baishya, M.C. Debnath, N.S. Dey, R. Maji, Lipid nanocarrier-based transport of docetaxel across the blood brain barrier, RSC Adv. 6 (2016) 85261–85274.
[49] S.E. Gratton, P.A. Ropp, P.D. Pohlhaus, J.C. Luft, V.J. Madden, M.E. Napier, J.M. DeSimone, The effect of particle design on cellular internalization pathways, Proc. Natl. Acad. Sci. 105 (2008) 11613–11618.
[50] B. Sahana, K. Santra, S. Basu, B. Mukherjee, Development of biodegradable polymer based tamoxifen citrate loaded nanoparticles and effect of some manufacturing process parameters on them: a physicochemical and in-vitro evaluation, Int. J. Nanomedicine 5 (2010) 621–630.
[51] E. Vaculikova, A. Cernikova, D. Placha, M. Pisarcik, P. Peikertova, K. Dedkova, F. Devinsky, J. Jampilek, Preparation of hydrochlorothiazide nanoparticles for solubility enhancement, Molecules 21 (2016) 1005.
[52] M.J. Masarudin, S.M. Cutts, B.J. Evison, D.R. Phillips, P.J. Pigram, Factors determining the stability, size distribution, and cellular accumulation of small, monodisperse chitosan nanoparticles as candidate vectors for anticancer drug delivery: application to the passive encapsulation of [14C]-doxorubicin, Nanotechnol. Sci. Appl. 8 (2015) 67–80.
[53] S.T. Crooke, Antisense drug technology: principles, strategies, and applications, second ed. CRC Press, Boca Raton, London, New York, 2007.
[54] T.K. Shaw, D. Mandal, G. Dey, M.M. Pal, P. Paul, S. Chakraborty, K.A. Ali, B. Mukherjee, A.K. Bandyopadhyay, M. Mandal, Successful delivery of docetaxel to rat brain using experimentally developed nanoliposome: a treatment strategy for brain tumor, Drug Deliv. 24 (2017) 346–357.
[55] B. Mukherjee, K. Santra, G. Pattnaik, S. Ghosh, Preparation, characterization and *in-vitro* evaluation of sustained release protein-loaded nanoparticles based on biodegradable polymers, Int. J. Nanomedicine 3 (2008) 487.
[56] V. Sanna, A.M. Roggio, A.M. Posadino, A. Cossu, S. Marceddu, A. Mariani, V. Alzari, S. Uzzau, G. Pintus, M. Sechi, Novel docetaxel-loaded nanoparticles based on poly (lactide-co-caprolactone) and poly (lactide-co-glycolide-co-caprolactone) for prostate cancer treatment: formulation, characterization, and cytotoxicity studies, Nanoscale Res. Lett. 6 (2011) 260.
[57] G.P. Sailema-Palate, A. Vidaurre, A.J. Campillo-Fernández, I. Castilla-Cortázar, A comparative study on poly(ε-caprolactone) film degradation at extreme pH values, Polym. Degrad. Stab. 130 (2016) 118–125.
[58] X. Zeng, R. Morgenstern, A.M., Nanoparticle-directed sub-cellular localization of doxorubicin and the sensitization breast cancer cells by circumventing GST-mediated drug resistance, Biomaterials 35 (2014) 1227–1239.
[59] J.P. Wise, B.C. Goodale, S.S. Wise, G.A. Craig, A.F. Pongan, R.B. Walter, W.D. Thompson, A.K. Ng, A.M. Abouelssa, H. Mitani, M.J. Spalding, Silver nanospheres are cytotoxic and genotoxic to fish cells, Aquat. Toxicol. 97 (2010) 34–41.
[60] X. Zhang, P. Sun, R. Bi, J. Wang, N. Zhang, G. Huang, Targeted delivery of levofloxacin-liposomes for the treatment of pulmonary inflammation, J. Drug Target. 17 (2009) 399–407.
[61] A. Sparreboom, C.D. Scripture, V. Trieu, P.J. Williams, T. De, A. Yang, B. Beals, W.D. Figg, M. Hawkins, N. Desai, Comparative preclinical and clinical pharmacokinetics of a cremophor-free, nanoparticle albumin-bound paclitaxel (ABI-007) and paclitaxel formulated in cremophor (taxol), Clin. Cancer Res. 11 (2005) 4136–4143.
[62] E. Bernabeu, G. Helguera, M.J. Legaspi, L. Gonzalez, C. Hocht, C. Taira, D.A. Chiappetta, Paclitaxel-loaded PCL–TPGS nanoparticles: *in vitro* and *in vivo* performance compared with Abraxane®, Colloids Surf. B: Biointerfaces 113 (2014) 43–50.
[63] R. Li, J.S. Eun, M.K. Lee, Pharmacokinetics and biodistribution of paclitaxel loaded in pegylated solid lipid nanoparticles after intravenous administration, Arch. Pharm. Res. 34 (2011) 331–337.

[64] C. Fonseca, S. Simoes, R. Gaspar, Paclitaxel-loaded PLGA nanoparticles: preparation, physicochemical characterization and *in vitro* anti-tumoral activity, J. Control. Release 83 (2002) 273–286.
[65] D. Le Broc- Ryckewaert, R. Carpentier, E. Lipka, S. Daher, C. Vaccher, D. Betbeder, C. Furman, Development of innovative paclitaxel-loaded small PLGA nanoparticles: study of their antiproliferative activity and their molecular interactions on prostatic cancer cells, Int. J. Pharm. 454 (2013) 712–719.
[66] P.N. Gupta, S. Jain, C. Nehate, N. Alam, V. Khare, R.D. Dubey, A. Saneja, S. Kour, S.K. Singh, Development and evaluation of paclitaxel loaded PLGA: poloxamer blend nanoparticles for cancer chemotherapy, Int. J. Biol. Macromol. 69 (2014) 393–399.
[67] F. Danhier, O. Feron, V. Préat, To exploit the tumor microenvironment: passive and active tumor targeting of nanocarriers for anti-cancer drug delivery, J. Control. Release 148 (2010) 135–146.
[68] Y. Zhong, F. Meng, C. Deng, Z. Zhong, Ligand-directed active tumor-targeting polymeric nanoparticles for cancer chemotherapy, Biomacromolecules 15 (2014) 1955–1969.
[69] B. Mukherjee, S. Chakraborty, L. Mondal, B.S. Satapathy, S. Sengupta, L. Dutta, A. Choudhury, D. Mandal, Multifunctional drug nanocarriers facilitate more specific entry of therapeutic payload into tumors and control multiple drug resistance in cancer, in: A. Grumezescu (Ed.), Nanobiomaterials in Cancer Therapy 2016, pp. 203–251.

Drug Delivery

ISSN: 1071-7544 (Print) 1521-0464 (Online) Journal homepage: http://www.tandfonline.com/loi/idrd20

Successful delivery of docetaxel to rat brain using experimentally developed nanoliposome: a treatment strategy for brain tumor

Tapan Kumar Shaw, Dipika Mandal, Goutam Dey, Murari Mohan Pal, Paramita Paul, Samrat Chakraborty, Kazi Asraf Ali, Biswajit Mukherjee, Amal Kumar Bandyopadhyay & Mahitosh Mandal

To cite this article: Tapan Kumar Shaw, Dipika Mandal, Goutam Dey, Murari Mohan Pal, Paramita Paul, Samrat Chakraborty, Kazi Asraf Ali, Biswajit Mukherjee, Amal Kumar Bandyopadhyay & Mahitosh Mandal (2017) Successful delivery of docetaxel to rat brain using experimentally developed nanoliposome: a treatment strategy for brain tumor, Drug Delivery, 24:1, 346-357, DOI: 10.1080/10717544.2016.1253798

To link to this article: https://doi.org/10.1080/10717544.2016.1253798

© 2017 The Author(s). Published by Informa UK Limited, trading as Taylor & Francis Group.

View supplementary material

Published online: 06 Feb 2017.

Submit your article to this journal

Article views: 1106

View related articles

View Crossmark data

Citing articles: 7 View citing articles

Full Terms & Conditions of access and use can be found at
http://www.tandfonline.com/action/journalInformation?journalCode=idrd20

http://informahealthcare.com/drd
ISSN: 1071-7544 (print), 1521-0464 (electronic)

Drug Delivery

Drug Deliv, 2017; 24(1): 346–357
© 2017 The Author(s). Published by Informa UK Limited, trading as Taylor & Francis Group.
DOI: 10.1080/10717544.2016.1253798

Taylor & Francis
Taylor & Francis Group

RESEARCH ARTICLE

Successful delivery of docetaxel to rat brain using experimentally developed nanoliposome: a treatment strategy for brain tumor

Tapan Kumar Shaw[1], Dipika Mandal[1], Goutam Dey[2], Murari Mohan Pal[1], Paramita Paul[1], Samrat Chakraborty[1], Kazi Asraf Ali[3], Biswajit Mukherjee[1], Amal Kumar Bandyopadhyay[1], and Mahitosh Mandal[2]

[1]Department of Pharmaceutical Technology, Jadavpur University, Kolkata, West Bengal, India, [2]School of Medical Science and Technology, Indian Institute of Technology Kharagpur, Kharagpur, West Bengal, India, and [3]Dr. B. C. Roy College of Pharmacy and Allied Health Sciences, Dr. Meghnad Saha Sarani, Bidhan Nagar, Durgapur, West Bengal, India

Abstract

Docetaxel (DTX) is found to be very effective against glioma cell *in vitro*. However, *in vivo* passage of DTX through BBB is extremely difficult due to the physicochemical and pharmacological characteristics of the drug. No existing formulation is successful in this aspect. Hence, in this study, effort was made to send DTX through blood–brain barrier (BBB) to brain to treat diseases such as solid tumor of brain (glioma) by developing DTX-loaded nanoliposomes. Primarily drug-excipients interaction was evaluated by FTIR spectroscopy. The DTX-loaded nanoliposomes (L-DTX) were prepared by lipid layer hydration technique and characterized physicochemically. *In vitro* cellular uptake in C6 glioma cells was investigated. FTIR data show that the selected drug and excipients were chemically compatible. The unilamellar vesicle size was less than 50 nm with smooth surface. Drug released slowly from L-DTX *in vitro* in a sustained manner. The pharmacokinetic data shows more extended action of DTX from L-DTX in experimental rats than the free-drug and Taxotere®. DTX from L-DTX enhanced 100% drug concentration in brain as compared with Taxotere® in 4 h. Thus, nanoliposomes as vehicle may be an encouraging strategy to treat glioma with DTX.

Keywords

Blood–brain barrier, nanoliposomes of Docetaxel, glioma, C6 cells, brain distribution

History

Received 4 August 2016
Revised 23 October 2016
Accepted 23 October 2016

Introduction

Astrocytoma (commonly known as glioma) is most prevalent among three different types of brain tumors, namely astrocytomas, oligidendrogliomas and oligoastrocytomas, in adults. This aggressive malignant form of cancer accounts for ~45–50% of all primary tumors resulting in death of patients within a couple of years (Guo et al., 2011; Nance et al., 2014). The characteristic features such as lack of sharp border, infiltration ability of the tumor cells in the brain of glioma as well as their wide distribution restrict their treatments by surgery and radiotherapy (Guo et al., 2011). Further, due to the strategic location of the blood–brain barrier (BBB) that allows a selective transport of drugs into the brain, chemotherapy becomes an auxiliary treatment for malignant glioma. In the last few decades, many drugs have been or being explored for the treatment of glioma. Most of them including docetaxel (DTX) are large hydrophobic molecules, which are unable to cross the BBB easily (Asperen et al., 1997) and may become an effective candidate for efflux by various efflux pumps governed by BBB as well as tumor cells (Beaulieu et al., 1997).

Docetaxel (DTX) is a complex diterpene alkaloid, isolated from the bark of *Texas baccata,* congener of paclitaxel. It has an efficient antineoplastic effect against a wide spectrum of solid tumors, such as ovarian, breast and lung cancer. It is found to be effective in the treatment of glioma *in vitro* but its *in vivo* efficacy is highly compromised due to its poor aqueous solubility and high molecular weight (Banks, 2009; Liu et al., 2011; Tan et al., 2012). Therefore, suitable design and development of appropriate vehicle for the transport of therapeutic payload is of prime importance in order to develop an effective therapy against glioma. In this context colloidal drug carrier especially nanoliposomes have gained significant interest among the researchers around the globe. (Jain, 2012; Zhang & Zhang, 2013; Hao et al, 2015; Sonali et al., 2016a; Sonali et al., 2016b; Sonali et al., 2016c).

Liposomes, the small spherical vesicle with single or multiple lipid bilayers, made from natural and/or synthetic lipids have been widely exploited due to their unique characteristics such as high biocompatibility, biodegradability, and non-immunogenicity (Laouini et al., 2012; Akbarzadeh et al., 2013). They usually improve biodistribution and pharmacokinetic profile of the therapeutic payload by sustained drug release from the formulation and

Address of correspondence: Biswajit Mukherjee, Department of Pharmaceutical Technology, Jadavpur University, Kolkata – 700032, West Bengal, India. Tel: +91-33-24146677. Fax: +91-33-24146677. E-mail: biswajit55@yahoo.com

This is an Open Access article distributed under the terms of the Creative Commons Attribution License (http://creativecommons.org/Licenses/by/4.0/), which permits unrestricted use, distribution, and reproduction in any medium, provided the original work is properly cited.

Edited by
ALEXANDRU MIHAI GRUMEZESCU

NANOBIOMATERIALS IN CANCER THERAPY

APPLICATIONS OF NANOBIOMATERIALS

Volume 7

Nanobiomaterials in Cancer Therapy

Applications of Nanobiomaterials

Nanobiomaterials in Cancer Therapy

Applications of Nanobiomaterials

Edited by

Alexandru Mihai Grumezescu

Department of Science and Engineering of Oxide Materials and Nanomaterials, Faculty of Applied Chemistry and Materials Science, University Politehnica of Bucharest, Bucharest, Romania

Department of Biomaterials and Medical Devices, Faculty of Medical Engineering, University Politehnica of Bucharest, Bucharest, Romania

ELSEVIER

AMSTERDAM • BOSTON • HEIDELBERG • LONDON
NEW YORK • OXFORD • PARIS • SAN DIEGO
SAN FRANCISCO • SINGAPORE • SYDNEY • TOKYO
William Andrew is an imprint of Elsevier

William Andrew is an imprint of Elsevier
The Boulevard, Langford Lane, Kidlington, Oxford, OX5 1GB, UK
50 Hampshire Street, 5th Floor, Cambridge, MA 02139, USA

Copyright © 2016 Elsevier Inc. All rights reserved.

No part of this publication may be reproduced or transmitted in any form or by any means, electronic or mechanical, including photocopying, recording, or any information storage and retrieval system, without permission in writing from the publisher. Details on how to seek permission, further information about the Publisher's permissions policies and our arrangements with organizations such as the Copyright Clearance Center and the Copyright Licensing Agency, can be found at our website: www.elsevier.com/permissions.

This book and the individual contributions contained in it are protected under copyright by the Publisher (other than as may be noted herein).

Notices
Knowledge and best practice in this field are constantly changing. As new research and experience broaden our understanding, changes in research methods, professional practices, or medical treatment may become necessary.

Practitioners and researchers must always rely on their own experience and knowledge in evaluating and using any information, methods, compounds, or experiments described herein. In using such information or methods they should be mindful of their own safety and the safety of others, including parties for whom they have a professional responsibility.

To the fullest extent of the law, neither the Publisher nor the authors, contributors, or editors, assume any liability for any injury and/or damage to persons or property as a matter of products liability, negligence or otherwise, or from any use or operation of any methods, products, instructions, or ideas contained in the material herein.

ISBN: 978-0-323-42863-7

British Library Cataloguing-in-Publication Data
A catalogue record for this book is available from the British Library.

Library of Congress Cataloging-in-Publication Data
A catalog record for this book is available from the Library of Congress.

For Information on all William Andrew publications
visit our website at http://www.elsevier.com/

Typeset by MPS Limited, Chennai, India

Contents

List of contributors

Udita Agrawal
Drug Delivery Research Laboratory, Department of Pharmaceutical Sciences, Dr. Hari Singh Gour Central University, Sagar, Madhya Pradesh, India

Ecaterina Andronescu
Department of Science and Engineering of Oxide Materials and Nanomaterials, Faculty of Applied Chemistry and Materials Science, University Politehnica of Bucharest, Bucharest, Romania

Bhawani Aryasomayajula
Center for Pharmaceutical Biotechnology and Nanomedicine, Northeastern University, Boston, MA, USA

Maria Vitória Lopes Badra Bentley
School of Pharmaceutical Sciences of Ribeirão Preto, University of São Paulo, Ribeirão Preto, São Paulo, Brazil

Archana Bhaw-Luximon
ANDI Centre of Excellence for Biomedical and Biomaterials Research, University of Mauritius, Réduit, Mauritius

Ioana Raluca Bucur
Department of Biomaterials and Medical Devices, Faculty of Medical Engineering, University Politehnica of Bucharest, Bucharest, Romania

Patrícia Mazureki Campos
School of Pharmaceutical Sciences of Ribeirão Preto, University of São Paulo, Ribeirão Preto, São Paulo, Brazil

Yu Cao
Key Laboratory of Pesticide and Chemical Biology (Ministry of Education), College of Chemistry, Central China Normal University, Wuhan, PR, China

Samrat Chakraborty
Department of Pharmaceutical Technology, Jadavpur University, Kolkata, India

Ankan Choudhury
Department of Pharmaceutical Technology, Jadavpur University, Kolkata, India

Luciana M. De Hollanda
Department of Internal Medicine, Hemocentro, School of Medical Science, Universidade Estadual de Campinas, Campinas, São Paulo, Brazil

Surbhi Dubey
Drug Delivery Research Laboratory, Department of Pharmaceutical Sciences, Dr. Hari Singh Gour Central University, Sagar, Madhya Pradesh, India

Lopamudra Dutta
Department of Pharmaceutical Technology, Jadavpur University, Kolkata, India

Elena Mikhailivna Egorova
Institute of General Pathology and Pathophysiology, Russian Academy of Medical Sciences, Moscow, Russia

Norhaizan Mohd. Esa
Universiti Putra Malaysia (UPM), Selangor, Malaysia

Yoshiya Furusawa
Research Center for Charged Particle Therapy, National Institute of Radiological Sciences, Chiba, Japan

Sharon E. Gao
Department of Pharmaceutical Sciences, University of Pittsburgh School of Pharmacy, Pittsburgh, PA, USA

Nowsheen Goonoo
ANDI Centre of Excellence for Biomedical and Biomaterials Research, University of Mauritius, Réduit, Mauritius

Alexandru Mihai Grumezescu
Department of Biomaterials and Medical Devices, Faculty of Medical Engineering, University Politehnica of Bucharest, Bucharest, Romania; Department of Science and Engineering of Oxide Materials and Nanomaterials, Faculty of Applied Chemistry and Materials Science, University Politehnica of Bucharest, Bucharest, Romania

Nidhi Gupta
Department of Biotechnology, The IIS University, Jaipur, Rajasthan, India

Dhanjay Jhurry
ANDI Centre of Excellence for Biomedical and Biomaterials Research, University of Mauritius, Réduit, Mauritius

Said Ibragimovitch Kaba
Institute of General Pathology and Pathophysiology, Russian Academy of Medical Sciences, Moscow, Russia

Samikannu Kanagesan
Materials Synthesis and Characterization Laboratory, Institute of Advanced Technology (ITMA), Universiti Putra Malaysia (UPM), Selangor, Malaysia

Katsumi Kobayashi
Photon Factory, Institute of Materials Structure Science, High Energy Accelerator Research Organization, Ibaraki, Japan

Aslan Amirkhanovitch Kubatiev
Institute of General Pathology and Pathophysiology, Russian Academy of Medical Sciences, Moscow, Russia

Claude Le Sech
Institut des Sciences Molélculaires d'Orsay—ISMO Bât 351, Université Paris, Orsay Cedex, France

Mădălina Lemnaru
Department of Biomaterials and Medical Devices, Faculty of Medical Engineering, University Politehnica of Bucharest, Bucharest, Romania

Song Li
Department of Pharmaceutical Sciences, University of Pittsburgh School of Pharmacy, Pittsburgh, PA, USA

Min Liu
Key Laboratory of Pesticide and Chemical Biology (Ministry of Education), College of Chemistry, Central China Normal University, Wuhan, PR, China

Shiying Luo
Key Laboratory of Pesticide and Chemical Biology (Ministry of Education), College of Chemistry, Central China Normal University, Wuhan, PR, China

Dipika Mandal
Department of Pharmaceutical Technology, Jadavpur University, Kolkata, India

Maria Minodora Marin
Department of Biomaterials and Medical Devices, Faculty of Medical Engineering, University Politehnica of Bucharest, Bucharest, Romania

Ştefania Marin
Department of Biomaterials and Medical Devices, Faculty of Medical Engineering, University Politehnica of Bucharest, Bucharest, Romania

Nishi Mody
Drug Delivery Research Laboratory, Department of Pharmaceutical Sciences, Dr. Hari Singh Gour Central University, Sagar, Madhya Pradesh, India

Laboni Mondal
Department of Pharmaceutical Technology, Jadavpur University, Kolkata, India

Shaker A. Mousa
The Pharmaceutical Research Institute, Albany College of Pharmacy and Health Sciences, Rensselaer, NY, USA

Jean Felix Mukerabigwi
Key Laboratory of Pesticide and Chemical Biology (Ministry of Education), College of Chemistry, Central China Normal University, Wuhan, PR, China

Biswajit Mukherjee
Department of Pharmaceutical Technology, Jadavpur University, Kolkata, India

Radhakrishnan Narayanaswamy
Universiti Putra Malaysia (UPM), Selangor, Malaysia; Laboratory of Natural Products, Institute of Bioscience (IBS), Universiti Putra Malaysia (UPM), Selangor, Malaysia

Surendra Nimesh
Department of Biotechnology, School of Life Sciences, Central University of Rajasthan, Ajmer, Rajasthan, India

Ashok Kumar Pandurangan
Department of Pharmacology, University of Malaya, Kuala Lumpur, Malaysia

Padmanabhan Parasuraman
Lee Kong Chian School of Medicine, Nanyang Technological University (NTU), Singapore

Kalyani C. Patil
Institute of Cancer Sciences, University of Glasgow, Glasgow, Lanarkshire, UK

Mehdi Rajabi
The Pharmaceutical Research Institute, Albany College of Pharmacy and Health Sciences, Rensselaer, NY, USA

Lucinda V. Reis
Department of Chemistry and CQ-VR, UTAD, Vila Real, Portugal

Antonello Santini
Department of Pharmacy, Università degli Studi di Napoli Federico II, Napoli, Italy

Bhabani Sankar Satapathy
Department of Pharmaceutical Technology, Jadavpur University, Kolkata, India

Soma Sengupta
Department of Pharmaceutical Technology, Jadavpur University, Kolkata, India

Patrícia Severino
Laboratory of nanotechnology and nanomedicine (LNMED), University of Tiradentes and Institute of Technology and Research, Aracaju, Brazil

Rajeev Sharma
Drug Delivery Research Laboratory, Department of Pharmaceutical Sciences, Dr. Hari Singh Gour Central University, Sagar, Madhya Pradesh, India

Amélia M. Silva
Department of Biology and Environment, University of Trás-os Montes e Alto Douro, Vila Real, Portugal; Centre for Research and Technology of Agro-Environmental and Biological Sciences (CITAB, UTAD), Vila Real, Portugal

Eliana B. Souto
Department of Pharmaceutical Technology, Faculty of Pharmacy, University of Coimbra (FFUC), Coimbra, Portugal; Center for Neuroscience and Cell Biology (CNC), University of Coimbra, Coimbra, Portugal

Selma B. Souto
Department of Endocrinology and Metabolism, Hospital of Braga, Braga, Portugal

Mathangi Srinivasan
The Pharmaceutical Research Institute, Albany College of Pharmacy and Health Sciences, Rensselaer, NY, USA

Roxana Elena Ţiplea
Department of Biomaterials and Medical Devices, Faculty of Medical Engineering, University Politehnica of Bucharest, Bucharest, Romania

Vladimir P. Torchilin
Center for Pharmaceutical Biotechnology and Nanomedicine, Northeastern University, Boston, MA, USA; Department of Biochemistry, Faculty of Science, King Abdulaziz University, Jeddah, Saudi Arabia

Noriko Usami
Photon Factory, Institute of Materials Structure Science, High Energy Accelerator Research Organization, Ibaraki, Japan

George Mihail Vlăsceanu
Department of Biomaterials and Medical Devices, Faculty of Medical Engineering, University Politehnica of Bucharest, Bucharest, Romania

Ruchi Vyas
Department of Biotechnology, The IIS University, Jaipur, Rajasthan, India

Suresh P. Vyas
Drug Delivery Research Laboratory, Department of Pharmaceutical Sciences, Dr. Hari Singh Gour Central University, Sagar, Madhya Pradesh, India

Jieni Xu
Department of Pharmaceutical Sciences, University of Pittsburgh School of Pharmacy, Pittsburgh, PA, USA

Jatinder Vir Yakhmi
Department of Atomic Energy, Homi Bhabha National Institute, Mumbai, Maharashtra, India

Peng Zhang
Department of Pharmaceutical Sciences, University of Pittsburgh School of Pharmacy, Pittsburgh, PA, USA

Yuannian Zhang
Key Laboratory of Pesticide and Chemical Biology (Ministry of Education), College of Chemistry, Central China Normal University, Wuhan, PR, China

CHAPTER

7

Multifunctional drug nanocarriers facilitate more specific entry of therapeutic payload into tumors and control multiple drug resistance in cancer

Biswajit Mukherjee, Samrat Chakraborty, Laboni Mondal, Bhabani Sankar Satapathy, Soma Sengupta, Lopamudra Dutta, Ankan Choudhury and Dipika Mandal

Department of Pharmaceutical Technology, Jadavpur University, Kolkata, India

7.1 INTRODUCTION

Cancer has instigated lots of interest among researchers around the globe due to its high mortality, unique nature, and inadequate treatment strategies. As per the published report of American Cancer Society, it is expected that by 2030 about 21.4 million new cancer cases will impose a serious global concern and cancer related death toll may reach up to 13.2 million due to the growth and aging of population. Despite the remarkable breakthroughs that have been achieved in understanding the disease, especially mapping and profiling of specific tumor biomarkers, characterization of cancer cells and the understanding of signal cascades involved in pathogenesis of cancer, the development of an appropriate treatment strategy is still in its infancy. This may be due to our inability to deliver the cargo of drug(s) specifically to the target site without imparting any adverse effect on healthy tissues and organs. Therefore, it would be very much essential to develop a smarter and more efficient carrier system that can overcome the biological barriers, distinguish between normal and cancerous cells, capable enough to exploit the heterogeneous and complex microenvironment to deliver cargo within an optimal dosage range (Mukherjee et al., 2014; Karra and Benita, 2012).

Traditional treatment options for cancer include surgical intervention, radiation, and chemotherapeutic drugs, which produce adverse effects on healthy cells, thus imparting toxicity to the patients. Moreover, most of the potent anticancer agents possess limited solubility in the biological environment, which has greatly

Nanobiomaterials in Cancer Therapy. DOI: http://dx.doi.org/10.1016/B978-0-323-42863-7.00007-4
© 2016 Elsevier Inc. All rights reserved.